PROPERTIES OF MACAQUE VENTRAL PREMOTOR CORTEX DURING GRASPING

Dissertation

zur

Erlangung der naturwissenschaftlichen Doktorwuerde

(Dr. sc. nat.)

vorgelegt der

Mathematisch-naturwissenschaftlichen Fakultaet

der

Universitaet Zuerich

von

MARIE-CHRISTINE FLUET

aus

Kanada

Promotionskomitee

Dr. Hansjoerg Scherberger

Prof. Kevan A.C. Martin

Prof. Bernhard Hess

Prof. Eric Rouiller

Zuerich, 2009

TABLE OF CONTENTS

SUMMARY

The hand is one of the most sophisticated biological motor systems and understanding the control strategies used by the brain to move this complex apparatus represents a major challenge. Previous studies have given evidence of multiple cortical representations of hand movements including primary motor cortex, supplementary motor area, inferior area 6 and parietal cortex. These findings raise questions about the specificity of each of theses areas for the planning and control of distal movements. In the present study, the main focus was to investigate the properties of area F5 (rostral part of inferior area 6). Firstly, we investigated the specificity of the response of F5 neurons to two parameters, grip type and target orientation, during a delayed grasping task. This task was divided into well defined periods that allow the analysis of the neural response during different phases of the action, namely the object observation, the planning of the movement and the movement execution. Secondly, we investigated the representation of partial instruction information by separating the instruction of the orientation from the instruction of the grip type in distinct task epochs. Thirdly, a decoding simulation was performed in order to attest the possibility of decoding grasp movement intentions from area F5 for the possible application of a prosthetic hand control from brain signals. Specifically, we recorded neural activity in two macaque monkeys while they were presented with a handle that could be rotated in five possible orientations (upright, 25 and 50 degrees to the right or left). Simultaneously with the object presentation, a colored light instructed how the handle had to be grasped, either with a power or with a precision grip. Our results revealed that the grip type and the object orientation are both encoded in area F5. Their representation was similar during the instruction, but while the representation of object orientation was maintained constant, the representation of grip type significantly increased during the movement execution. These results suggest a major role of area F5 for shaping the fingers during grasping movement while its role for the positioning of the hand in the correct orientation might be reduced. Furthermore, cells with different tuning onset for grip type and orientation had been found. These different types of cells also showed differences in the simultaneous encoding of grip type and orientation. Moreover, the cue separation task revealed that the orientation representation was present in F5 even without a grip

type instruction, but that the grip type was not encoded in F5 in the absence of the presentation of an object. Finally, the decoding simulation using a Bayesian classifier showed that grip type and orientation could both be decoded from area F5, but the performance was better for decoding the grip type than the orientation. In sum, the present thesis brings new insight to the representation of hand movement in area F5, in particular for the combined encoding of object orientation and grip type. It also reveals that hand movements can be decoded from higher order planning areas and that area F5 could be suitable for the implementation of a brain-machine interface for hand grasping which might have potential value for future applications in paralyzed patients.

ZUSAMMENFASSUNG

Die Hand ist eines der am höchsten entwickelten biologisch-motorischen Systeme und das Verständnis der vom Gehirn verwendeten Kontrollmechanismen für die Bewegung dieses komplexen Apparates stellt eine grosse Herausforderung dar. Ergebnisse früherer Studien zeigten, dass mehrere Hirnregionen an der Kontrolle von Handbewegungen beteiligt sind, darunter der primär-motorische Kortex, das supplementär-motorische Areal, das inferiore Areal 6 und der Parietalkortex. Diese Ergebnisse führten zu weiteren Fragestellungen über die Spezifität dieser Regionen für die Planung und die Kontrolle von Handbewegungen. Der Schwerpunkt der vorliegenden Studie liegt auf der Untersuchung der Hirnregion F5 (dem rostralen Teil des inferioren Areals 6). Erstens untersuchten wir mit einem delayed grasping task Neuronen in der Region F5 auf ihre Spezifität für zwei Parameter, die Art des Handgriffes und die Griff-Orientierung. Diese Aufgabe war zur Analyse der neuronalen Aktivität in zeitlich deutlich voneinander getrennte unterschiedliche Handlungsabschnitte unterteilt: der Beobachtung des Zielobjektes, der Planung der Bewegung, und der Ausführung der Bewegung. Zweitens untersuchten wir mit einem cue seperation task die Repräsentation von unterschiedlichen Instruktionen, indem wir die Anweisungen für die Orientierung und die Art des Griffes in klar getrennte Zeitabschnitte unterteilten. Zum Dritten wurde ein Decoding simuliert, um die Möglichkeit des Entschlüsselns der Planung von Greifbewegungen in der Region F5 für die etwaige Kontrolle einer Hand-Prothese durch Gehirn-Signale zu zeigen. Im Detail zeichneten wir während des delayed grasping task die Hirnaktivität von zwei Makaken auf, denen ein Handgriff in fünf möglichen Orientierungen präsentiert wurde (vertikal, sowie 25 und 50 Grad nach links oder rechts rotiert). Zeitgleich mit der Präsentation dieses Objektes wurden die Tiere durch ein farbiges Lichtsignal instruiert, mit welchem von zwei Griff-Arten, entweder einem Kraft- oder einem Präzisions-Griff, das Objekt ergriffen werden sollte. Unsere Ergebnisse zeigen, dass sowohl die Art des Griffes als auch die Orientierung des Objektes in der Region F5 kodiert sind. Ihre Repräsentation war in der Instruktionsphase ähnlich, aber während die Repräsentation der Objektorientierung während der Bewegungsausführung stabil blieb, nahm die Repräsentation der Griff-Art signifikant zu. Diese Ergebnisse deuten darauf hin, dass die Region F5 eine grosse Rolle für die Kodierung der Fingerstellung

beim Greifen spielt, wohingegen ihre Bedeutung für die Orientierung der Hand untergeordnet wäre. Weiterhin wurden Zellen mit unterschiedlichem Tuning onset für die Art des Griffes und der Orientierung gefunden, welche die Greifart und Handorientierung auch unterschiedlich repräsentieren. Des weiteren zeigte der cue seperation task, dass die Repräsentation der Orientierung in F5 auch ohne vorherige Instruktion über die Art des Griffes vorhanden war, wohingegen die Art des Griffes in Abwesenheit eines Objektes nicht in F5 kodiert wurde. Schliesslich zeigte die Simulation eines Decoding mit einem Bayesian Classifier, dass sowohl die Art des Griffes als auch die Orientierung von neuronaler Aktivität in der Region F5 dekodiert werden konnten wobei die Dekodierung der Griff-Art besser als die der Orientierung war. Zusammengefasst gewährt diese Dissertation neue Einblicke in die Repräsentation von Handbewegungen in der Region F5, insbesondere für die kombinierte Kodierung von Objekt-Orientierung und der Art des Griffes. Auch zeigt sie, dass Handbewegungen aus neuronaler Aktivität höherer Planungsareale dekodiert werden können und die Region F5 damit für die Verwirklichung einer Gehirn-Maschine-Schnittstelle für Handgreifbewegungen geeignet wäre. Dies könnte für zukünftige Anwendung bei gelähmten Patienten potentiell nützlich sein.

DECLARATION

All procedures involving animal subjects were in accordance with the guidelines set by the Veterinary Office of the Canton of Zurich and the Guidelines for the care and use of mammals in neuroscience and behavioral research (National Research Council, 2003).

Training of the monkeys was performed by Markus Baumann and myself with the help of Bernadette Disler.

Surgeries were performed by Hansjoerg Scherberger assisted by Markus Baumann.

Electrophysiological recordings were performed by Markus Baumann and myself.

Most of the software programmed in Matlab for the data analyses was written by myself. Some programs used for the decoding were written by Hansjoerg Scherberger and a program to convert the raw data in an easily accessible structure was written by Markus Baumann. Discussions with Hansjoerg Scherberger and Markus Baumann were important to develop the analyses.

Perfusion was performed by Hansjoerg Scherberger and fixation by Nuno Da Costa.

Histology slices were prepared by Simone Rickauer.

ACKNOLEDGMENTS

First, I would like to thank Steven Fry for introducing me at the INI and Kevan Martin and Rodney Douglas for their support and trust during the application process to the PhD program. Furthermore, I would like to thank my supervisor Hansjoerg Scherberger from which I learned new techniques and for teaching me a rigorous way of working. Thanks to my inseparable colleague and partner Markus Baumann. I am glad that we could go through all the steps of this great accomplishment together. Thanks to Bernhard Hess and Eric Rouiller for being part of my thesis committee. Thanks to all my colleagues and friends who made the life at the INI enjoyable. Finally, I would like to thank my parents Claudette Drouin and Rene Fluet for giving me the chance to get a good education.

1. INTRODUCTION

This chapter first introduces to the history of the discovery of the excitable motor cortex and the initial concepts about movement generation emerging from it. It is followed by the current view of the motor cortex, including premotor and parietal areas, which is based on more recent findings and the focus will be made on the areas specialized in the control of hand and finger movements. As the present study concentrates mainly on the rostral part of the ventral premotor cortex (or area F5), an overview of the afferent and efferent connections of that area will be provided as well as a review of what is known up to now about its function. Finally, the possibility to decode hand grasping movements from high-order brain areas in paralyzed patients will be discussed.

1.1 Discovery of the excitable motor cortex

The localization of motor functions within the cerebral cortex was first proven by electrical stimulation studies performed by Gustav Fritsch and Edvard Hitzig in 1870 (Fritsch and Hitzig, 1870; Hitzig, 1870) (for a review see (Gross, 2007)). When electrically stimulating a rostral part of the cortex of dogs using brief pulses of monophasic direct current, they could elicit muscle twitches and contractions in contralateral body parts. Their experiment also showed a topographic representation of the body in the brain. The rest of the cortex was believed to be sensory. A confirmation of the excitability of the cortex came from David Ferrier in 1873 (Ferrier, 1873). Ferrier wanted to reproduce the experiment of Fritsch and Hitzig in other species, especially in monkeys. To electrically stimulate the brain, he used a long duration biphasic current and elicited complex movements rather than simples muscle twitches. Ferrier also found a larger excitable region which covers the precentral, postcentral and parietal convolutions of the monkey brain but this finding of a widespread excitable cortex was strongly criticized by Fritsch and Hitzig. In order to firmly establish the concept of an excitable motor cortex, further investigations led by Horsley, Schafer and Beevor were performed in order to produce a precise topographic mapping of the cortex (Beevor and Horsley, 1887; Horsley and

Schafer, 1888) (for a review see (Gross, 2007)). The fingers, the hands and the mouth were found to represent most of the surface of the primary motor cortex. Even though the motor cortex could be localized by electrical stimulation, its function was still unclear. Two views opposed each other. The first one stated that the excitable cortex represents the unique place where organization and initiation of a movement occurs while the opposing view proposed that the excitable cortex was only the point of departure and not the center of movements. The answer to that debate came from observations in conscious patients performed by Penfield in 1937 which reports that the movements elicited by electrical stimulation were clearly purposeless. It became obvious that the motor cortex was only the last cortical level before projecting to the pyramidal tract and not the center of purposeful movements. This led to the conclusion that other areas must fulfill the functions of movement organization. Earlier, based on the study of epileptic patients, J. Hughlings Jackson had proposed a hierarchical model composed of three levels of motor organization (for a review see (Swash, 2005)). The lowest level would be constituted by the spinal cord and the middle one by the primary motor cortex. In 1905, Campbell suggested that the premotor cortex would represent the higher level of Johnson's model (for a review see (Wise, 1985)). Experiments conducted by Fulton in which he performed the ablation of premotor areas in monkeys led to deficits in execution of skilled movements, then showing that other areas than the primary motor cortex were involved in motor functions (Fulton et al., 1932; Fulton, 1934; Kennard et al., 1934; Fulton, 1935; Kennard, 1935) (for a review see (Wise, 1985)). The lack of precision about the location of the ablations performed by Fulton engendered controversy. It was finally Woolsey who established the concept of a nonprimary cortex by discovering the supplementary motor cortex which also displays a somatotopic representation of the body, but Woolsey concluded that the premotor cortex played no role in the control of movements based on his observation that the ablation of the premotor cortex, in addition to the ablation of the primary motor cortex or the supplementary motor cortex, did not produce additional substantial deficits (Woolsey et al., 1952). Few neuroanatomists continued studying the premotor cortex and their work showed that the premotor cortex is strongly interconnected with other cortical (primary motor cortex, supplementary motor area) (Matsumura and Kubota, 1979; Muakkassa and Strick, 1979) and subcortical (thalamus, cerebellum, basal ganglia) (Schell and Strick,

1984) structures involved in the control of movement and should then be considered as part of the motor cortex.

1.2 Nomenclature

There have been several denominations for the different subdivisions of the frontal cortex based on different studies and different criteria (connectivity patterns, topographic map, physiological function, etc.). The agranular frontal cortex was classically divided into two areas, areas 4 and 6, according to Brodmann's cytoarchitectonic map (Figure 1.1A). Later, Woolsey proposed another denomination based on the functional role of these areas. Area 4 and the portion of area 6 located on the lateral convexity were thought to have the same function and were referred to as the primary motor cortex (or M1), while the mesial portion of area 6 constituted a separate functional area referred to as the supplementary motor area (or SMA) (Figure 1.1B). Recent anatomical and functional studies have shown that the motor cortex is composed of many more distinct areas. The premotor cortex was subdivided into the ventral and dorsal premotor cortex and each of these subdivisions have a rostral and a caudal part (Figure 1.1C). The most recent denomination was proposed by Matelli (Matelli et al., 1985) and is composed of seven distinct functional areas (Figure 1.1D) each one dealing with different effectors. More details are provided in the section 1.3 about the function of each of these seven subdivisions. In the present study, we will refer to the different subdivisions of the motor cortex using the most recent denominations.

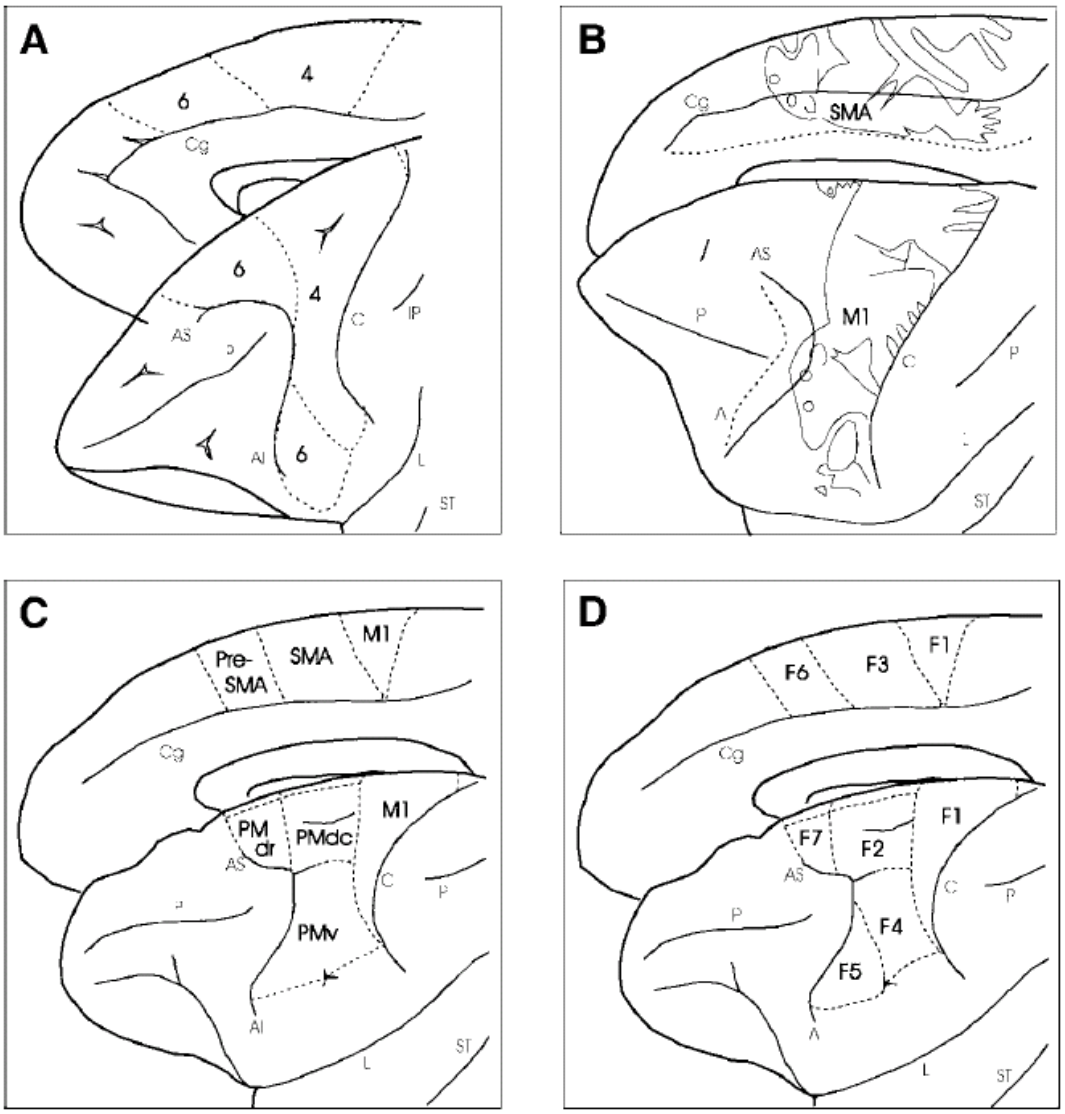

Figure 1.1 Comparative views of some of the proposed subdivisions of the agranular frontal cortex of the monkey.
A) cytoarchitectonic map of Brodmann; B) functional map of Woolsey et al.; C) modern, functional subdivision; D) histochemical and cytoarchitectonic map of Matelli et al.. AI, inferior arcuate sulcus; AS, superior arcuate sulcus; C, central sulcus; Cg, cingulate sulcus; F1-F7, agranular frontal areas; IP, intraparietal sulcus; L, lateral fissure; M1, primary motor cortex; P, principal sulcus; PMdc, dorsal premotor cortex, caudal; PMdr, dorsal premotor cortex, rostral; PMv, ventral premotor cortex; SMA, supplementary motor area; ST, superior temporak sulcus. (Luppino and Rizzolatti, 2000)

1.3 Current view of the motor cortex

The extremely simplistic view of the motor cortex including only the precentral gyrus (primary motor cortex) and the medial wall of the frontal lobe (supplementary motor area) has radically changed in the last decades. The involvement of the

premotor areas in movement control was strongly supported by the study of its connectivity (reviewed in section 1.4). The motor cortex is now considered as covering the entire agranular part of the frontal cortex, being the caudal part of the frontal cortex, and is composed of many anatomically and functionally distinct areas. Seven divisions were established based on cytoarchitectural and histochemical data (Matelli et al., 1985) as presented in Figure 1.2. By single-neuron recordings, intracortical microstimulation and corticospinal projection studies, these divisions were also found to have functional differences and to have different motor representations. Leg representation was found in areas F1, F2 and F3, while arm representation was found in F1, F2, F3, F4 and F5 and more specifically, hand and fingers representation was restricted to area F1 and F5. As for areas F6 and F7, they have been shown to have strong input from the prefrontal cortex and to project to all the premotor areas except F1 making them as the entrance point of prefrontal cortex into the motor cortex. The prefrontal cortex is usually considered as being involved in working memory, motivation and temporal planning of actions. Beside the prefrontal lobe, the parietal lobe was found to have important projections to the frontal motor areas. Some authors even suggest that the posterior parietal cortex should be considered as part of the motor system (Luppino and Rizzolatti, 2000) because the activity in that area was found to be correlated with motor actions (Goldberg et al., 1990; Batista et al., 1999). Anatomical data revealed that some areas in the parietal cortex even project to the cervical spinal cord (Martino and Strick, 1987). These studies have given evidence of a multiple cortical representation of movements and raise questions about the specificity of each of theses areas for the planning and control of movements. The organization of the parietal cortex seems to be rather similar to the premotor cortex. It is formed by many areas, each one dealing with a different effector and specific sensory information. Anatomical studies have shown that the parietal areas tend to project specifically to only one frontal area and reciprocally the frontal areas are also specifically projecting to the same parietal areas, thus forming segregated parietofrontal circuits working in parallel. These circuits are thought to be dedicated to specific sensorimotor transformations, which consist in transforming sensory representation, like visual, tactile or auditory information, into a motor representation for action execution (Luppino et al., 1999).

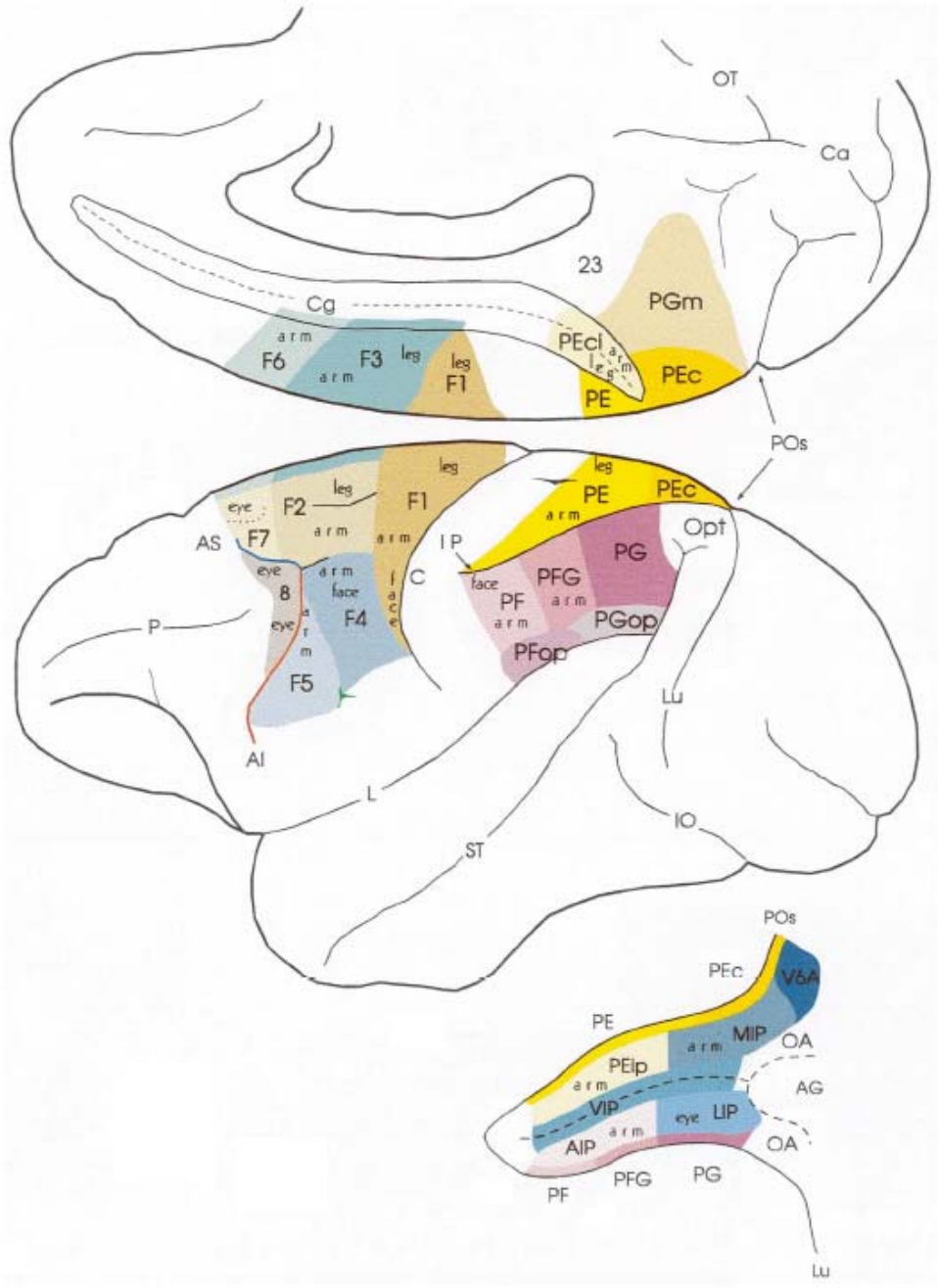

Figure 1.2 Mesial and lateral views of the macaque brain showing the cytoarchitectonic parcellation of the agranular frontal cortex and the posterior parietal cortex.
Motor areas are defined according to Matelli et al. (Matelli et al., 1985, 1991). All parietal areas except those buried within the intraparietal sulcus are defined according to Pandya and Seltzer (Pandya and Seltzer, 1982). The areas located within the intraparietal sulcus (IP) are defined according to physiological data and are shown in an unfolded view of the sulcus in the lowest part of the figure. On the basis of the available data, the various body-parts representations are reported. In the prefrontal cortex the frontal eye field (FEF) is also defined according to physiological criteria. The superior arcuate sulcus (AS), the inferior arcuate sulcus (AI) and the inferior precentral dimple are drawn in blue, red and green, respectively. AG, annectant gyrus; C, central gyrus; Ca, calcarine fissure; Cg, cingulate sulcus; IO, inferior occipital sulcus; L, lateral fissure; Lu, lunate sulcus; OT, occipitotemporal sulcus; P, principal sulcus; POs, parieto-occipital sulcus; ST, superior temporal sulcus. (Rizzolatti et al., 1998).

1.4 Connectivity of the motor cortex

The afferent and efferent connections of the motor areas are examined in the following section with an emphasis on premotor area F5 in order to give a better understanding of the input provided to that area and the output generated by this area as well as a comprehension of the sensorimotor transformation loop in which it is involved.

1.4.1. Subcortical connections

Retrograde injection studies have shown that the cerebellum and the basal ganglia project via the thalamus to the motor areas (Schell and Strick, 1984). Those studies have shown that the primary motor cortex, the supplementary motor area and the premotor cortex receive input from separate subdivisions of the ventrolateral thalamus. The actual scheme of connections is the following: the primary motor cortex receives input from the rostral portions of the deep cerebellar nuclei via the pars oralis subdivision of nucleus ventralis posterior lateralis (VPLo), the supplementary motor area receives input from the globus pallidus in the basal ganglia via the pars oralis subdivision of nucleus ventralis lateralis (VLo) and the premotor cortex receives input from the caudal portions of the deep cerebellar nuclei via area X. The cerebellum and the basal ganglia have been shown from lesion studies to be involved in motor control. Patients with cerebrocerebellar damage show delays in the initiation of movements and irregularities in the timing of movement components while disorders of the basal ganglia lead to either diminished movements (Parkinson disease) or excessive movements (Huntington disease). The primary motor cortex as well as the ventral, dorsal and medial premotor areas, were found to project to the parvocellular red nucleus with the strongest projections coming from the medial premotor area (supplementary motor area) (Kuypers and Lawrence, 1967; Monakow et al., 1979). The red nucleus additionally receives input from the cerebellum and is thought to play a major role in feedback control of movements (Figure 1.3).

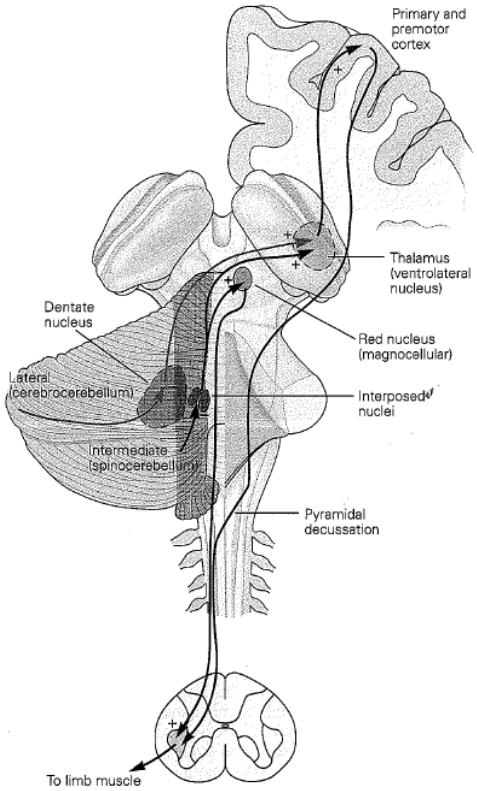

Figure 1.3 Projections from the cerebellum to the motor cortex via the thalamus and to the spinal cord via the red nucleus.
The lateral zone (cerebrocerebellum) influences the motor and premotor cortices via the ventrolateral nucleus of the thalamus. The intermediate zone (spinocerebellum) controls the dorsolateral descending systems (rubrospinal and corticospinal tracts).

Studies in which retrograde tracers were injected in the second cervical segment of the spinal cord revealed that most of the corticospinal projections originate from the primary motor cortex and the premotor areas (Dum and Strick, 1991). The primary motor cortex contributes for about 40% of the corticospinal projections originating from the frontal cortex while the premotor areas contribute for 60% of the projections. The premotor areas in the medial wall alone (SMA and CMA) contribute to 40% of the projections from the frontal cortex with 18% from the supplementary motor area. About 5% of the corticospinal projections originate from PMv (Wise, 2006). Tracer injections in the arm region of the primary motor cortex also revealed that the premotor areas projecting to the spinal cord are the same that project to the arm area of the primary motor cortex (Dum and Strick, 2005). Parietal areas have also been found to have direct projections to the spinal cord (Martino and Strick, 1987), suggesting that these areas can control hand movements independently of the primary

motor cortex and raising questions about viewing the primary motor cortex as the final common pathway for movement control. This also shows that corticospinal projections are not restricted to the frontal cortex.

1.4.2 Corticocortical connections

The primary motor cortex, the premotor areas and the supplementary motor area have been found to be strongly interconnected. More specifically, area F5 strongly projects to the primary motor cortex and these projections are topographically organized (Matsumura and Kubota, 1979; Muakkassa and Strick, 1979; Godschalk et al., 1984). The neurons located in the posterior bank of the inferior limb of the arcuate sulcus and in the arcuate spur have reciprocal connections with the hand area of the primary motor cortex while the neurons situated below the inferior limb of the arcuate sulcus projects to the mouth area of the primary motor cortex via area F4 (Matelli et al., 1986). Area F5 was also found to have reciprocal connections with the supplementary motor area organized in a topographic way and the density of those connections seems to be equivalent in both directions unlike the connection of F5 with the primary motor cortex where the projections are denser from F5 to the primary motor cortex than vice versa (Matelli et al., 1986).

The premotor cortex receives direct input from the parietal cortex. This is not the case for the primary motor cortex. These connections are organized in distinct parallel parietofrontal circuits (Luppino et al., 1999). PMd is connected to the superior parietal lobule while PMv is connected to the ventral bank of the intraparietal sulcus and the rostral part of the inferior parietal lobule (Chavis and Pandya, 1976; Jones et al., 1978). While PMd receives proprioceptive information, PMv receives tactile and visual information (Matelli et al., 1986). One of the major afferent inputs from the parietal cortex to area F5 comes from area 7b (or PF). This input from area 7b seems to convey the visual information coming from the occipital gyrus (area OA). F5 also receive input from the area situated immediately medially to area PF, in the bank of the intraparietal sulcus, namely the anterior intraparietal area (AIP). Another source of visual information to area F5 comes from the area POa which receives direct projections from the prestriate cortex (Godschalk et al., 1984). Another major afferent

from the parietal cortex to area F5 originates from the operculum of the lateral fissure, more specifically in a region of the postcentral operculum called the secondary somatosensory area (SII) (Matelli et al., 1986). This input from SII seems to convey the somatosensory information. Interestingly, the secondary somatosensory area, in addition to its projections to F5, also projects to area 7b.

The premotor areas were also found to receive inputs from the prefrontal cortex. PMd receives afferent connections from the dorsal part of the prefrontal cortex, while PMv is connected to the ventral part. Area F5 is reciprocally connected with the prefrontal cortex, more precisely to the ventral bank of the principal sulcus and the cortex on the adjacent convexity (area 46) (Matelli et al., 1986). The prefrontal cortex is thought to be involved in planning, initiation, facilitation and inhibition of motor responses and also in motivation. The premotor areas seem to play a major role in connecting the frontal cortex to the primary motor cortex, or in other words, to bring volition into action.

1.4.3 Distinction between PMd and PMv

Distinction between the superior and the inferior premotor areas should be made based on anatomical, functional and evolutionary findings (Matelli et al., 1986). These areas have been found to receive input from different cortical areas (reviewed in the previous subsection 1.4.2). Additionally, enzymatic methods show a clear separation of these two areas at the level of the spur of the arcuate sulcus. The cytoarchitectonic organization differs also largely. The superior premotor area is very similar to the organization of the primary motor cortex but with less pyramidal cells. The inferior premotor area shows differences between its more caudal part which is similar to the primary motor cortex and the more rostral part which contains a thin granular layer. Finally, PMd and PMv seem to have evolved from different structures. PMd would originate from the cingulated gyrus while PMv would originate from the insular cortex (Sanides, 1964). Functionally, both areas are involved in planning and execution of arm movements. Functional distinctions were nevertheless observed. More recently, in an experiment performed by Hoshi (Hoshi and Tanji, 2006), the activity of PMv and PMd neurons was recorded during a task in which two cues were

presented successively in a central position, one cue instructed the location to be reached and the other one instructed the arm to be used. Additionally, a white square appeared to the left or right of the central position. PMd and PMv showed different responses. While PMv response represented the spatial position of the visual cue, PMd response reflected the motor information instructed by the arbitrary cue. These results led the authors of the study to conclude that PMv is involved in direct sensorimotor processing while PMd is involved in indirect sensorimotor processing.

1.5 Descending pathways for motor control

There are several motor descending pathways, each one having specific characteristics concerning the origin of the pathway, the trajectory of the fibers, the termination of the pathway, etc. Some of those pathways are originating in the brainstem and are thus referred to as brainstem pathways while the pathway involving cortical structures is called the corticospinal tract (or CST) (Figure 1.4). The frontal cortex contributes to most of the cortical projections to the spinal cord, but some projections also originate in the parietal lobe (Martino and Strick, 1987). Important differences of the CST exist across species. One of these main differences resides in the extend of the direct, monosynaptique cortico-motorneuronal (CM) connections in primates. This system was discovered in 1954 by Bernhard and Bohm (Bernhard and Bohm, 1954) and is specific to primates. Direct connections to motor neurons occur in the lateral intermediate zone and lateral motor nuclei. These connections are very important for the control of individual muscles, mainly for independent control of fingers. These connections have been shown to originate exclusively from the primary motor cortex suggesting that the other motor areas of the brain must use this route to exert motor effects (for a review see (Lemon, 2008)). In parallel to the CM system, the cortex also projects to interneurons. These connections are important for coordinating large group of muscles, like in reaching or walking. Many CST fibers cross to the contralateral side of the spinal cord in the pyramidal decussation. Nevertheless, a non negligible number of fibers also project ipsilaterally.

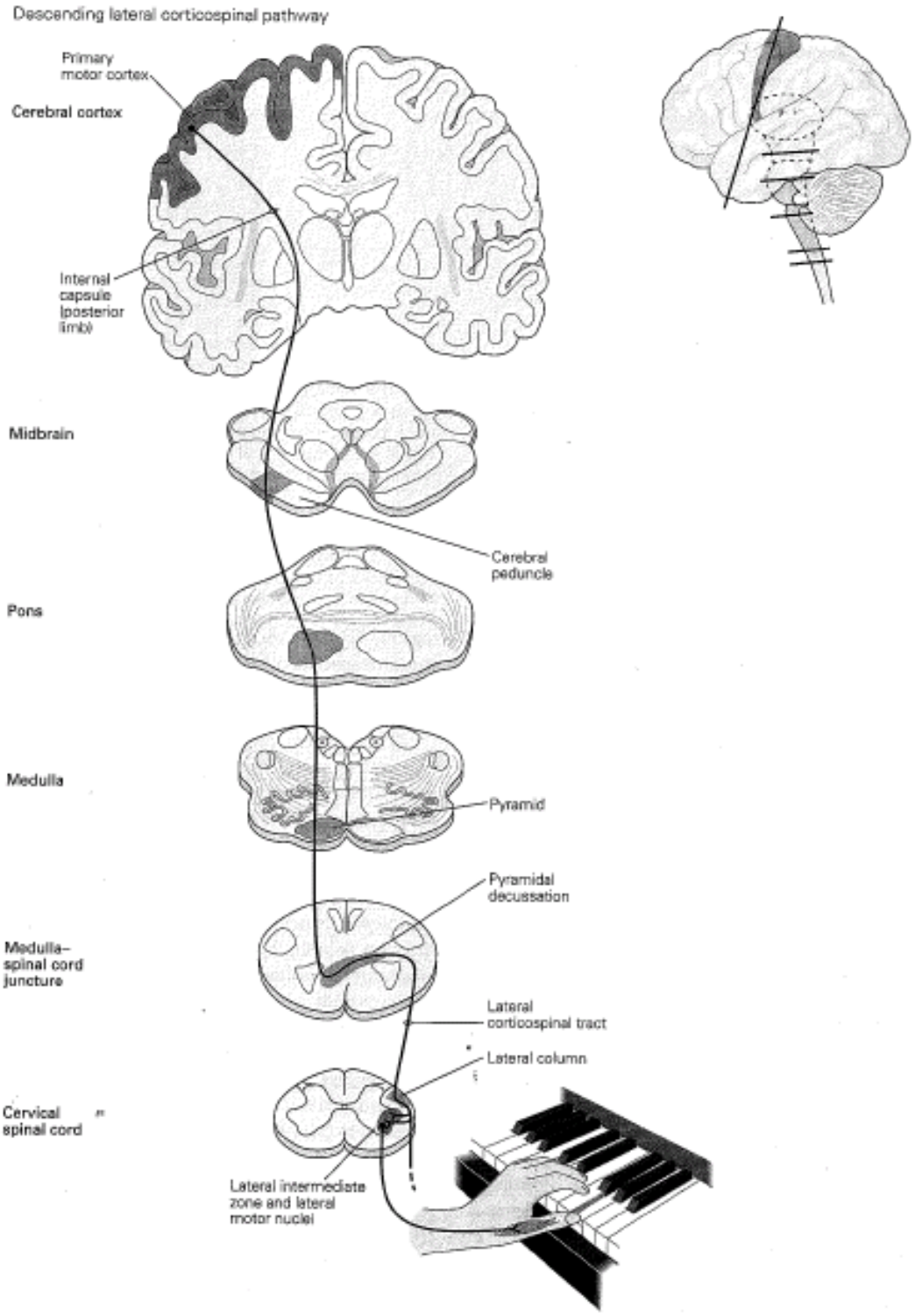

Figure 1.4 Descending lateral corticospinal pathway.
Fibers that originate in the primary motor cortex and terminate in the ventral horn of the spinal cord constitute a significant part of the corticospinal tract. The same axons can be found at various spinal levels among the internal capsule, the cerebral peduncle, the medullary pyramid, and the lateral corticospinal tract.

1.6 Prehensile classifications

Our hands play a very important role in our daily life by manipulating objects for the achievement of a large variety of tasks. We can execute hand movements with great ease even though the hand is a very complex system with many degrees of freedom. The main functions of the hands during grasping are the following: first, to transfer motion to an object in order to move it in a purposeful way; second, to apply forces to oppose to external forces (ex: gravitational force); third, to gather sensory information about the state of the interaction in order to readjust the grasp. Many attempts have been made to classify the variety of hand movements. One classification was developed by Schlesinger in 1919 in order to build prosthetic hands for the many amputees of the First World War. He started by taking many objects from his environment and tried to find a tool that could hold it and then named the different grip types according to either the tool that he used or the object that was grasped. For example, he named the hook grip according to the tool, cylindrical and spherical grips where named according to the object and tip, palmar and lateral grip were named according to the surface of the hand which was in contact with the object. This classification had the advantage to be quite simple but did not reflect the task and the intention of the movement. In 1956, Napier developed another classification more closely related to the requirements of the task (Napier, 1956). For Napier, prehension constituted the application of forces. His classification resulted into two categories: power and precision grasps. The power grasp is made by the flexion of all the fingers holding the object in a stable grasp while the precision grip is the ability of the hand to make small adjustments to control the object. To Napier, all other movements represented variation of these two categories. Many following studies concerning hand grasping explored the neural representation of these two types of grasp.

1.7 Visuomotor transformation for grasping

The control of the hand movements represents a great challenge for the brain. Among different kind of movements, reflexes represent a category of actions in reaction to external stimuli but they are rather elementary movements and do not involve the cortex, but only the spinal cord and brain stem. In contrast, voluntary

movements are organized to perform a purposeful task and require planning. They are not only a reaction to an external stimulus but are generated internally. Voluntary movements involve three steps: firstly, the selection of an appropriate response to the sensory information, out of a repertoire of possible responses; secondly, the planning of the movement in physical terms, meaning defining the characteristics of the selected response as the sequence of muscle contractions required to carry it out; thirdly, the execution of the movement. Grasping movements are thus goal-directed movements and require sensorimotor transformation, a process by which sensory representations of the environment is transformed into muscle-control signals. Grasping is mainly driven by object characteristics, like shape and size, making the transformation of visual information crucial for hand shaping. Although the primary motor cortex detains strong spinal projections, its access to visual information is very limited. It is then unlikely that this area would be the site where visuomotor transformation for hand grasping occurs. The areas that are thought to perform this visuomotor transformation for grasping are area F5 in the frontal cortex (Gentilucci et al., 1983; Murata et al., 1997; Fogassi et al., 2001) and the anterior intraparietal area (or AIP) in the parietal cortex (Taira et al., 1990; Sakata et al., 1995). The circuit responsible for transforming visual information about the properties of objects roughly connects the primary visual system to AIP along the so-called dorsal stream of visual information processing (Goodale and Milner, 1992), and further projects to F5 with strong reciprocal connections between AIP and F5 (Luppino et al., 1999; Matelli and Luppino, 2001), and F5 further projects to the hand area of the primary motor cortex (for review see (Jeannerod et al., 1995; Castiello, 2005)).

1.8 Function of area F5

The present thesis will focus on area F5 and understanding its function. A quick review of inactivation and electrophysiological recordings studies will be given first. The remaining questions about the function and the meaning of the internal representation of information in area F5 will be highlighted. We will finally expose the way that we adopted in the present study in order to try to answer these remaining questions.

1.8.1 Dual properties

Accumulating evidences suggest that area F5 is formed of two distinct areas, one corresponding to the bank of area F5 and the other to the convexity. A type of neurons called the canonical neurons can be found in the bank and on the convexity while another type of neurons called mirror neurons can be found exclusively on the convexity. These two populations of neurons discharge when the monkey executes an action with a specific goal (grasping, tearing, manipulating, etc). The majority of the neurons encode grasping and they fire selectively for a specific type of grip, either precision grip, power grip, opposition of all fingers, etc. Some neurons discharge indifferentially to different grip types and are thought to encode the temporal structure of the action, for example the beginning of the transport phase, contact with the object, etc (Arbib, 1985; Jeannerod et al., 1995). The difference between these two populations lies in their response to different visual stimuli.

1.8.1.1 Canonical neurons

Canonical neurons discharge at the presentation of objects which characteristics, like size and shape, correlate with the grip type encoded by the neurons (Murata et al., 1997). It was suggested that these neurons extract a motor plan from the visual characteristics of the objects, thus being involved in visuomotor transformation. As the function of area F5 is commonly attributed to visuomotor transformations, these neurons were called canonical neurons. The bank area was found to be strongly interconnected with the parietal area AIP. Inactivation studies revealed similar deficit in execution of visuomotor transformation after inactivation of AIP and the bank of area F5 (Gallese et al., 1994; Fogassi et al., 2001). These studies are explained in more details in section 1.8.2.

1.8.1.2 Mirror neurons

Mirror neurons have been discovered recently in F5 and were first described by Gallese (Gallese et al., 1996). These neurons were exclusively found on the convexity of area F5. They discharge during the observation of a hand action executed by

another individual when this action corresponds to the same action for which the neuron fires when the monkey executes that action itself. The actions that are most encoded by F5 mirror neurons are grasping, placing and manipulating objects. The observation of an object only is not sufficient to trigger a response from these neurons. Additionally, full view of the action is not required as long as the goal of the action can still be understood (Umilta et al., 2001). Mirror response of F5 neurons was also reported during mouth actions and is thus not restricted to hand actions (Ferrari et al., 2003). Some mirror neurons were also found to discharge when performing an action and when hearing the related sound, such as the breaking of a peanut shell (Kohler et al., 2002). Some studies have shown that the mirror system is not restricted to premotor areas, but is also present in parietal cortex (Rozzi et al., 2008). A possible explanation of the role played by these neurons is the creation of an internal representation of the action observed for either action imitation or action understanding. It is still under debate whether monkeys can imitate actions, but this system is known to be highly evolved in humans. The activation of the mirror system was suggested to be the source of action and emotion understanding and to play an important role in social cognition in humans (Gallese et al., 2004). The mirror neurons were nevertheless not the focus of the present thesis, so the mirror properties of the recorded neurons were not tested.

1.8.2 Inactivation studies

Inactivation of brain regions is one of the techniques used to gain more insight into the function of those areas. Studies have been performed in which the primary motor cortex and the premotor areas (Matsumura et al., 1991; Fogassi et al., 2001), including both the ventral and the dorsal parts of the premotor cortex (Kurata and Hoffman, 1994), have been reversibly inactivated. Most of the inactivation studies were examined with a lever relieved task or a wrist flexion and extension task, but only few of those studies were tested with a grasping task. In the study by Matsumura (Matsumura et al., 1991), a GABA agonist (muscimol) and an antagonist (bicuculline) were used to inactivate the primary and premotor cortex and the hand grasping performances were tested during a raisin pick up task and a visual reaction time task. During the raisin pick up task, they obtained similar results using muscimol and

bicuculline, namely a deterioration of digital manipulation after injection in both primary and premotor cortex, but the deficit was stronger when inactivating the primary motor cortex as compared to the premotor cortex. For the visual reaction time task, injection of muscimol increased the reaction time while injection of bicuculline produced high variability in the reaction times. Performance deficits were again stronger after inactivation of primary motor cortex. The authors concluded that the appropriate level of GABA in primary motor cortex is necessary for the control of voluntary muscles movements, while it does not strongly affect the functioning of the premotor cortex in the simple tasks that they tested. However, the premotor cortex could play a role in more complex tasks.

More recently, in an inactivation study performed by Fogassi (Fogassi et al., 2001), monkeys had to reach and grasp objects of different size, shape and orientation. Inactivation was performed by injection of muscimol in the bank of area F5, in the convexity of area F5 and in the primary motor cortex. Following small inactivation of the bank of area F5, no misreaching was observed, but deficits in hand shaping were detected which were more pronounced for small objects than for big ones. Nevertheless, monkeys could perform the grasp, but only after contact with the object and under tactile feedback. Furthermore, the grip force was lower and monkeys experienced problems in rotating the wrist in the correct orientation. Following small inactivation of the convexity of area F5, no clear hand shaping deficits were observed. Movements were executed more slowly, but the relationship between the transport velocity and the size of the object was preserved. Following large inactivation of the convexity, a difficulty in properly orienting the wrist was observed. Finally, following injections in the hand field of the primary motor cortex, grasping of all objects was impaired. In contrast to the inactivation of the bank of area F5, appropriate shaping of the fingers was not possible even after the hand was in contact with the object. With these results, the authors demonstrated a clear distinction in the function of the bank and the convexity of area F5. The bank of area F5 shows a clear involvement in visuomotor transformation.

A similar study in which the anterior part of the lateral bank of the intraparietal sulcus (area AIP) had been reversibly inactivated was performed (Gallese et al.,

1994). Monkeys had to grasp objects of different shape, size and orientation. Deficits in preshaping the fingers during the transport phase were observed, but no misreaching. These observations are very similar to those following inactivation of F5 and support the involvement of area AIP in visual guidance of hand movements. The observation that no misreaching was observed suggests that the control of proximal and distal movement could be subserved by two separate pathways.

1.8.3 Recording studies

Initial studies performing single neuron recordings in the postarcuate sulcus of anesthetized monkeys have shown that these neurons respond to somatosensory and visual stimuli. The neurons responding to somatosensory stimuli mostly represented the hand and the mouth, pointing to a role in controlling distal movements and contradicting the commonly accepted idea that this area is exclusively responsible for axial movements (Rizzolatti et al., 1981). Recordings in awake behaving monkeys during a visually guided reaching task have shown that neurons in the postarcuate sulcus area change their firing rate even before movement execution (Godschalk et al., 1981). Some neurons increase their firing rate already at the moment when a piece of food that the monkey will have to retrieve is presented, revealing a fundamental difference with the neurons situated in the primary motor cortex who discharge with the beginning of the movement only. Further investigations have led to the important finding that F5 neurons discharge in relation to the aim of a movement such as grasping, holding and tearing (Rizzolatti et al., 1987; Rizzolatti et al., 1988). Furthermore, grasping neurons are the most common in F5 and they have been shown to fire specifically for a certain grip type (e.g. precision grip, whole hand prehension). However, the beginning of the activation with respect to the movement seems to vary from neuron to neuron.

1.8.4 Ambiguity of the visual response

The finding that F5 neurons discharge already during the visual presentation of an object appeared to be contradictory for an area which was known to have direct projections to the spinal cord and strong connections to primary motor cortex. That

area was originally mainly seen as a motor area and was though to play its main role during movement planning and movement execution (Rizzolatti et al., 1988). An important study performed by Murata aimed to investigate the nature of the response of F5 neurons during the visual presentation of an object (Murata et al., 1997). In that study, they presented six different objects to a monkey in four different conditions: grasping in light, grasping in dark, object fixation and LED fixation. They found two types of neurons, motor and visuomotor neurons, that responded selectively to one object or a subgroup of objects. The motor neurons responded only during grasping while the visuomotor neurons responded additionally during the visual presentation of objects and thus, even in the absence of a subsequent movement. They concluded from these results that the visual response of F5 neurons might represent a potential motor action. However, in that study each object was associated to a specific grip type and did not allow investigating the visual characteristics of the object independently of the grip type. In order to find an answer to the meaning of the visual response in F5, the objects presented to the monkeys should have the possibility to be grasped with different grip types, keeping an ambiguity during the observation of the object about what is the required motor behavior.

In the paradigm that we used for the present study, the monkeys had to grasp a handle in two different manners, either power or precision grip, meaning that the object characteristics remained the same for all trials while the grip type could alternate between the two grip types. The monkeys also had to perform an associative learning task, which consists of the association between a particular sensory event with a specific movement. In the present paradigm, they had to associate a light colored cue to the execution of a specific grip type. Additionally, we developed two related paradigms. In the first one, the object observation and the grip type instruction were given at the same time, while in the second paradigm we instructed the grip type in a separate time epoch than the object observation, which allowed us to analyze the response to each instruction independently.

1.8.5 Presence of orientation representation

The question whether the spatial orientation of a grasping movement is represented in area F5 was studied only very coarsely. There is one study made by Raos (Raos et al., 2006) that tested the response of F5 neurons during the presentation and grasping of a plate and a ring in a vertical and a horizontal position. As the neurons responded specifically to one object in one orientation (Figure 1.5), they proposed that the grip type and the wrist orientation are encoded in a combined fashion rather than a simple rotation of the wrist. However, the orientation representation was not thoroughly studied. One of the limitations of Raos study is that they had a bias already when they recorded the cells. Indeed, they only looked at the cells that showed grip type specificity and did not investigate the orientation alone. In turn, they did not study the cells that were only orientation specific. That bias would then lead to the recording of only the cells that combined both grip type and orientation. In the present study, we investigated the representation of orientation in a more systematic way. Instead of presenting only two orientations, we presented an object in five possible orientations (-50, -25, 0, 25, 50 degrees with zero being vertical). This procedure allowed a better comparison between different spatial orientations. Furthermore, the study of Raos reported only few neurons showing orientation representation. We explored the extent of this orientation representation in F5 in a quantitative way.

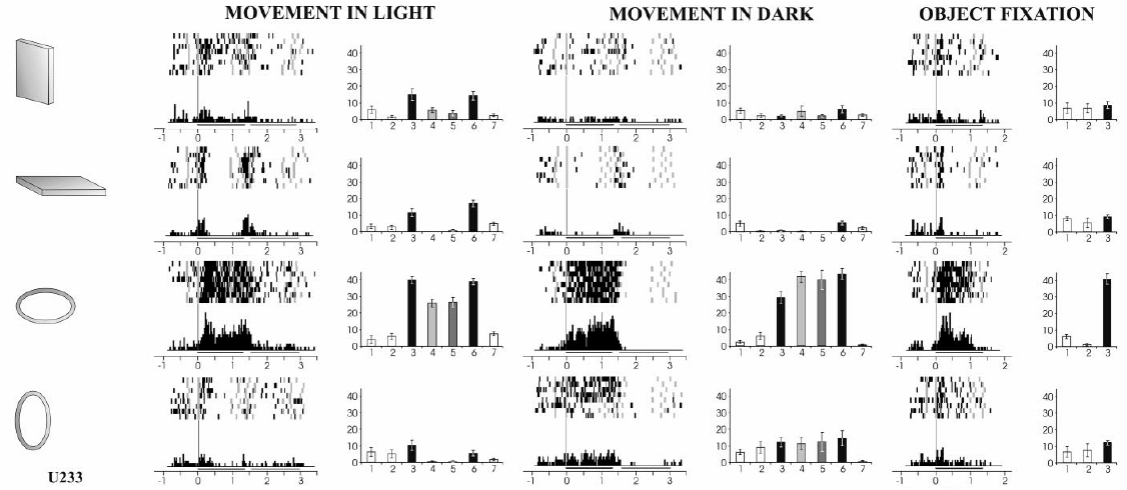

Figure 1.5 Example of an F5 visuomotor neuron tested with objects of different orientation axis. For each object, rasters of 8 trials, the resulting histogram and a bar graph with the mean firing rate and standard error during each task epoch of the movement in light, movement in dark and object fixation conditions are presented. First and second horizontal lines below each histogram indicate the object presentation and object holding periods, respectively, averaged across trials. Rasters and histograms are aligned (vertical bar) with key press (object illumination). Bar graph abscissa: task epoch for movement in light and in dark (1: spontaneous activity; 2: key press; 3: object presentation; 4: set; 5: premovement; 6: movement; 7: holding), task epoch for object fixation (1: spontaneous activity; 2: key press; 3: object presentation). This example shows specificity for the ring oriented horizontally. (Raos et al., 2006)

1.9 Hand grasping decoding

People affected by lesions of the central nervous system or neurodegenerative disorders often suffer from motor deficits and up to now there is no existing cure to mitigate the suffering of these patients. The first solution explored by researchers was to try to restore the motor functions by reconstructing the connectivity and functionality of the damaged nerve fibers. Although promising, theses attempts did not yet provide a definitive cure (Ramon-Cueto et al., 1998; Uchida et al., 2000; Bomze et al., 2001; Bunge, 2001; Schwab, 2002). An alternative solution would be to bypass the spinal cord and connect the cortical motor areas directly to artificial effectors. Most of the paralyzed patients are indeed still able to plan movements, even if unable to move their limbs. Therefore, it might be possible to record these planning signals and interpret them for the control of a prosthetic limb or other external devices. Recent developments on recording electrodes and signal-processing technologies in real time facilitated the exploration of this solution. Over the last years, several research groups have started to decode neural signals from rodents

(Chapin et al., 1999) and primates (Wessberg et al., 2000; Serruya et al., 2002; Taylor et al., 2002; Carmena et al., 2003; Musallam et al., 2004; Kemere et al., 2008) and used the signals to guide computer cursors and prosthetic devices. The most promising work achieved more recently was by the group of Donoghue who implanted an electrode array in the primary motor cortex of a human patient three years after a spinal cord injury (Hochberg et al., 2006). That patient could open simulated e-mail, operate a television and open and close a prosthetic hand. This work demonstrated that a brain-machine interface (BMI) device could dramatically improve the independence of paralyzed patients. There are still many technical problems to overcome. The need for a wireless and portable device represent some of the issues that need to be improved as well as the longevity of the electrode implants which is limited to few months due to the development of a reactive response from the brain tissues. Following electrode implantation, the brain seems to show first an acute response which consist in an anti-inflammatory response produced by damage of small capillaries. Later, the brain develops a chronic response in which the increase of microglia surrounding the electrodes leads to a neurotoxic environment. The fast advances in technologies nevertheless suggest that these problems are not impossible to solve.

One of the aims of this thesis was to explore the possibility to decode grasp movement commands from higher order cortical areas for the control of hand prosthesis. Until now, most of the attempts have been performed using the primary motor cortex, which constitutes the main cortical area projecting to the spinal cord. Therefore, the encoding is highly correlated with muscle activation. The signal derived from that area is usually translated into a movement direction that can be used for the control of a robotic arm. However, a more realistic reproduction of human movements would involve the control of a prosthetic hand that could reproduce some of the complex grasping movements of the hand. For that case, the primary motor cortex does not necessarily constitute the ideal source of signal. It might be easier to interpret signals from higher level cognitive areas to decode hand movements since these areas could encode a motor goal or a movement type instead of the details of a movement execution (e.g., muscle forces or movement trajectories) (Musallam et al., 2004). One interesting candidate area for such a high-level decoder could be area F5

as it was shown that this area encodes specific grip types. In this thesis, we also explored the possibility to use area F5 for a brain-machine interface for the control of hand prosthesis. We simulated a decoder using the neural activity recorded over multiple recording sessions and tested simple Bayesian techniques to explore the decoding performance of different grip types and spatial orientations. We also explored the number of cells necessary for good performances.

1.10 Specific aims

It has been shown that most of the neurons in area F5 discharge during hand grasping movements and the discharge is specific for certain grip types. Some neurons fire during grasping execution or slightly before. These neurons are referred to as motor neurons. Other neurons already fire during object presentation and are called visuomotor neurons. In the present study, we investigated the nature of the response of the visuomotor neurons by dissociating the object characteristics from the grip type. This experiment allowed a better understanding of the role of area F5 in visuomotor transformation. Furthermore, we investigated the orientation representation in area F5. Finally, we studied the feasibility of decoding the grasp type information and the object orientation from area F5 for the control of a prosthetic limb.

1.11 Organization of the thesis

In the following chapters, we present the experiments that we performed, the results that we obtained and a summarizing discussion. Chapter 2 presents the general methods used to perform the experiments. Chapter 3 explores the representation of different grip types and spatial orientations in area F5 during a delayed grasping task and the specific role of that area for the planning of motor behavior. Chapter 4 explores in more details the representation of grasp movement intentions in the presence of only partial informations necessary to perform the task. Chapter 5 shows a comparison of the results obtained in F5 with the results of a population of neurons recorded simultaneously in AIP during the delayed grasping task and the cue separation task. Chapter 6 presents the results of the decoding of grasping information

and the possibility to use the signals from area F5 for a brain-machine interface for the control of a prosthetic hand. Chapter 7 presents the anatomical location of the recordings and the histology observations. Finally, Chapter 8 discusses the results of the present work in relation to the other studies.

2. MATERIALS AND METHODS

This chapter describes the animal training, the imaging and surgical procedures as well as the recording procedures and the signal processing performed to obtain our results.

2.1 Experimental setup

The animals used for this experiment were two adult female rhesus macaque monkeys. All procedures were in accordance with the guidelines set by the Veterinary Office of the Canton of Zurich and the Guidelines for the care and use of mammals in neuroscience and behavioral research (National Research Council, 2003). Monkeys were trained to sit in a primate chair (Crist Instrument Co., Maryland, USA) and habituated to be moved in that chair to the experimental setup room. They learned to perform a grasping task with their left hand. They faced a handle (Figure 2.1) placed at a distance of about 30 cm. The handle could be grasped either with a power grip (opposition of fingers and palm) or a precision grip (opposition of index and thumb pads). Sensors on the handle permitted to assess the correct behavior. For the power grip, a light barrier detected that the monkeys placed their hand inside the handle and a force sensor located in the axis of the handle monitored the pulling force of the handle. For the precision grip, simultaneous pressure on force sensors placed in a hole on each side of the handle (red circle in Figure 2.1, only one sensor is visible) assessed the correct execution of the grip. The grip type was instructed by two colored LEDs that were projected on the middle of the handle through a half mirror situated between the monkeys' eyes and the target. The handle could be rotated in different positions and we tested 5 different orientations (upright, 25 and 50 degrees to the left and right). Two spotlights were positioned on each side of the target to illuminate the handle in the otherwise dark experimental room. The half mirror ensured that the object was not visible when the spotlights were off. Two handrest buttons (model EC 3016 NPAPL, Carlo Gavazzi, Italy) were situated at the level of the animals' waist and animals had to place each hand on a handrest button in order to initiate a trial. Monkeys were required to fixate a red LED also projected on the center of the handle

during the fixation, cue and planning epochs. Eye movements were measured using an optical eye tracker (RK-826PCI, ISCAN Inc, Burlington, MA, USA). In that system, the eye was illuminated with a low-level infrared light reflected from a dichroic mirror. The pupil absorbed the infrared light while the cornea reflected it back to a camera (ISCAN high-speed camera), yielding to "dark pupil" eye images. The corneal reflection corresponded to a bright reflection of the infrared light and was used to measure the pupil/corneal reflection difference for determining the horizontal and vertical eye position. A custom-written software implemented in LabView Realtime (National Instruments, Austin, TX, USA) was used for controlling the behavioral task (Figure 2.2). Behavioral signals were sent to a data storage computer (Cerebus, Cyberkinetics Neurotechnology Systems Inc., Salt Lake City, USA). Correct trials were rewarded with a small amount of fluid (ice tee without caffeine) that was delivered through a reward system (Crist Instrument Co., Maryland, USA). The mouth piece of the reward tube was adjusted in a way that monkeys could easily lick it in front of their mouth. Prior to training and recording sessions, monkeys' weights were measured and a reference weight was determined. During the training and recording sessions, monkeys were water restricted up to 24 hours prior to the experimental session. The minimal amount of fluid given daily corresponded to 20ml/kg of the weight of the monkey. The weight was measured on every working day to ensure that it would not decrease more than 10% of the reference weight. Monkeys had unrestricted access to water during the week end. A schematic of the setup is presented in Figure 2.3.

Figure 2.1 Sketch of the handle.
Two sensors in groove (red circle, only one sensor visible) detected the execution of the precision grip while a light barrier (red line) detected the insertion on the monkey hand in the handle during the execution of the power grip.

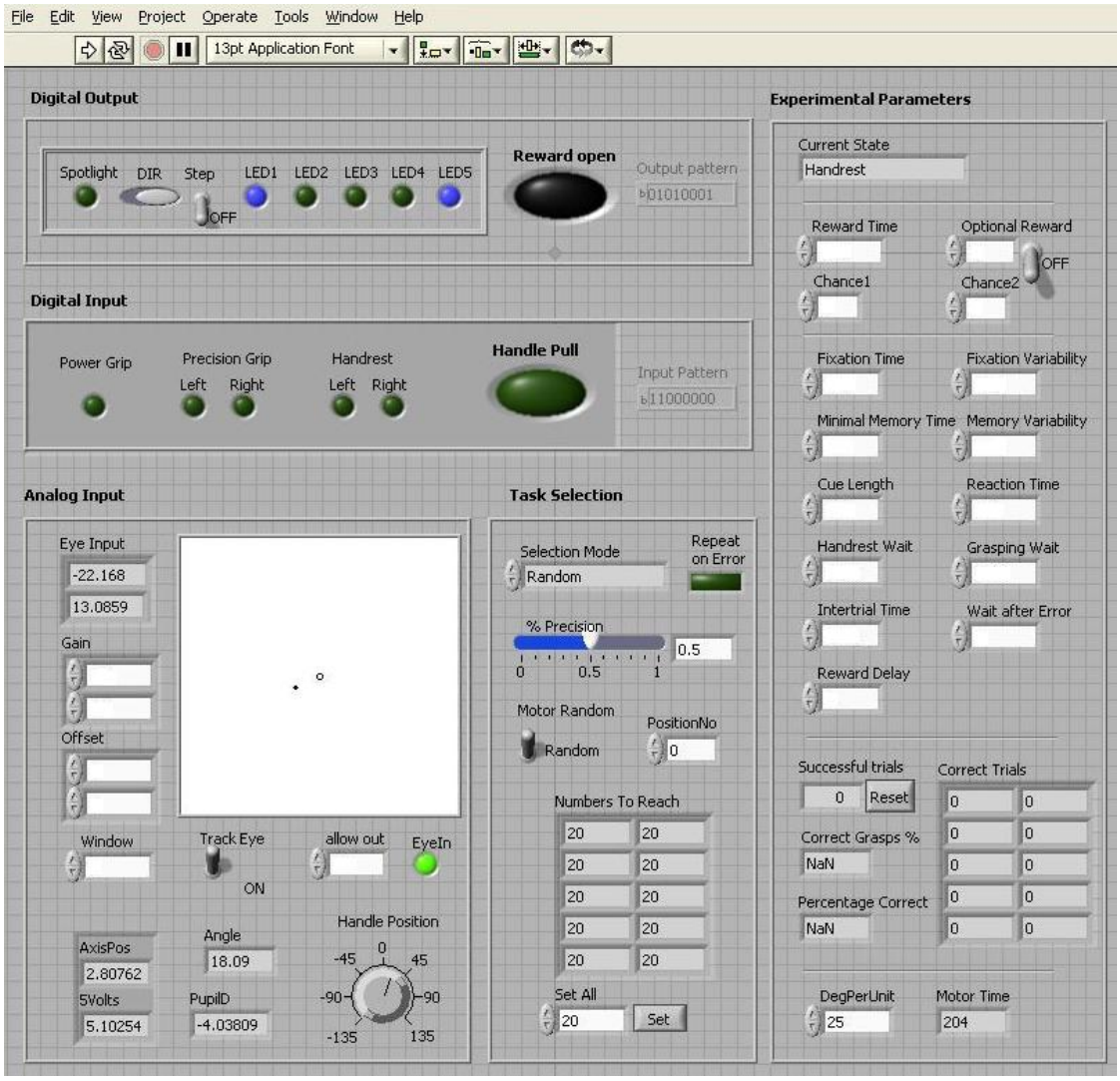

Figure 2.2 Labview software interface for the control of the task.
On the left upper corner, the light and sensors states are displayed. Below on the left, eye position was visualized and window size was determined and right to it, the task randomization parameters were controlled. The time for each epoch and other time intervals were specified on the right column.

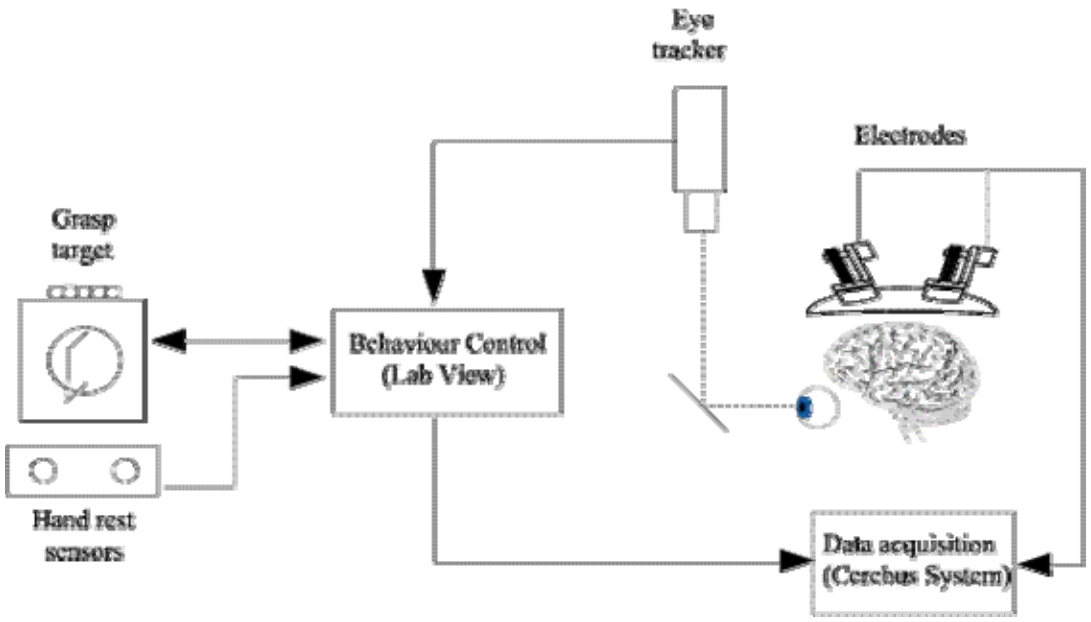

Figure 2.3 Overview of the recording setup.
The handle orientation, LEDs display, sensors monitoring and eye position were achieved by a software implemented in LabView that controlled the behavioral task. The behavioral signals and the neural recorded signals were acquired by a data acquisition system (Cerebus) and stored on a computer for offline processing.

2.2 Training in the delayed grasping task

The monkeys were first trained in a delayed grasping task where they were seated in front of a handle that could be grasped in two different ways, either with a power grip or a precision grip. The handle could be rotated in 5 possible orientations (upright, 25 and 50 degrees to the right or left). In view of the two possible grip types and the five orientations, 10 different grasping conditions were presented pseudo-randomly to the monkey. Monkeys initially sat in darkness and were required to place each hand on a handrest button (Figure 2.4A). After both handrests had been pressed, a red fixation LED was switched on. Monkeys were required to fixate it for a variable period (700-1100 ms, mean = 900 ms) and to maintain the hands at the handrests (fixation period). During that interval, the handle was positioned in one of the five possible orientations. After the fixation period, the object was illuminated to reveal its orientation and an additional LED was presented next to the fixation LED indicating, by its color, which grip type the monkey had to perform: a green LED required the execution of a power grip (Figure 2.4B) while a white LED required a precision grip (Figure 2.4C). This

period lasted 600 ms and is referred to as the cue period. The spotlights as well as the instructing LED were then switched off and only the fixation light remained on for a variable period (700-1100 ms, mean = 900 ms) during which the monkeys had to remember the grasping instructions (planning period). After the red fixation LED was switched off, the animal had to reach and grasp the object in the dark within 1.5 sec. The movement period ended when the sensors on the handle were activated. Correct trials were rewarded with juice. The trial sequence is presented in Figure 2.5. The complete training period, from the habituation in the chair until the first recording session, lasted about 8 months. The task was learned in successive steps. The power grip was taught first because of its higher simplicity. Monkeys received reward for grasping and slightly pulling the handle in a vertical position. They further learned to pull only after the go signal (extinction of the red light). The precision grip was taught afterward and each execution of a precision grip was rewarded. The two grip types were then interleaved in blocks and monkeys had to associate the colored LED to the corresponding grip type and execute the grasp when the red light and the cue were extinguished at the same time. There was initially no planning period. Afterward, monkeys were required to press the two handrest buttons between each trial to initiate the task. A planning phase was later introduced and the grip types were completely randomized. The handle was then presented in different orientations. Following the head post implantation, monkeys learned to fixate the red fixation light during the whole trial.

Figure 2.4 Initiation of a trials and execution of grasps.
A) Animal sitting in front of the grasping target and pressing the handrest sensors. B) Animal performing a power grip. C) Animal performing a precision grip.

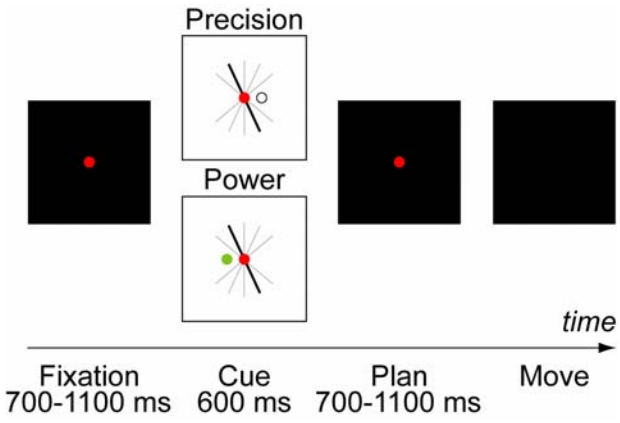

Figure 2.5 Representation of the time course of the delayed grasping task.
The task consisted of four epochs: fixation, cue, planning, and movement. The entire task was performed in the dark except for the cue period in which the handle was visible and a colored LED was shown to indicate the grip type. The lights were projected onto the middle of the handle through a half mirror.

2.3 Training in the cue separation task

The monkeys were further trained in a modified grasping task. The initial paradigm was modified to present the two different cues, one about the orientation of the object and the other about the grip type, in two separate epochs. This paradigm was therefore called the cue separation task. In one version of the tasks, the orientation was presented first (600 ms) followed by a planning phase (600-1000 ms, mean = 800 ms) and then the grip type was instructed (600 ms), also followed by a planning phase (600-1000 ms, mean = 800 ms) before giving the go signal for the execution of the movement. This task is later referred to as the OT-task (orientation first, type of grip second). In the second version of this task, the grip type was presented first followed by a planning phase and then the orientation followed by another planning phase before the movement execution. This task was referred to as the TO-task (type of grip first, orientation second). During animal testing, trials of the OT-task and the TO-task were randomly interleaved with trials of the delayed grasping task. The time course of the cue separation tasks is presented in Figure 2.6.

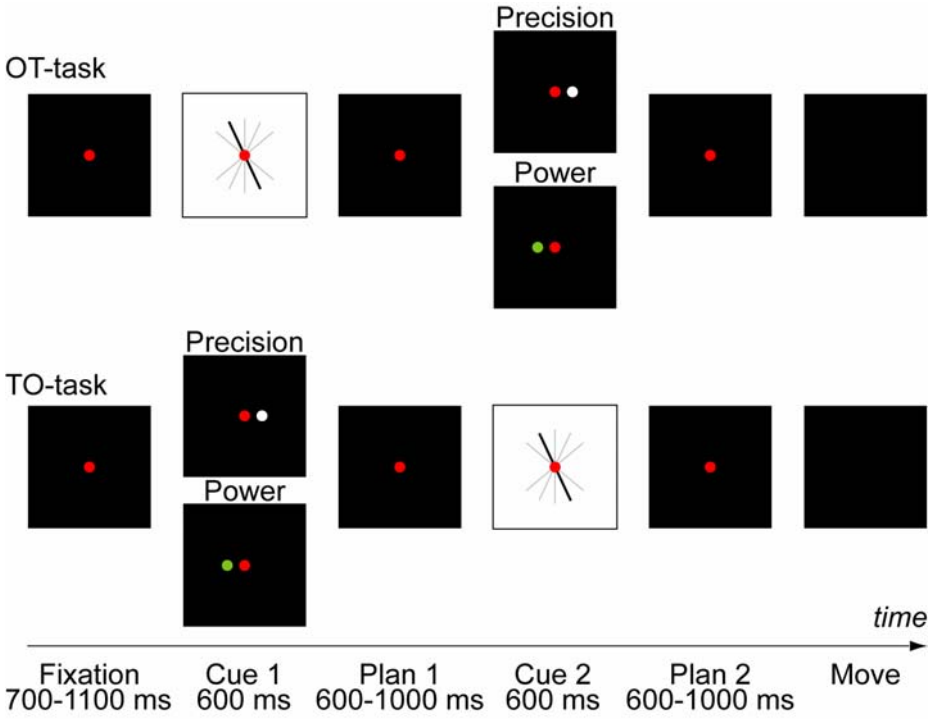

Figure 2.6 Representation of the time course of the cue separation task.
In this task, the cues indicating the grip type and the orientation were presented in two different epochs, each one followed by a planning epoch. In the OT-task presented above, the orientation was presented first followed by the type, while in the TO-task presented below, the type was presented first followed by the orientation.

2.4 Imaging and surgical procedures

Once the animals were fully trained in the task, an MRI scan was performed to locate anatomical landmarks in order to plan the location of implantation of the recording chamber. The animals were anesthetized using ketamine (10 mg/kg i.m.), xylazine (0.5 mg/kg i.m.), and atropine (0.05 mg/kg s.c.) and supplemented with O2 (1 l/min). Heart rate, O2 saturation and end-tidal CO2 level were continuously monitored while the animals were placed in the scanner (Siemens 1.5T) in a prone position. T1-weighted volumes images of the brain were obtained (voxel size 0.7 mm isometric, TR 7.6 ms, TE 3.16 ms, flip angle 12 deg, 400 ms inversion time) and stored in DICOM format. The images were realigned in stereotaxic coordinates using AFNI 3.0.

Next, a surgery was performed to implant the head post (material: titanium, cylindrical shape, diameter: 18mm) and the recording chamber (material: PEEK, oval

shape, outer dimensions: 40mmX25mm). The animals were anesthetized using ketamine (10 mg/kg i.m.) and atropine (0.05 mg/kg s.c.). They were intubated and continuously anesthetized with isoflurane (1-2%) and analgesia was done with buprenorphene (0.01 mg/kg s.c.). Pulse, blood oxygenation and body temperature were continuously monitored and kept in the desired physiological range. Animals were placed in a stereotaxic frame and the skull was exposed by an incision of the skin at midline. The head post was placed rostral at midline (inclination angle of 20 degrees towards the animal nose). Ten to fifteen titanium and ceramic bone screws (Synthes, Switzerland; Thomas Recording, Germany) were fixed in the skull to anchor the implant (Figure 2.7A). The materials for the chamber, head post and screws were chosen for their biocompatibility, their strength and their compatibility with MRI scan. One disadvantage for the use of titanium is that it can produce artifacts on MRI images (Figure 2.7B). The recording chamber was placed between stereotaxical anterior33-posterior07 with the reference being the ear canal and centered at lateral20 (following MRI guidance) over the right hemisphere. No skull trephination was performed. Head post and chamber were fixed using bone cement (Palamed, Biomet Orthopaedics, Switzerland). Anesthesia was terminated and animal woke up easily. After surgery, analgesics were given (buprenorphine 0.01 mg/kg s.c.) as well as antibiotics (synulox 0.15 ml/kg i.m., composition amoxicillin and clavulanic acid) once daily for 5 days. Animals were kept separate from the group until they were active and eating normally.

After recovery from the surgery, a second MRI scan was taken to map the brain in the coordinates of the recording chamber. The same procedure as described above was adopted. In addition, the chamber was filled with a contrast medium (Gadolinium solution diluted in saline 1:2000). The MRI images were visualized and rotated in the chamber coordinates which allowed the precise planning of the recording penetrations.

Finally, a second surgery was done to perform the craniotomy inside the recording chamber. The anesthesia protocol was the same as in the first surgery. The bone cement and the skull were removed in two locations inside the recording chamber, one on top of the intraparietal sulcus and the other on top of the inferior limb of the

arcuate sulcus. This allowed the simultaneous recording in parietal and frontal cortex. The dura was not penetrated. Post-operational precautions were the same as in the first surgery.

Following the craniotomy, the inside of the recording chamber was regularly cleaned with saline (before and after recording and otherwise three times per week). The growth of granulation tissues was controlled using 5 Fluorouracil (5 minutes three times per week) (Spinks et al., 2003). Approximately once per month, a dural scrape was performed under light anesthesia (ketamine 2.5 mg/kg i.m.), using a scoop and a hook in order to remove some excess tissue grown on the dura.

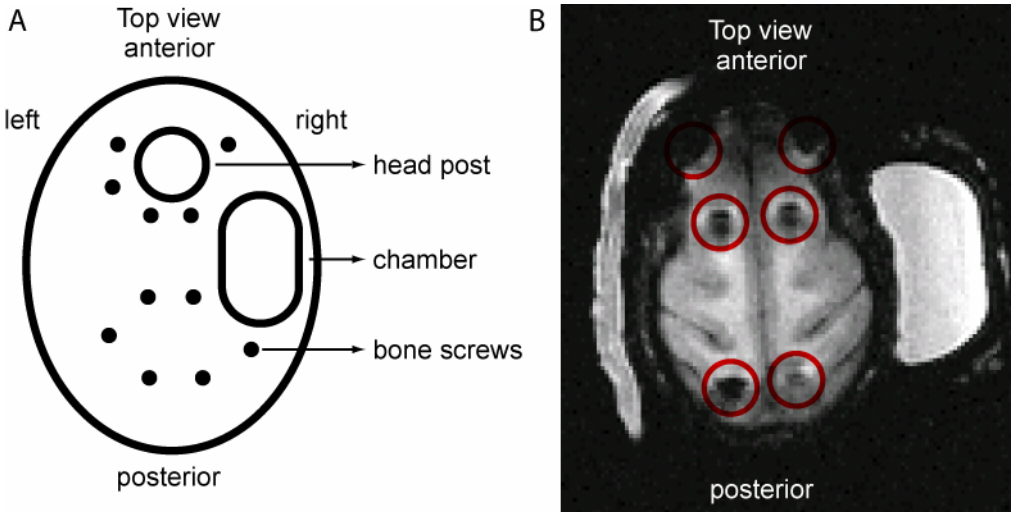

Figure 2.7 Screws map and artifacts produced in MRI image.
A) Top view of monkey's skull showing the approximate locations of the recording chamber (oval), head post (circle) and bone screws (small black dots). B) MRI image with artifacts caused by the screws (circled in red).

2.5 Neural recordings

Recordings were performed in an electrically shielded room in order to reduce the noise in the signal. For recording sessions, the head of the animals were fixed using the implanted head post. The recording chamber was opened and two 5-channel microelectrode manipulator drives (Thomas Recording, Germany) were fixed on it with a clamp and two xyz-manipulators (maximum path length: ± 10 mm in all directions, Thomas Recording, Germany) as illustrated in Figure 2.8. The

microelectrode manipulators head configuration was organized in a one linear row of five guide tubes (Figure 2.9) that served to guide the electrodes. The interelectrode spacing was 305 μm. The drives were dialed down until the blunt guide tubes touched the dura and slightly depressed it. Two chamber clamps allowing different drive configurations have been used. In one clamp configuration, the drives were parallel to each other, and consequently perpendicular to the brain surface. This configuration facilitated the calculation of the recording point but allowed a minimum distance of only 18 mm between the two recording points. In the other clamp configuration, one drive was perpendicular to the brain surface but the other one was tilted by 10 degrees. This configuration permitted reducing the minimal distance between the recording points to 7.5 mm. For the tilted configuration, the position indicated by the xyz-manipulator had to be corrected for the tilt.

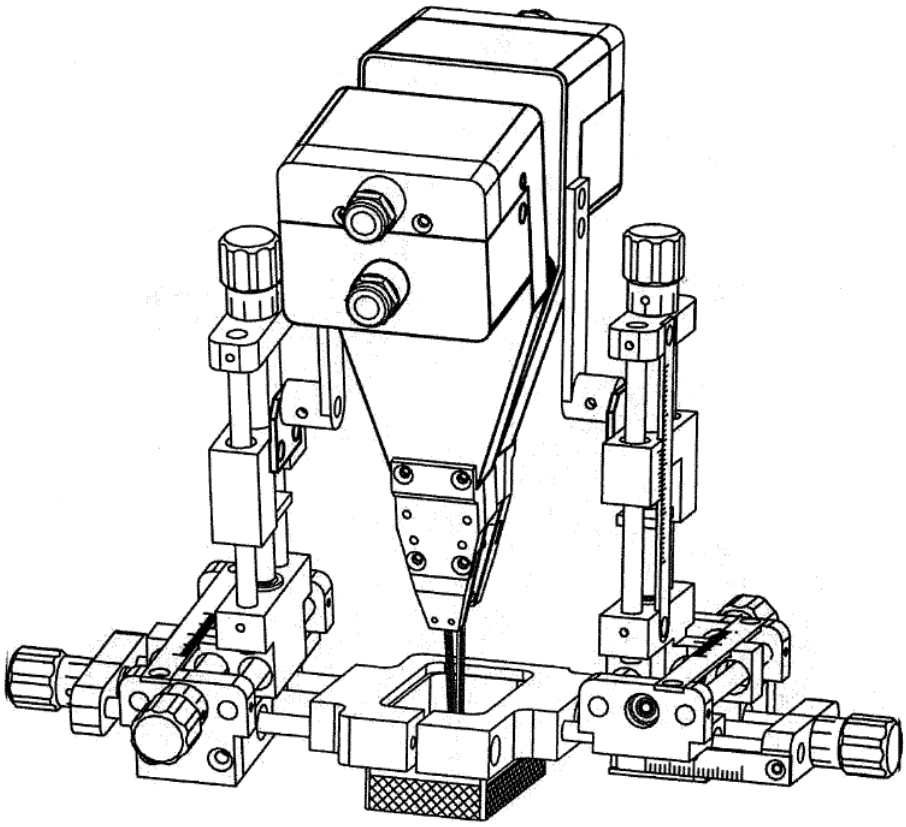

Figure 2.8 Two 5-channel microelectrode manipulators with xyz-manipulators mounted with a chamber clamp on a recording chamber.
The positions of the drives were adjusted using the xyz-manipulators and the depth of the electrodes was controlled by motors in the microelectrode drive.

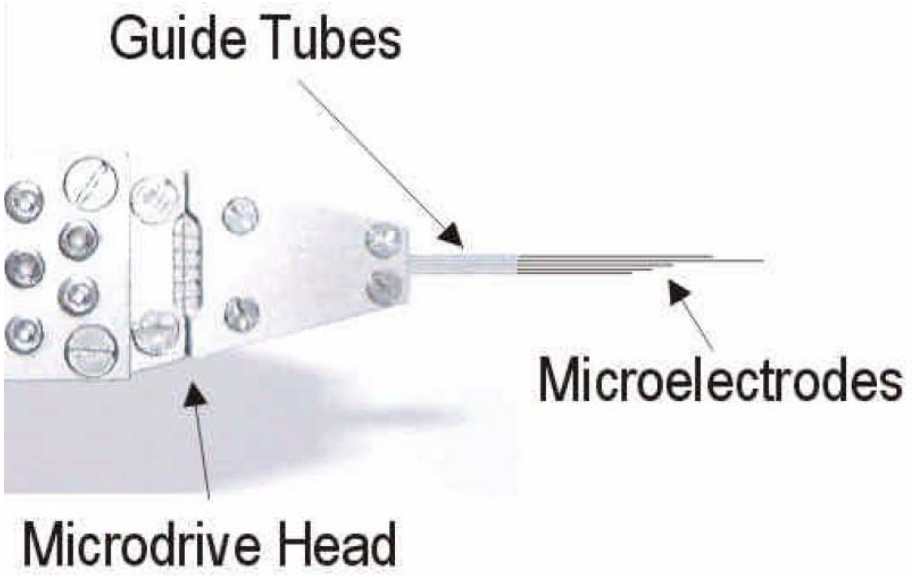

Figure 2.9 Microelectrode manipulator drives head.
Linear configuration of five guide tubes with no spacing between them, leading to 305 μm spacing between the electrodes.

Single-unit activity was recorded from area F5 in the posterior bank of the inferior limb of the arcuate sulcus using platinum/tungsten fiber-electrodes with quartz-glass coating (diameter 80 μm, impedance 1-2 MΩ measured at 1 kHz, Thomas Recording, Germany). Exploration of the area at different depths permitted assessment of the position of the arcuate sulcus. Figure 2.10A presents a coronal view of monkey J and the red line indicates the recording plane. Recording maps for each monkey are presented in Figure 2.10B-C. Signals detected by the electrodes were amplified by two stages, first by the microelectrode preamplifier (20X amplification) and second by an external amplifier (Thomas recording, 20X amplification). Then, the signal was acquired by a data acquisition system (Cerebus, Cyberkinetics Neurotechnology Systems Inc., Salt Lake City, USA) and recorded at a sample rate of 30 kS/s and saved on disk. The full bandwidth was recorded and no filtering was applied nor threshold crossing to allow all possible offline processing. During the recording sessions, an Ethernet switch allowed the Cerebus interface software to run simultaneously on two computers. Additionally, the signal could be monitored online using a software implemented with Matlab. Even though task modulation could be observed online, all neurons that could be isolated were recorded without discrimination relative to task modulation. The signal was filtered offline using a high pass filter (cutoff 400 Hz) and single units were isolated using principal component

analysis techniques (Plexon Inc, Dallas, TX, USA). This sorting technique is based on the shape of the waveforms. The parameters of the waveforms are converted into a set of vectors and this set of vectors is transformed into a lower dimension in order to maximize the distances between the different units. The interface of the Plexon program is shown in Figure 2.11.

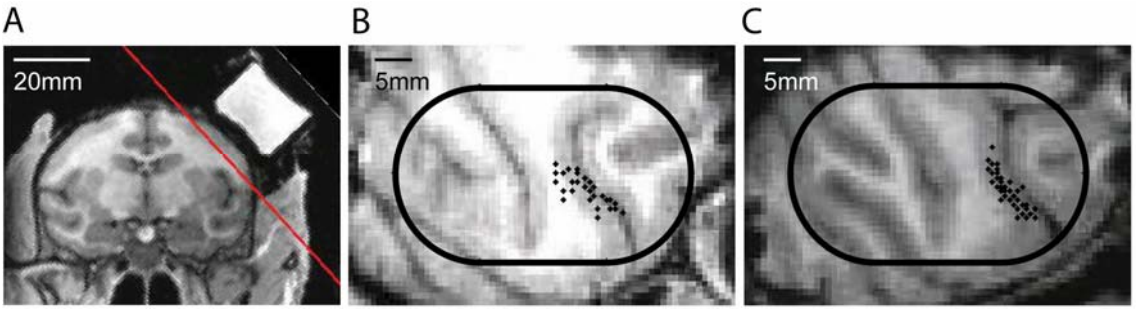

Figure 2.10 Coronal view and recording sites.
A) MRI image showing the coronal view of a macaque brain. Red line indicates the plane of the recording chamber. B) MRI image of the right hemisphere of monkey L in the plane of the recording chamber. Superimposed to the image are the recording sites in area F5 and the recording chamber which is represented by an ellipse (the chamber extend far posterior in order to reach the tip of the IPS). C) Same for monkey J.

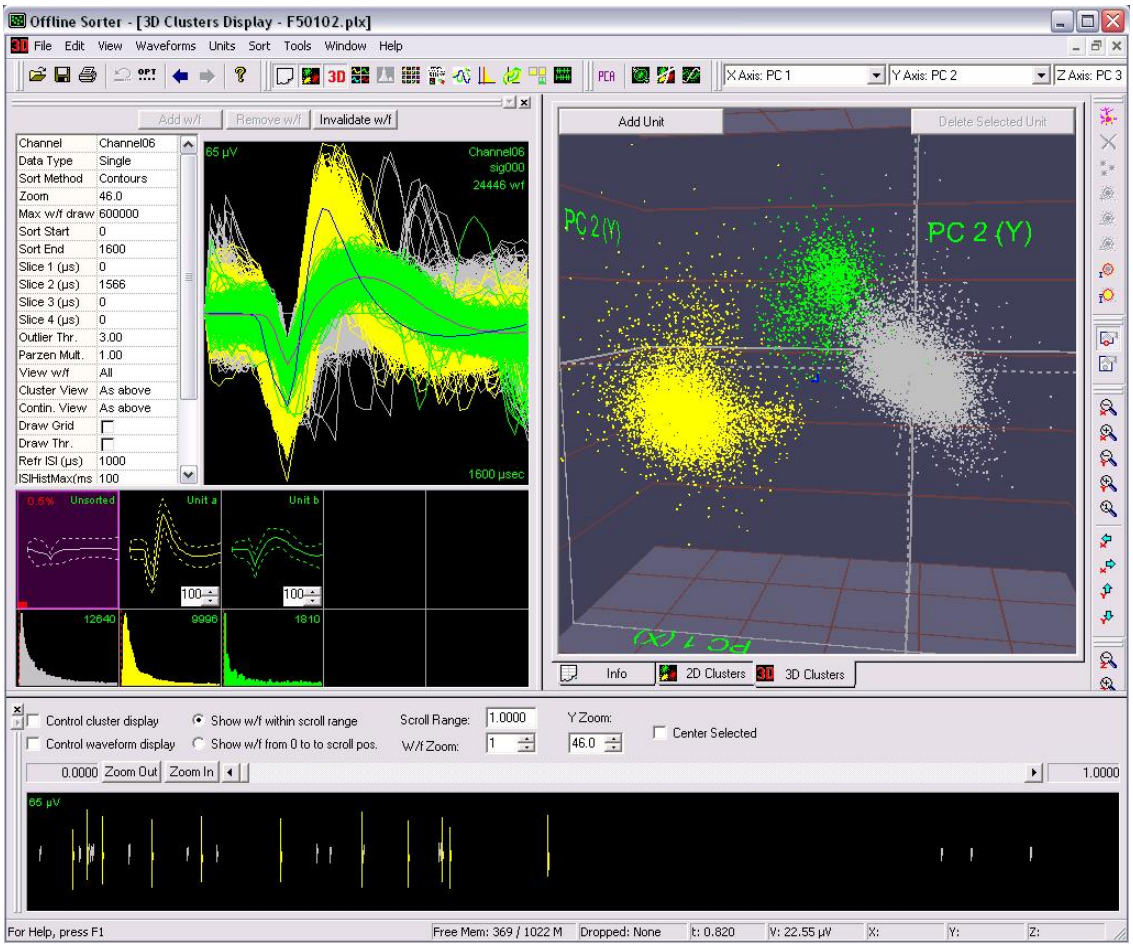

Figure 2.11 Offline spike sorter.
The waveforms of each unit are displayed in different colors (noise is white and units are in yellow and green) on the left side of the panel. A 3-dimensional representation of the principal components analysis is presented on the right side of the panel. The spikes timing of all spikes is shown in the bottom panel

3. DELAYED GRASPING TASK

In this chapter, we studied the response of F5 neurons during the grasping of an object using a delayed grasping paradigm in which the different steps required for the execution of the movement were separated into very distinctively defined periods. These different periods consisted of object observation, movement planning and movement execution (for details, see section 2.2). We investigated the specificity of the response to different grip types as well as to different spatial orientations of the object in order to find to which extend these two parameters are encoded in the F5 population. A fine time resolution analysis was performed in order to study the representation progression of grip type and orientation and the tuning onset in the neural population. The detailed encodings of each grip type and orientation were further explored. Finally, the activation and suppression of the neuronal response during the different task epochs were compared to the baseline (fixation period).

3.1 Data analysis

For the delayed grasping task, we included in our database all single-units that were stably recorded during at least 7 trials per condition (minimum of 70 trials). The peristimulus-time histograms were generated using a gaussian kernel (standard deviation = 50 ms). Because of the variable length of the different trials, the activity was aligned at different time points. The first alignment was situated at the end of the cue presentation and the second at the beginning of the movement execution (vertical dotted line in Figure 3.1), leading to a discontinuity in the plot that we fixed at 0.5 sec during the planning period. For the example neurons, results from all 10 conditions are presented. For the population histogram, only four of the 10 conditions are drawn in order to reduce the image complexity. The four conditions correspond to: 1) preferred grip type and orientation, 2) preferred grip type and non preferred orientation, 3) non preferred grip type and preferred orientation, 4) non preferred grip type and non preferred orientation. The preferred grip type was determined by pooling the five conditions of each grip type together and comparing the mean activity of the two grip types from the beginning of the cue until the end of the movement execution.

The preferred grip type was defined as the grip type with the highest mean firing rate while the non-preferred grip type corresponded to the other grip type. The preferred orientation was determined by pooling the two conditions of each orientation together and comparing the mean activity of the five orientations from the beginning of the cue until the end of the movement execution. The preferred orientation corresponded to the orientation with the highest mean firing rate. For the population histogram, the non-preferred orientation corresponded to the orientation that was 75 degrees apart from the preferred orientation. This definition was chosen in order to select the non-preferred direction not only exclusively from the two extreme orientations. For the vertical position, since there was no existing position 75 degrees apart, we selected randomly between -50 or 50 degrees.

In order to investigate the specificity for grip type and object orientation of F5 neurons, we performed a two-way ANOVA (factor grip type and orientation, p = 0.01) for each task epoch. The number of cells encoding one of the parameters in at least one epoch (cue, planning, and movement) as well as the number of cells showing grip type or orientation specificity in at least one epoch were determined from that analysis without correcting the p value due to multiple testing. This allowed keeping these results congruent with the analysis of the encoding of theses two parameters in different task epochs. A two-proportion z-test was performed in order to compare the results between two different epochs and determine whether the difference between two proportions was significant. The standard error (SE) of the sampling distribution difference between two proportions was calculated in the following way:

$$SE = \sqrt{p*(1-p)*\left[(\frac{1}{n_1})+(\frac{1}{n_2})\right]} \qquad \text{with } p = \frac{n_1 * p_1 + n_2 * p_2}{n_1 + n_2}$$

In the previous equations, n_1 corresponds to the size of sample 1, n_2 to the size of sample 2 (in our case $n_1 = n_2 = 489$ cells), p_1 is the first proportion to be compared, p_2 is the second proportion and p is the pooled sample proportion. The z-score is then calculated in the following way:

$$z = \frac{p_1 - p_2}{SE}$$

The probability of statistical difference between two proportions was then obtained from the z-score with conversion tables. A one-tailed test was used in order to attest if the encoding of grip type significantly increased and if the encoding of orientation significantly decreased.

We further investigated the grip type and orientation specificity in an unconstrained sliding window analysis. We performed a two-way ANOVA ($p = 0.01$) in bins of 200 ms shifted by 50 ms. The number of significant cells in each bin was plotted in the middle of the bin. The time of the half maximum activity during the cue period was calculated by subtracting the firing rate at the beginning of the cue period from the maximal activity during the cue and taking the middle value. The time delay between the start of grip type and orientation representation corresponds to the difference between the times of the half maxima.

The tuning onset for grip type or orientation was determined from the two-way ANOVA analysis in small window bins and was defined as the first of five consecutive significant bins. Cells were classified according to the time of their tuning onset falling in a particular task epoch (cue, planning, movement, or never) and the combined encoding of grip type and orientation was investigated for the different classes of neurons.

The preferred grip type and orientation were further analyzed during each task epoch for the whole neuronal population and for the different classes of neurons that were established based on their tuning onset. This analysis allowed us to investigate the representation differences of grip type and orientation in the early (during cue), middle (during planning) and late (during movement) tuned cells. The preferred grip type and orientation were determined as described previously but based on the mean activity in each task epoch instead of for the complete task.

In order to investigate and compare the tuning depth of the encoding of grip type and orientation, we calculated the tuning index (TI) of each cell for each parameter in each task epoch by dividing the difference between the firing rate during the preferred (f_p) and non preferred (f_n) conditions by their sum as expressed in the following equation:

$$TI = \left| \frac{f_p - f_n}{f_p + f_n} \right|$$

The tuning index could vary between 0 and 1. A value of 0 indicates that the cell fires with the same rate during the preferred and the non preferred condition while a value of 1 reflects a high activity difference. However, the tuning depth for grip type is not directly comparable with the tuning depth for orientation due to the unequal numbers of different grip types and orientations (2 possibilities for grip type and 5 possibilities for orientation). We then performed a normalization of the tuning indices. We shuffled the trials 1000 times in order to get the probability distribution of having a tuning index of 0. The significance level was chosen as the value of the last 5% and the tuning indices were divided by the significance level.

3.2 Results

3.2.1 Tuning for grip type and orientation

Single-unit activity was recorded from area F5 during the delayed grasping task. A total of 489 single-units were isolated in two animals (182 neurons from monkey L and 307 neurons from monkey J). Three typical neurons are presented in Figure 3.1A-C. The first example shows a neuron encoding the orientation and the grip type from the cue presentation until the end of the movement execution. The neuron prefers the precision grip with the handle oriented at 50 degrees to the left. The second example presents a neuron with grip type encoding only, with a preference for precision grip, from the cue presentation until the end of the movement execution. Finally, the third example presents a neuron that encodes only the grip type, with a preference for

power grip, during the movement execution. These three examples reflect important categories of F5 neurons: first, cells that show early orientation specificity, second, cells that shows early grip type specificity, and third, cells that show late grip type specificity. The Figure 3.1D presents the population histogram of the recorded population in four of the 10 conditions, i.e. with all combinations of preferred and non-preferred grip types and orientations. This graph reveals an early separation during the cue presentation between the preferred versus the non preferred orientations without distinction for the grip type. Then, after a delay of approximately 100 ms the response also differentiates for the grip type. This suggests that the orientation is first represented in the neural population rapidly after the object presentation, followed by the representation of the grip type. This issue will be further investigated later in this section. For the rest of the task, grip type and orientation were both represented in the neural population. Nevertheless, during the movement execution, we see an inversion of the light blue curve (preferred type, non preferred orientation) and the red one (non preferred type, preferred orientation), suggesting that even though the orientation encoding is preserved, the grip type is encoded with a stronger tuning depth than the orientation. This issue will be discussed in section 3.2.5. Finally, the results were essentially the same in the normalized population histogram confirming that the results were not only due to few cells with a high firing rate.

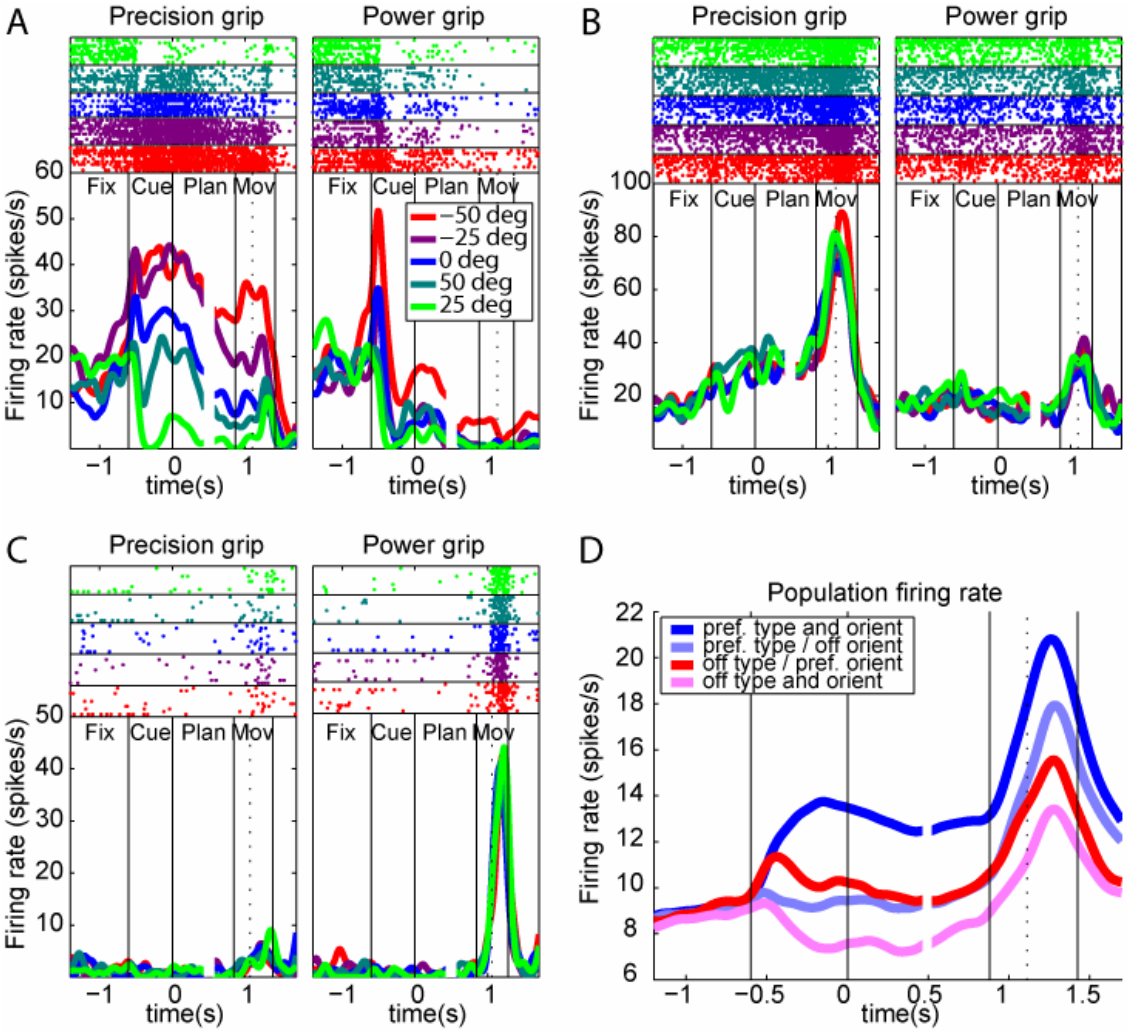

Figure 3.1 Firing rate histograms and raster plots of three example neurons and population firing rate histogram during the delayed grasping task.
Trials with precision grips are presented in the left panel, while the power grips are presented in the right panel. Each orientation is represented by a different color. Curves are aligned to the end of the cue and the beginning of the movement. The transition was fixed at 0.5sec. A) Neuron modulated by the grip type and the orientation from the cue and keeps the tuning for both parameters during the entire task. B) Neuron modulated by the grip type during the cue and keeps the tuning for grip type during the entire task. C) Neuron showing no modulation at the beginning of the trial, but then grip type tuning during the movement period. D) Population firing rate histogram for the 489 cells during the preferred and non preferred conditions (grip type and orientation).

To quantify the grip type and the orientation tuning of F5 neurons in each task epoch, we performed a two-way ANOVA ($p = 0.01$). This analysis revealed that 68% of the neurons were tuned for at least one of these two parameters in at least one epoch (cue, planning, or movement). Furthermore, we found that 59% of the cells were tuned for grip type and 38% of the cells were tuned for orientation in at least one task epoch. These two parameters did not only show a large difference of

representation, but also showed different progressions (Figure 3.2). During the cue period, the percentage of grip type tuned neurons (23%) was similar to the percentage of orientation tuned neurons (22%). This was followed by an important increase in the number of grip type specific cells (planning: 28%, movement: 39%) and a slight decrease in the number of orientation specific ones (planning: 22%, movement: 17%). A two-proportion z-test revealed that the increase in the number of grip type specific cells was not significant from cue to planning, but was significant from planning to movement. For the number of orientation specific cells, the decrease was not found significant for any period transition (cue to planning, planning to movement, cue to movement) and was thus constant across the task ($p = 0.01$). The stronger representation of grip type comparing to the representation of orientation during the movement period suggests differences in the encoding of these two parameters and possibly of the role played by area F5 in the control of theses two aspects of the movement, namely finger shaping and wrist orientation. The grip type was maximally represented during the movement execution suggesting an important involvement of area F5 in finger shaping for the execution of grasping movements, while the object orientation was represented equally during the whole task by about 20% of the cells suggesting that area F5 might play a less important role for the control of wrist orientation. The details about the encoding of each grip type and orientation will be explored later (section 3.2.3).

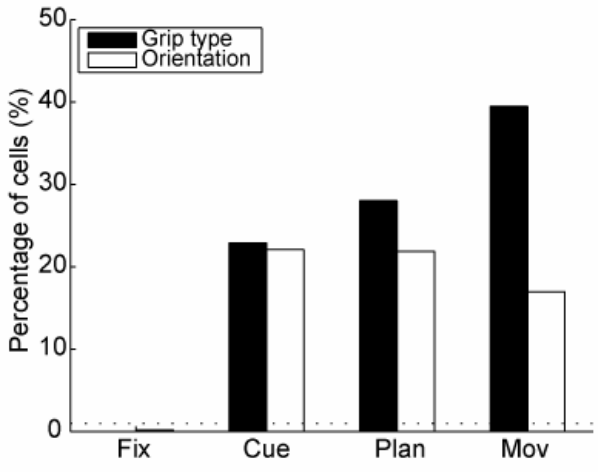

Figure 3.2 Grip type and orientation tuning in the neural population (n = 489).
Percentage of grip type specific (black) and orientation specific (white) cells (two-way ANOVA, p = 0.01) during each task epoch (fixation, cue, planning and movement). Grip type and orientation specificity during the fixation period is below chance (chance level = 1%.).

To further investigate how the grip type and the orientation tuning progressed across the different task epochs in individual neurons, we calculated the percentage of cells for each possible tuning combination for grip type and orientation during cue, planning and movement. This led to eight possible combinations. For the grip type (Table 3.1A), the most represented combination corresponded to the tuned cells during movement execution only (3rd row). Among the 23% of the cells that were grip type tuned during the cue period, 8% maintained their grip type tuning across the task, while 15% lost it in at least one of the following epochs. For the orientation (Table 3.1B), the different combinations were represented more heterogeneously. Only 6% of the cells showed orientation tuning exclusively during the movement period. Furthermore, among the 22% of cells that were orientation tuned during the cue period, 6% stayed tuned for the rest of the task, while 16% lost their tuning in at least one of the following epochs. These results showed that a population of neurons becomes grip type tuned early during the task, but most neurons loose their tuning, while another population becomes grip type tuned during movement execution. For the orientation, most of the orientation tuned cells became tuned during the cue and the majority of cells lost their tuning in the following epochs. These results show that the grip type and orientation tuning in individual cells is often lost. The tuning is nevertheless well represented in the population, as shown in Figure 3.2.

A Grip type

Cue	Plan	Move	Percent.
+	-	-	8%
-	+	-	6%
-	-	+	21%
+	+	-	5%
-	+	+	9%
+	-	+	2%
+	+	+	8%
-	-	-	41%

B Orientation

Cue	Plan	Move	Percent.
+	-	-	8%
-	+	-	8%
-	-	+	6%
+	+	-	6%
-	+	+	2%
+	-	+	2%
+	+	+	6%
-	-	-	62%

Table 3.1 Grip type and orientation tuning combinations across epochs.
A) Percentage of cells for all possible combinations for grip type tuning during cue, planning and movement. Tuning is indicated by a +, while non-tuning is indicated by a – for each epoch. B) Same for orientation tuning.

To investigate the grip type and orientation representation over time, we performed a two-way ANOVA (p = 0.01) in small time windows (window size = 200 ms, step size = 50 ms) rather than in task epochs. The orientation tuning reached its maximum during the cue period and slightly decreased during the planning period, before it peaked again at the time of the start of the movement (Figure 3.3). The grip type tuning reached a first peak during the cue, it slightly decreased during the planning period and it peaked a second time during the movement execution at the moment when the fingers entered in contact with the object. The larger number of grip type tuned cells compared to the orientation tuned cells during the movement execution suggests a more important role of F5 in controlling the shaping of the fingers compared to the wrist orientation. Furthermore, during the cue presentation, the orientation representation appeared slightly earlier than the grip type representation, as previously seen in the population firing rate histogram (Figure 3.1D). We calculated the time lag between the half maximum of the two curves during the cue period and found a delay of 93 ms between the orientation representation and the grip type representation. This delay showed that the orientation is more rapidly retrieved while the grip type needed more time in order to be retrieved from the associated light cue. These two cues could possibly be processed by two different pathways with the pathway for the grip type involving more synapses.

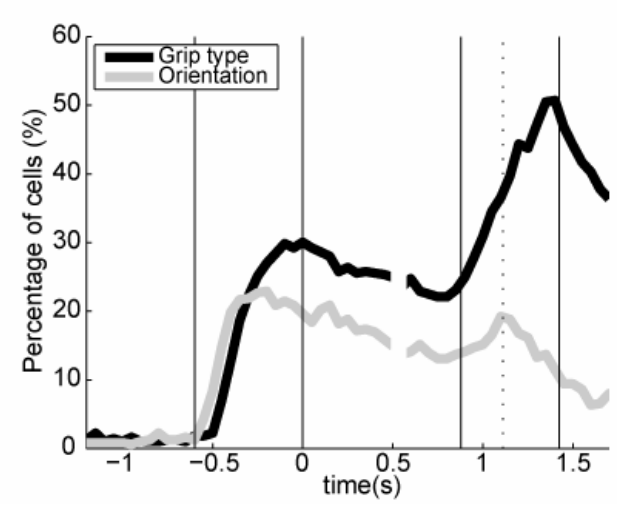

Figure 3.3 Percentage of grip type specific cells (black) and orientation specific cells (gray) determined by a two-way ANOVA in 200 ms time windows (p = 0.01, step = 50ms, centered in the middle of the 200ms window).

3.2.2 Tuning onset

To determine the tuning onset of each cell for grip type and orientation, we used the results from the two-way ANOVA in small windows and defined the tuning onset as five consecutively tuned windows. The cells were ranked according to the time of their tuning onset. The tuning for all cells of the population (489 cells) in each bin is presented in Figure 3.4A and B for grip type and orientation respectively, where black represents a significant tuning. A large percentage of cells were grip type tuned during the task with a first population becoming grip type tuned during the cue and a second population becoming tuned during the movement execution. Additionally, the grip type tuning seems to get lost by many cells after their tuning onset. A much smaller percentage of cells were orientation tuned during the task with most of the cells becoming tuned during the cue followed by a slow progression. Many cells seemed to loose their orientation tuning. Figure 3.4C and D present the number of cells in function of time of tuning onset for grip type and orientation respectively. The histogram of the grip type tuning onset clearly displays two peaks, revealing that a large number of cells becomes grip type specific during the cue period while another population of cells become grip type tuned during the movement period. For the orientation tuning onset, we found only one major peak during the cue period, revealing a large number of cells becoming orientation tuned during the cue period. Unlike the grip type tuned cells, there is no strong additional increase during the movement period. These results reveal three important classes of neurons based on their tuning onset: early grip type tuning, late grip type tuning and early orientation tuning. These three classes of neurons were well illustrated by the three example neurons in Figure 3.1A-C. The first neuron was an example of early orientation and early grip type tuning, the second neuron was an example of early grip type tuning alone and the third neuron was an example of late grip type tuning. The late grip type tuned cells (21% of the population, see Table 3.1) could correspond to the motor cells described in previous studies (Murata et al., 1997) while the early grip type tuned cells keeping their tuning during the whole task (8% of the population, see Table 3.1) could correspond to the visuomotor cells also described in the study by Murata.

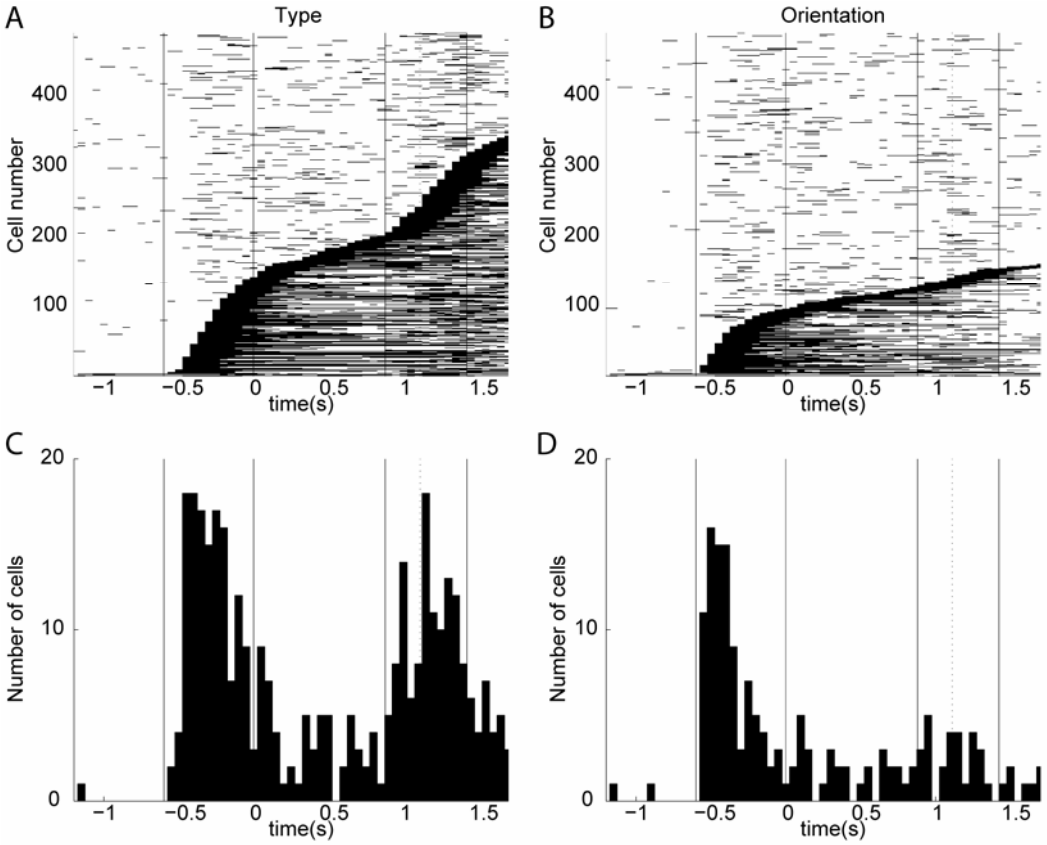

Figure 3.4 Tuning and tuning onsets for grip type and orientation.
A) Cells are ordered in function of the time when the tuning for the grip type becomes significant for 5 consecutives bins and is indicated in black (ANOVA, p = 0.01, window size = 200 ms, step = 50 ms, centered in the middle of the 200 ms bin). B) Same for orientation. C) Histogram of tuning onset for grip type and D) orientation.

As the first example neuron suggested, early grip type and early orientation tuning could be present simultaneously in the neural activity. Additionally, early grip type tuning could be found alone but few cells showed only early orientation tuning. We then further investigated the simultaneous tuning for grip type and orientation in order to determine the dependence between these two parameters. We divided the population of cells according to their tuning onset for grip type and orientation into the following categories: cue, plan, move, and never (Table 3.2). We found that most of the orientation tuned cells become tuned during the cue period (90 cells out of 149 cells). Among these early orientation tuned cells, most are also grip type tuned (79 cells out of 90 cells) and this grip type tuning usually arose during the cue period (49 cells out of 79 cells). For the grip type tuned cells, a large population became tuned during the cue period (135 cells out of 310 cells) and another one during the

movement period (113 cells out of 310 cells). About half of the grip type tuned cells during the cue period never showed orientation tuning (67 cells against 68), but when they did show orientation tuning it was also during the cue period. Most of the cells that became grip type tuned during the movement epoch were never orientation tuned (87 cells against 26). These results suggest a strong dependency of the orientation representation with the grip type, while early grip type tuned cells showed only a moderate dependency with the orientation and the late grip type tuned cells exhibited a complete independence with the orientation.

Orient / Grip type	Cue	Plan	Move	Never	Sum
Cue	49	12	7	67	135 (28%)
Plan	20	7	5	30	62 (13%)
Move	10	5	11	87	113 (23%)
Never	11	8	4	156	179 (37%)
Sum	90 (18%)	32 (7%)	27 (6%)	340 (70%)	489

Table 3.2 Interaction between grip type and orientation tuning in populations with different tuning onset.
Comparison of the grip type (rows) and orientation (columns) tuning for the neural population (n = 489) divided in subpopulations with different tuning onset (cue, planning, movement, and never).

3.2.3 Specific coding

In order to further investigate the differences in the grip type and the orientation encoding in area F5, we studied the representation of each grip type and each orientation during each task epoch for the total population (Figure 3.5A-B). For power versus precision grip, we found that the percentage of cells preferring each grip type increased across the task (precision: cue: 13%, planning: 17%, movement: 25%; power: cue: 10%, planning: 11%, movement: 14%). Using the two-proportion z-test, we found that the increase of the number of cells preferring precision grip was not significant from cue to planning, but was significant from planning to movement

while the increase of the number of cells preferring power grip was not significant for any period transition. These results show that the significant increase of grip type representation from the planning to the movement (Figure 3.2) is predominantly due to an increase of the precision grip representation. Additionally, we found that the percentage of cells preferring precision grip was higher than the percentage of cells preferring power grip in each task epoch and the ratio between the percentage of precision and power preferring cells also increased during the task (cue: 1.3, planning: 1.5, movement: 1.8). The representation of the two grip types was found significantly different during planning and movement periods. The representation difference of precision versus power grip during the movement execution could be due to the need for the brain to recruit more cells for the accurate execution of the grip type with higher complexity that might require more coordination. For the orientation, the results showed a higher representation of the extreme orientations (-50 and 50 degrees) compared to the middle orientations (-25, 0 and 25 degrees) in each task epoch. We further compared the results of the extreme orientations with the middle ones and found that the representation of the extreme stayed constant across the task while the representation of the middle orientations decreased from planning to movement (extremes orientations: cue: 13%, planning: 12%, movement: 13%; middle orientations: cue: 9%, planning: 10%, movement: 3%). The two proportion z-test showed no significant change in the representation of the extreme orientations, but the representation of the middle orientations significantly decreased from the planning to the movement period. We also observed an increase of the ratio between the extreme and the middle orientations during the movement period (cue: 1.4, planning: 1.2, movement: 4.3). The representation of the extreme orientations compared to the middle ones was found significantly different during the movement period. The higher representation of the extreme orientations could be due to the limited range of orientations that we tested (100 degrees). In that case, the orientation tuned cells preferring orientations outside the tested range (above 50 degrees or below -50 degrees from vertical) would contribute to the overrepresentation of the extreme orientations. Alternatively, the overrepresentation of the extremes could reflect a push-pull coding scheme of the wrist orientation, either clockwise or counterclockwise rotation. In sum, the unequal representations of each grip type and of each orientation seem to indicate a motor representation of the grip type and the

orientation already during the cue presentation and a strong increase of this motor representation during the movement period.

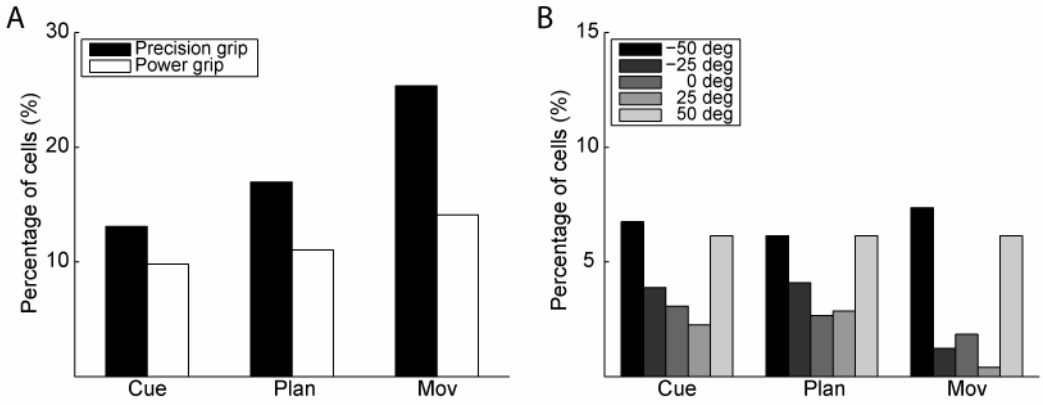

Figure 3.5 Preference for each grip type and orientation in each task epoch for all significantly tuned cells.
A) Percentage of grip type specific cells preferring precision (black) versus power grip (white) during the different task epochs (cue, planning and movement). B) Percentage of orientation specific cells preferring each of the 5 orientations (-50, -25, 0, 25, 50 degrees form the vertical) during the different task epochs (cue, planning and movement).

The preference for each grip type and orientation was further analyzed for the subpopulation of early (during cue), middle (during planning) and late (during movement) tuned cells in order to investigate the representation differences between theses populations (Figure 3.6). We found that early grip type tuned cells showed a constant representation of each grip type (precision: cue: 12%, planning: 10%, movement: 9%; power: cue: 8%, planning: 7%, movement: 5% from the total population). Nevertheless, the percentage of cells preferring precision grip was higher in each epoch and was found significantly higher during movement. The late grip type tuned cells also showed a preference for precision grip with a significantly higher representation of precision grip during the movement. These results showed that the significant increase of precision grip representation during the movement period is due to a new population of cells coding late precision grip, but also to the early tuned cells that showed a significantly higher representation of precision grip during movement, which therefore also contributed to the increasing difference between the precision and the power grip. For the early orientation tuned cells, we found that the early orientation tuned cells showed a constant representation of the extreme

orientations for each period transition, but a significant decrease of the middle orientations representation from planning to movement (extreme: cue: 10%, planning: 7%, movement: 6%; middle: cue: 6%, planning: 5%, movement: 2% from the total population). The percentage of cells preferring the extreme orientations was higher in each epoch and was found significantly higher during cue and movement. The late orientation tuned cells did not show a significantly different representation between the extremes and the middle orientations, but there were only few late orientation tuned cells. These results showed that the early orientation tuned cells contribute to the significant difference between the extreme and middle orientations.

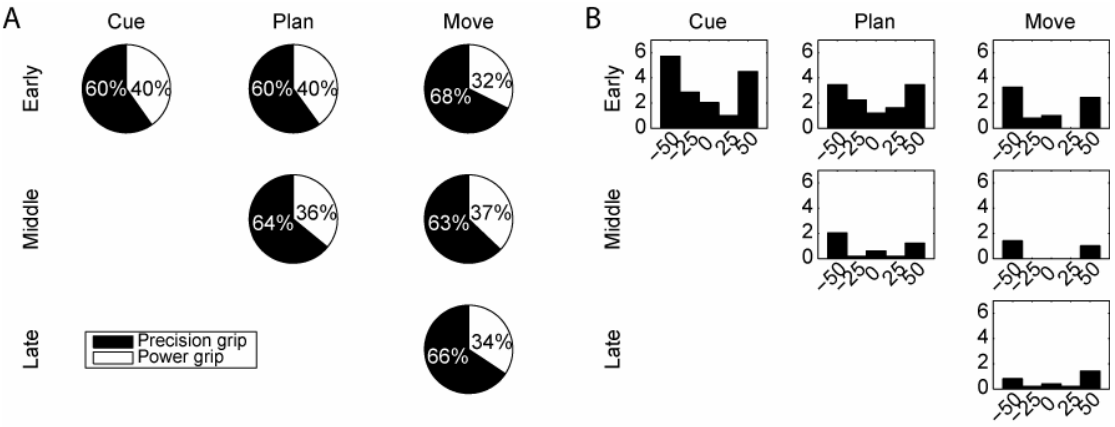

Figure 3.6 Preference for each grip type and orientation in each task epoch separately shown for early, middle and late tuned cells.
A) Percentage of grip type specific cells preferring precision (black) versus power grip (white) during the different task epochs (cue, planning, and movement) for the early, middle and late grip type encoding cells. B) Percentage of cells preferring each of the 5 orientations (-50, -25, 0, 25, 50 degrees from the vertical) during the different task epochs (cue, planning and movement) for the early, middle and late orientation encoding cells.

We further analyzed the preference consistence for grip type and orientation across the task. The preference for a certain grip type and orientation was investigated by calculating the percentage of neurons that consistently maintained the same preference, the one that changed their preference and the one that lost their tuning from cue to planning, from planning to movement and from cue to movement. For the grip type tuned cells, we found that between consecutive epochs, very few cells change their tuning preference (Figure 3.7A). Most of the cells kept the same preference and another large percentage lost its tuning. For the orientation tuned cells, we compared the results for all the cells and separately for the cells that preferred the

extreme orientations and those that preferred the middle orientations (Figure 3.7B). Most of the cells lost their tuning, but from the cells that stayed tuned, most showed no shift in their preferred orientation. When comparing the orientation tuned cells that prefer the extreme orientations with the orientation tuned cells that prefer the middle orientations, we found similar amount of cells that lost their tuning from one epoch to the next, but the extreme preferring cells tend to maintain their tuning while the middle preferring cells did not stay tuned, nor did they shift their preference to other orientations. In conclusion, most of the cells were encoding the grip type and the orientation in a consistent manner across epochs. Additionally, the loss of tuning for the middle orientations tuned cells represents an argument in favor of the push-pull mechanism of encoding wrist orientation.

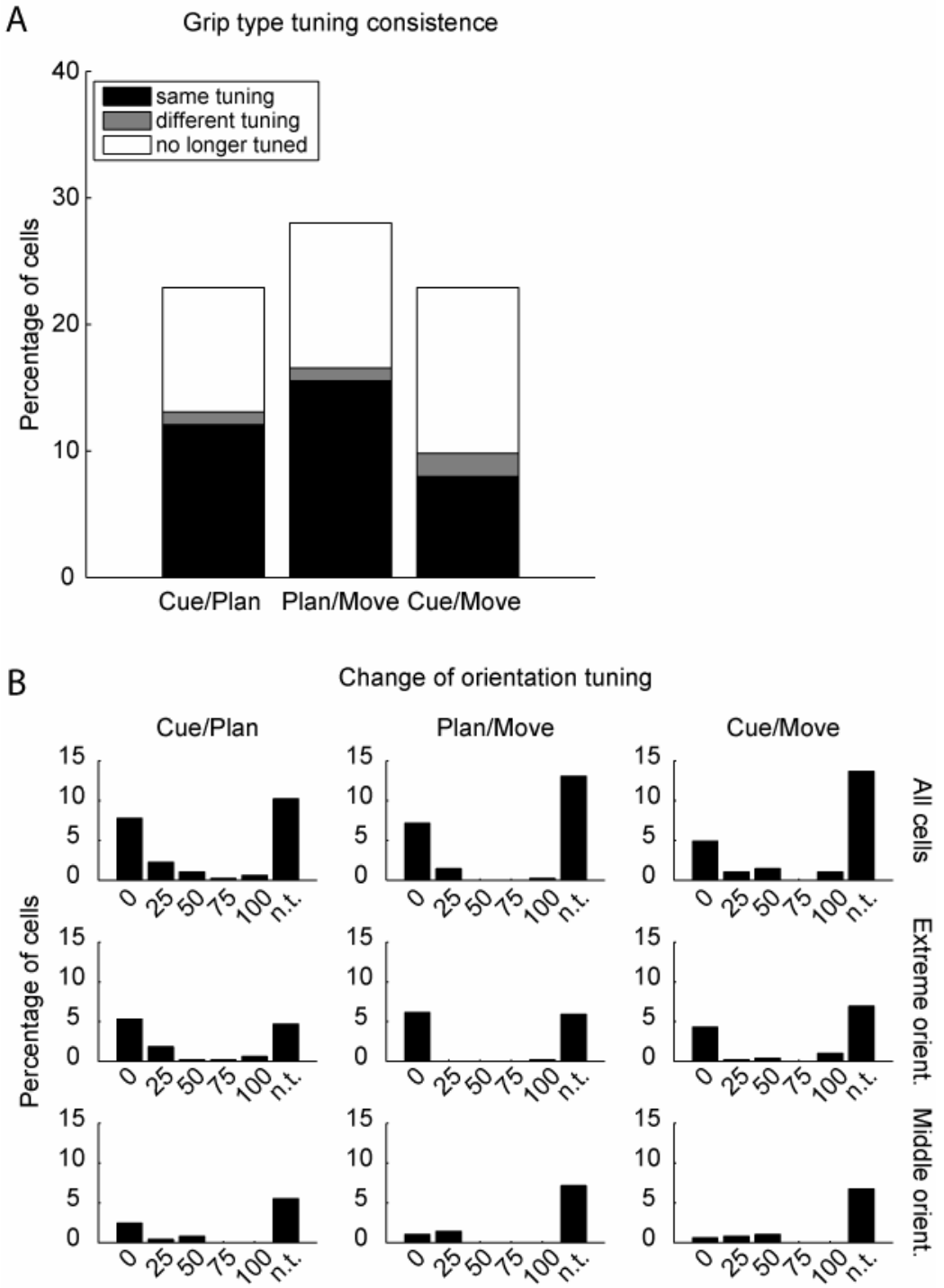

Figure 3.7 Tuning consistence between different task epochs.
A) Grip type tuning consistence. Percentage of cells that kept the same tuning (black), changed their tuning preference (gray) and lost their tuning (white) from cue to planning, from planning to movement and from cue to movement. B) Orientation tuning consistence. Percentage of cells in function of the shift in their preferred orientation from cue to planning, from planning to movement and from cue to movement for all cells, for the cells that preferred the extreme orientations and for the cells that preferred the middle orientations.

3.2.4 Visual response

Our paradigm was designed in order to present to the monkeys only one object that could be grasped with two different grip types. With that design, the visual characteristics of the object were always the same in order to answer the question whether the response of F5 neurons during the object presentation reflects the visual characteristics of the object or the upcoming movement. The preferred grip type was determined for all cells based on their firing rate from the beginning of the cue until the end of the movement. We found that 61% of the cells preferred precision grip against 39% of the cells that preferred power grip. The population firing rate of the precision and power preferred cells during the preferred versus non preferred grip type is presented in Figure 3.8. We observed that each population of cells has a similar firing rate during the fixation period. Each population then showed different activation during the cue period between the conditions with the preferred versus the non preferred grip type, with an increase of the firing rate for the preferred condition and a suppression of the activity for the non preferred condition. The comparison of the two populations in their preferred and non preferred condition revealed similar level of activation for each population during the cue and planning period. A slightly higher activity for the power preferring cells can be seen at the end of the cue period. During the movement period, the precision preferring cells fired with a higher rate during the preferred condition than the power preferring cells. The similar level of activation of both populations during the preferred grip type condition on one side and the non preferred grip type condition on the other side during the cue period suggests that the object characteristics activate each cell population similarly. Furthermore, the early separation of activity during object presentation between the preferred versus non preferred grip type conditions suggests that the visual response during cue reflects the upcoming grip type rather than the object characteristics.

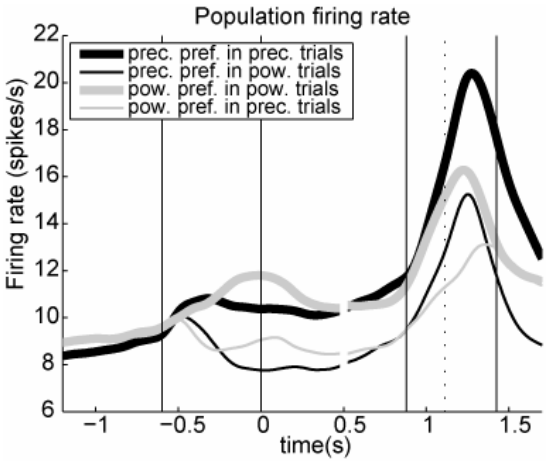

Figure 3.8 Population histograms of the cells preferring precision grip and power grip during the conditions with preferred versus non preferred grip type.
The population preferring precision grip is drawn in black while the population preferring power grip is drawn in gray. The trials with the preferred condition are drawn with a thick line while the trials with the non preferred condition are drawn with a thin line.

3.2.5 Tuning depth

The population histogram presented in Figure 3.1D suggested that the orientation is encoded with a higher activity than the grip type during the cue and first half of the planning period (red curve higher than the light blue one) while the grip type is encoded with a higher activity during the movement period (light blue curve higher than the red one). The population histogram of the preferred versus non preferred grip type is shown in Figure 3.9A and the population histogram of the preferred versus non preferred orientation is shown in Figure 3.9B. These plots also suggest that the grip type is encoded with a higher tuning depth during the movement compared to the cue and that the orientation is encoded with a higher tuning depth during the cue compared to the movement. The tuning indices for grip type and orientation during each task epochs are presented in Figure 3.10A. The median of each distribution was calculated for grip type and orientation and are presented by a black line and a gray line respectively. These results confirm a decrease of the orientation tuning depth and an increase of the grip type tuning depth (Figure 3.10B). Nevertheless, the tuning depth for grip type is not directly comparable with the tuning depth for orientation due to the unequal numbers of different grip types and orientations (2 possibilities for grip type and 5 possibilities for orientation). We then performed a normalization of the

tuning indices. We shuffled the trials 1000 times in order to get the probability distribution of having a tuning index of 0. The significance level was chosen as the value of the last 5%. The tuning indices were divided by the significance level and the results are presented for all the cells in Figure 3.11A. The median of each distribution was calculated for grip type and orientation. The results for the total population show a constant tuning depth for the orientation and an increase of the tuning depth for the grip type during the task (Figure 3.11B). Furthermore, the tuning depth for orientation was higher than for grip type during the cue, the same during planning and smaller during movement. Nevertheless, when looking only at the significantly tuned cells, we found that the tuning depth of grip type was always higher than the tuning depth for orientation. These results then suggest a stronger encoding of grip type in area F5 than orientation.

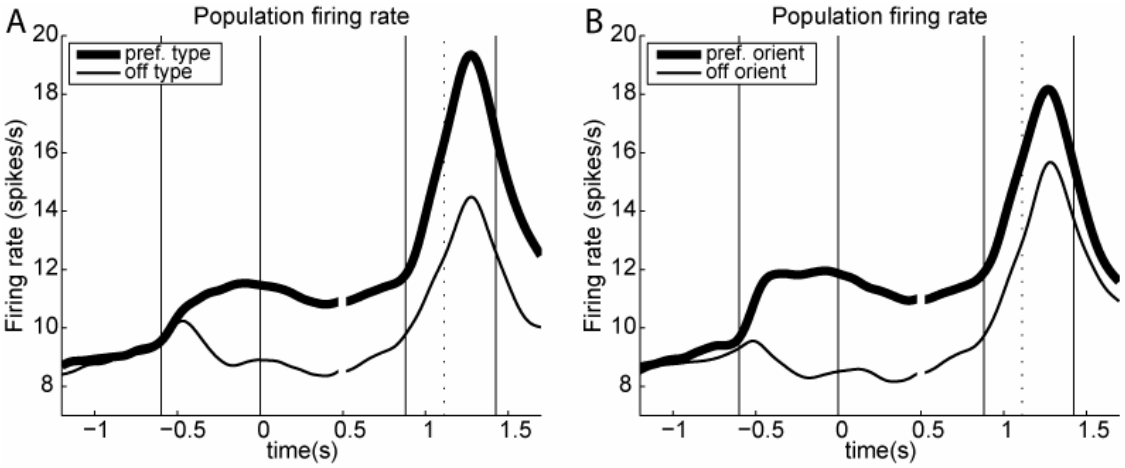

Figure 3.9 Population histograms of all cells during the condition with preferred versus non preferred grip type and orientation.
A) The preferred grip type is drawn with a thick line and the non preferred grip type with a thin line. B) The preferred orientation is drawn with a thick line and the non preferred orientation with a thin line.

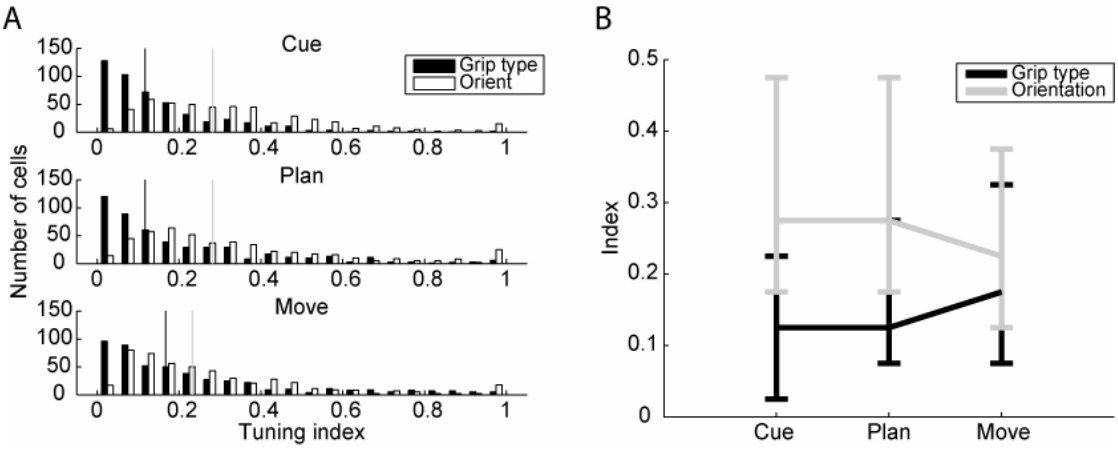

Figure 3.10 Tuning index and median for grip type and orientation.
A) Number of cells in function of the tuning index for grip type (black) and orientation (white) for all cells in the different task epochs (cue, planning, and movement). The median of the distribution for grip type is shown by a black vertical line and for orientation by a gray vertical line. B) Median, 25 percentile and 75 percentile of the distribution of the tuning index during each task epoch.

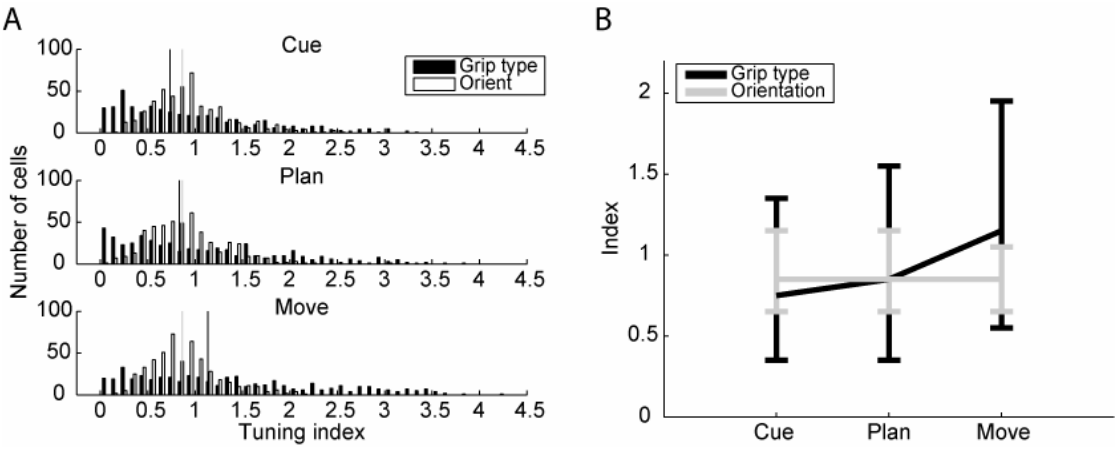

Figure 3.11 Normalized tuning index and median for grip type and orientation.
A) Number of cells in function of the normalized tuning index for grip type (black) and orientation (white) for all cells in the different task epochs (cue, planning, and movement). The median of the distribution for grip type is shown by a black vertical line and for orientation by a gray vertical line. B) Median, 25 percentile and 75 percentile of the distribution of the normalized tuning index during each task epoch.

3.2.6 Task modulation and time coding

The task modulation of the neural population was analyzed for each of the ten conditions using a one-way ANOVA ($p = 0.001$) by comparing the mean firing rate during the different epochs (cue, planning, and movement) to the mean firing rate during the baseline period (fixation). We found that 75% of the cells were task modulated in at least one condition of one epoch. The percentage of task modulated

cells in at least one of the ten conditions was 29% during the cue, 41% during the planning and 63% during the movement epoch (Figure 3.12A). The increase in the percentage of task modulated cells points to a major involvement of area F5 during the movement execution. The task modulation is the result of either an increase of the firing rate compared to baseline or a decrease. In order to determine whether the task modulated cells increased or decreased their firing rate compared to baseline in a certain epoch, we compared the mean activity of that epoch to the mean activity during fixation in each of the ten conditions and compared the results for all ten conditions. Some cells showed either increased or decreased activity in one or more conditions while others showed increase in some conditions and decrease in others. The percentage of cells showing these three behaviors are reported in Figure 3.12B. Only few cells showed both increase and decrease of activity in different conditions. We found more cells that increased their activity relative to baseline than cells decreasing their activity in all task epochs. The percentage of cells increasing their firing rate increased across the task while the percentage of cells decreasing their firing rate reached a maximum during the planning period. Inhibitory activity in area F5 has been reported previously (Romo et al., 2004; Hoshi and Tanji, 2006). The explanation proposed up to now suggest that increase and decrease of neuronal activity both reinforced the chosen motor plan and reject the other options. Most of the task modulated cells were also grip type or orientation specific. We reported previously that 68% of the cells were either grip type or orientation specific. We found that 58% of the cells were grip type or orientation specific and task modulated while 10% of the cells were neither grip type nor orientation specific and not task modulated in any condition of any epoch (with $p = 0.001$). Of the total population, 32% of the cells were not tuned for grip type or orientation. We found that 17% of the cells were neither tuned for grip type nor for orientation but were nevertheless task modulated, and 15% were not tuned for grip type or orientation and also not task modulated. The activity of the tuned cells for grip type or orientation have been explore in the previous sections. In Figure 3.13, we show the peristimulus time histogram and raster plot of two example neurons that showed no specificity for grip type or orientation, but were nevertheless task modulated. The first example neuron increased its activity during the planning period and peaked during the movement execution while the second example neuron decreased its activity during movement.

For both examples, the response was the same for all ten conditions independently of the grip type and the orientation. Such neurons could possibly be tuned for a grip type that was not tested in the current experiment or it could code the temporal structure of the action, for example the beginning of the transport phase, contact with the object, etc., as it was suggested in previous work (Arbib, 1985; Jeannerod et al., 1995).

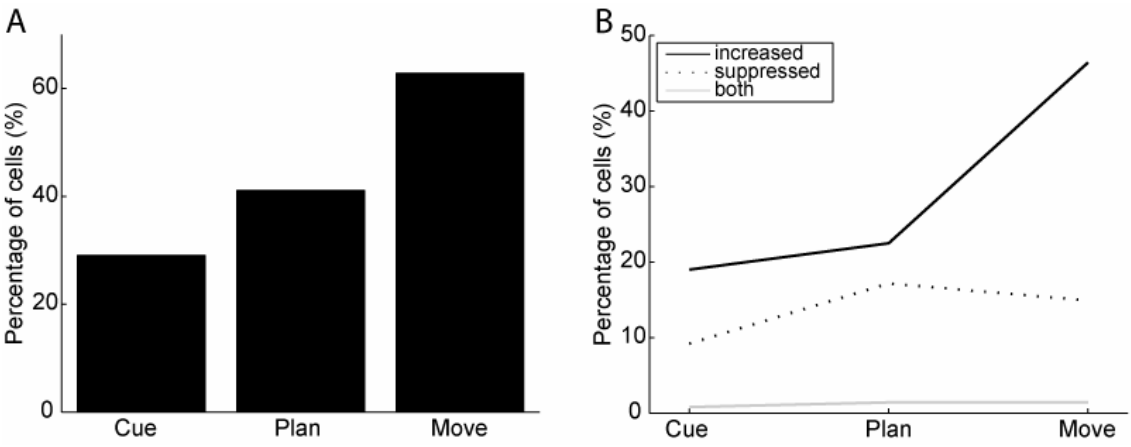

Figure 3.12 Percentage of task modulated cells during each task epoch.
A) Percentage of cells with significantly different activity during cue, planning, and movement relative to fixation. B) Percentage of task modulated cells that increased (black full line), decreased (dotted line), and both increased and decreased (gray line) their activity compared to baseline.

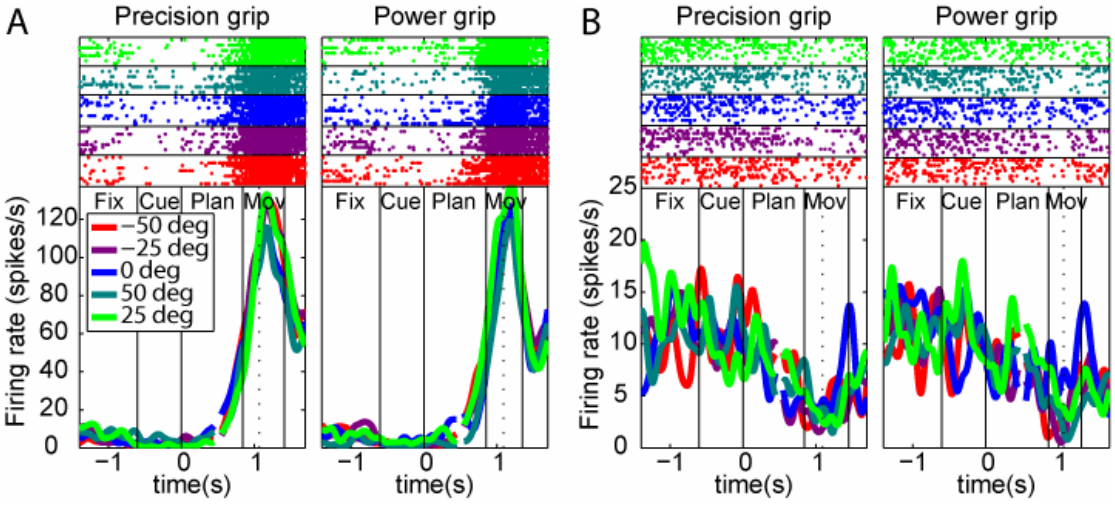

Figure 3.13 Peristimulus time histograms (PSTH) and raster plots of two task modulated cells that were unspecific for grip type and orientation.
Trials with precision grips are presented in the left panel, while the power grips are presented in the right panel. Each orientation is represented by a different color. Curves are aligned to the end of the cue and the beginning of the movement. The transition was fixed at 0.5sec. A) Neuron showing a significant increase of activity during planning and movement with no specific tuning for grip type or orientation. B) Neuron showing a significant decrease of activity during movement with no specific tuning for grip type or orientation.

Finally, we further investigated the task modulation across the different task epochs for the non tuned cells as well as the precise timing of their maximal activity. We calculated the percentage of cells for each possible task modulation combination during cue, planning and movement. The results are presented in Table 3.3. The results showed that most of the unspecific task modulated cells were modulated during the movement period and most of them showed an increase of activity. The timing at which each unspecific task modulated cells fired maximally was calculated and averaged across the 10 task conditions. Although the cells fired in a large variety of timing, most of the cells fired maximally during the movement epoch (Figure 3.14). This result suggests that the unspecific task modulated cells could code principally the precise timing of movement execution.

Cue	Plan	Move	Task mod	increase	decrease
+	-	-	4%	1%	2%
-	+	-	11%	5%	6%
-	-	+	47%	40%	7%
+	+	-	7%	2%	5%
-	+	+	20%	7%	8%
+	-	+	4%	1%	1%
+	+	+	8%	2%	4%

Table 3.3 Task modulation combinations across epochs for neither grip type nor orientation tuned cells (83 cells, 17% of total population).
Percentage of task modulated but unspecific tuned cells for all possible task modulation combinations during cue, planning and movement. Results for all type of modulation, for increase activity only and for decrease activity only are presented in three different columns. Task modulation is indicated by a +, while non modulation is indicated by a -.

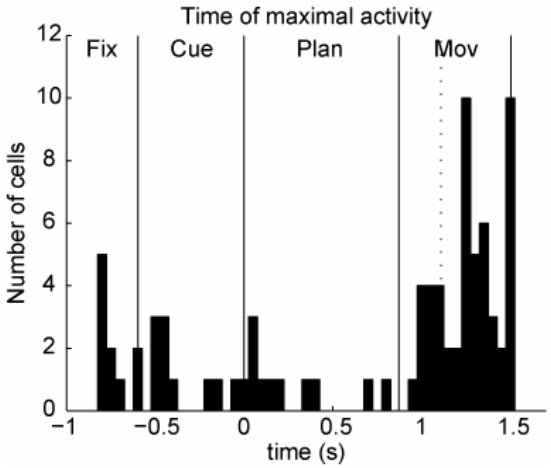

Figure 3.14 Time coding of the unspecific task modulated cells.
Number of unspecific task modulated cells in function of the time of their maximal firing activity averaged across the 10 grasp conditions.

3.3 Summary

We found that the neural activity in area F5 encodes the grip type and the hand orientation. The orientation was encoded in a constant way across the task by about 20% of the population while the grip type representation increased from about 20% during the cue to almost 40% during movement execution. These results support the previous findings that area F5 plays a significant role in planning and executing hand grasping movements. The low percentage of orientation tuned cells suggests that area F5 might only play a minor role in controlling hand orientation. Additionally, we found three classes of neurons with different tuning onset: early orientation tuning, early grip type tuning and late grip type tuning. These three classes showed differences in the simultaneous representation of grip type and orientation. Most of the early orientation tuned cells represented the grip type as well, while half of the early grip type tuned cells represented the orientation and very few late grip type tuned cells represented the orientation. Furthermore, the cells were found to keep or to loose their preference for a certain grip type or orientation, but rarely changed their preference. Finally, each specific grip type and orientation was found to be unequally represented suggesting a motor representation of grip type and orientation rather than an abstract representation.

4. CUE SEPARATION TASK

In this chapter, we studied the response of F5 neurons during the cue separation task in which the instructions about the orientation of the object and the grip type to grasp the object were given in two separate periods. Recordings were performed during the two possible combinations of the task, when the orientation was presented prior to the grip type (OT-task) and when the grip type was presented prior to the orientation (TO-task). Each instruction period was followed by a planning period and grasping execution was required after a go signal (for details, see section 2.3). This paradigm allowed investigating the response of F5 neurons to each parameter, grip type and orientation, separately. A fine time resolution analysis was performed in order to study the representation progression of grip type and orientation. Finally, the detailed encodings of each grip type and orientation were further explored.

4.1 Data analysis

For the cue separation task, we included in our database all single-units that were stably recorded during at least 5 trials per condition (10 conditions for each of the three tasks, standard delayed grasping task, OT-task, and TO-task, for a total of 150 trials). The peristimulus-time histograms were generated using a gaussian kernel (standard deviation = 50 ms). Because of the variable length of the different trials, the activity was aligned at three different time points. The first alignment was situated at the end of the first cue, the second one at the end of the second cue and the third one at the beginning of the movement execution (vertical dotted line), leading to two discontinuities in the plot during each planning period. All the analyses were performed similarly as for the delayed grasping task and had already been described in section 3.1. The analysis of the specificity for grip type and object orientation with a two-way ANOVA was performed with a p-value of $p = 0.05$ (instead of $p = 0.01$ as in Chapter 3 to accommodate for the reduced number of trials). The task epochs were also slightly different than in the delayed grasping task. The epochs for the cue separation task were the following: fixation, cue 1 (either orientation or grip type), planning 1, cue 2 (either orientation or grip type), planning 2, movement.

4.2 Results

4.2.1 Tuning for grip type and orientation

Single-unit activity was recorded from area F5 during the cue separation task. A total of 55 single-units were isolated in two animals (21 neurons from monkey L and 34 neurons from monkey J). An example neuron is presented during the standard delayed grasping task (Figure 4.1A), the OT-task (Figure 4.1B) and the TO-task (Figure 4.1C). Only four of the ten conditions are presented in order to simplify the plots. The four conditions are the preferred and non-preferred grip types and orientations in all possible combinations. During the delayed grasping task, the neuron showed early orientation tuning during the cue period and the orientation tuning was maintained for the rest of the task. The neuron was also grip type tuned during the planning and the movement period. During the OT-task, the neuron was orientation tuned from the first cue period when the object was presented and before the grip type was instructed. The orientation tuning was maintained until the end of the movement period. The neuron became first grip type tuned during the second planning period and stayed grip type tuned during the movement period. In the TO-task, the neuron showed no grip type tuning following the first cue period when the grip type was instructed. It was only during the second planning period, and thus after the object was illuminated, that the neuron became grip type tuned and remained tuned until the end of the task. The neuron became orientation tuned during the object presentation in the second cue period. This neuron represents an example of orientation representation independently of the grip type and with no grip type representation without visualization of the object. A second example neuron is presented in Figure 4.2. This neuron was grip type tuned during the movement period only and showed no representation of the object orientation.

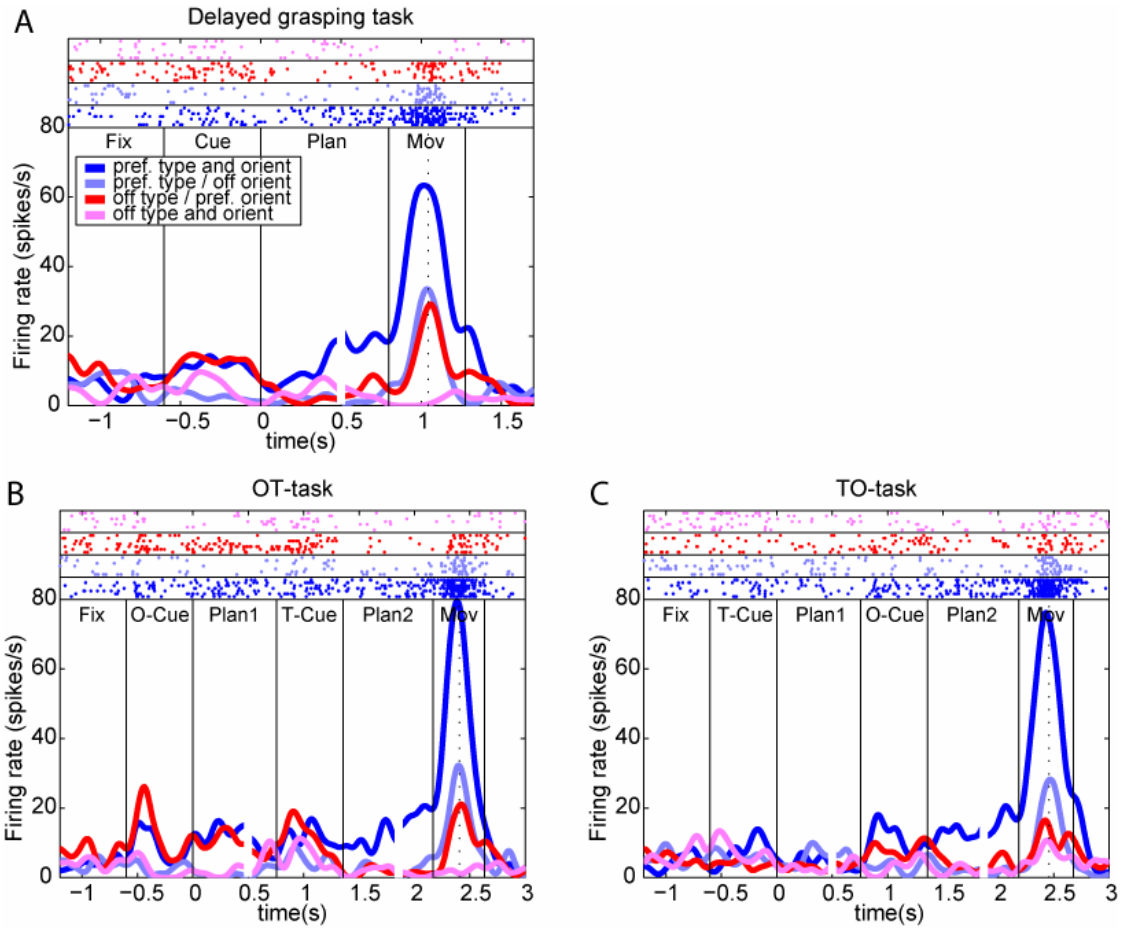

Figure 4.1 Firing rate histograms and raster plots of one example neuron during the delayed grasping task and both cue separation tasks.
In each panel, four conditions are presented with all combinations of the preferred and the non preferred grip type and orientation. Curves are aligned at the end of each cue and at the beginning of the movement execution (vertical dotted line). A) During the delayed grasping task, the neuron was modulated by the object orientation during the cue period and was later modulated by the grip type during the planning and the movement period. B) In the OT-task, this neuron encoded orientation after the presentation of the object and represented the grip type from the second planning epoch onward. C) When the grip type was presented first, the neuron was not encoding the grip type alone, but showed grip type and orientation tuning only after the object had been presented.

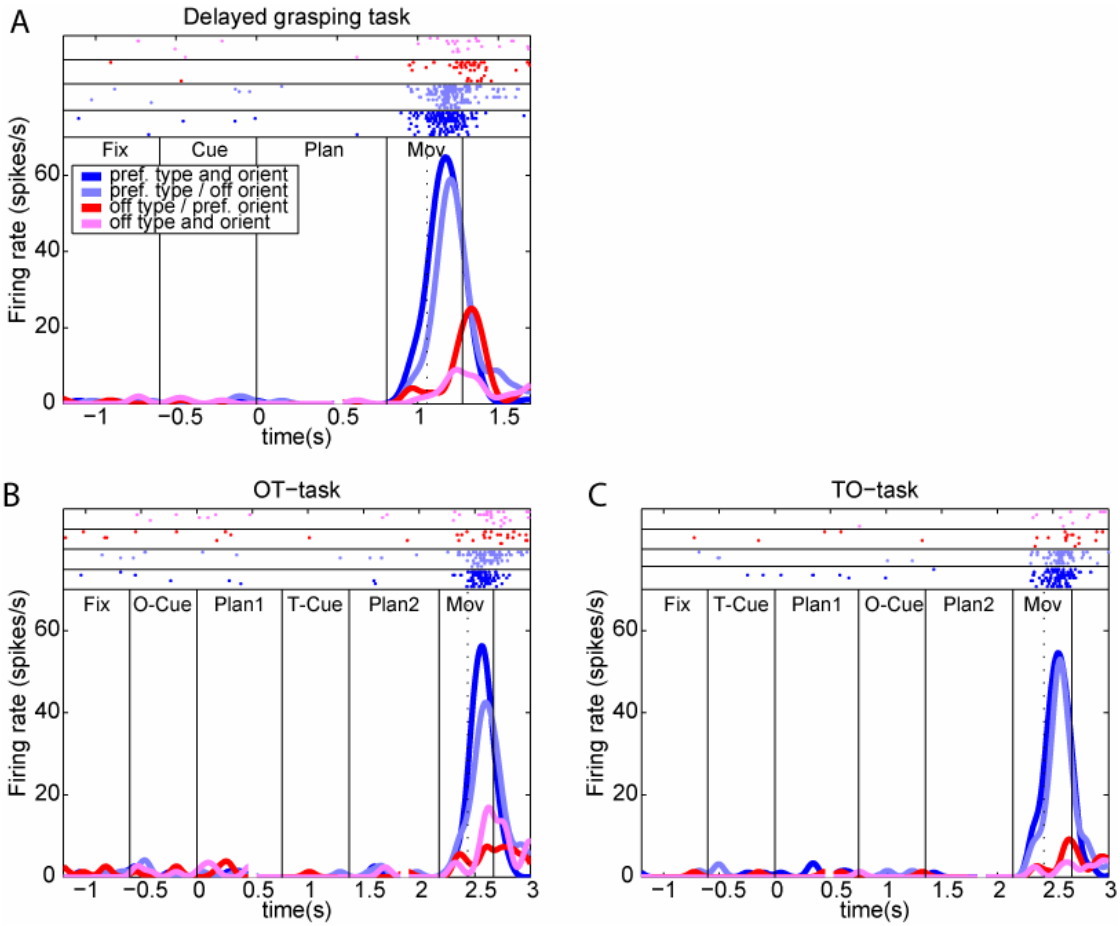

Figure 4.2 Firing rate histograms and raster plots of a second example neuron during the delayed grasping task and both cue separation tasks.
In each panel, four conditions are presented with all combinations of the preferred and the non preferred grip type and orientation. Curves are aligned at the end of each cue and at the beginning of the movement execution (vertical dotted line). A), B) and C) During all tasks, the neuron was modulated by the grip type during the movement period.

The population histograms of the 55 recorded cells are presented in four of the ten conditions (Figure 4.3). The population histogram during the delayed grasping task (Figure 4.3A) was consistent with the results of the total population of 489 cells (Figure 3.1D). It shows an initial increase of the two curves with the preferred orientation independently of the grip type and is followed by an increase of the condition with the preferred grip type after approximately 200 ms. These results allowed us to consider this relatively small sample as being representative of the total population. The population histogram during the OT-task revealed a separation of the activity during the first cue presentation between the preferred versus the non preferred orientations independent of the grip type. After the second cue presentation,

the response became different for the two grip types (Figure 4.3B). The population histogram during the TO-task revealed no separation during the first cue presentation between the preferred versus the non preferred grip type. After the second cue presentation, the response represented both the orientation and the grip type (Figure 4.3C).

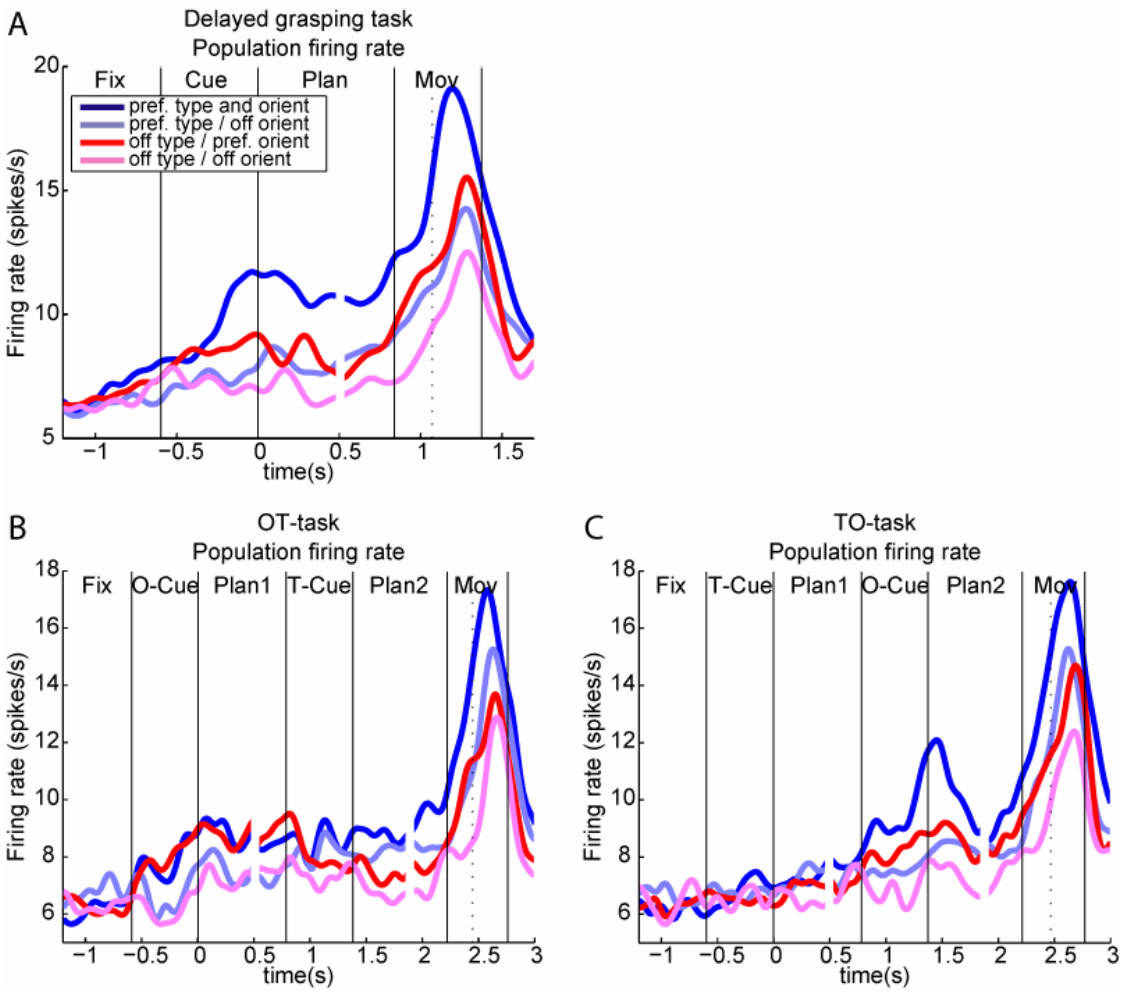

Figure 4.3 Population firing rate histogram during the delayed grasping task and the cue separation task (55 cells).
In each panel, four conditions are presented with all combinations of the preferred and the non preferred grip type and orientation. Curves are aligned at the end of each cue and at the beginning of the movement execution (vertical dotted line). A) Population firing rate histogram during the delayed grasping task. B) Population firing rate histogram during the OT-task. C) Population firing rate histogram during the TO-task.

To quantify the grip type and the orientation tuning of F5 neurons in each task epoch of the delayed grasping task and the cue separation task, we performed a two-way ANOVA ($p = 0.05$). The results of this analysis showed an increase of the number of

grip type tuned cells (cue: 18%, planning: 33%, movement: 44%) and a constant number of orientation tuned cells (cue: 24%, planning: 25%, movement: 22%) during the course of the delayed grasping task (Figure 4.4A). The two-proportion z-test revealed that the increase in the percentage of grip type tuned cells was not significant from one epoch to the following one, but was significant between the cue and movement period. For the orientation, no significant difference in the tuning was found between the different epochs. These results confirmed again that this sample was representative for the entire population (Figure 3.2). For the OT-task, we found orientation tuning during the first cue presentation and the following planning period, followed by a significant decrease in the representation of orientation during the second cue presentation. Grip type tuning was found during the second cue presentation and the number of cells showing grip type tuning increased until movement execution (Figure 4.4B). Theses results suggest that the orientation representation can be encoded without the grip type information being known. However, our results from the previous chapter have shown that most of the early orientation tuned cells also encode the grip type in combination. In the present task, we then verified if the early orientation encoding cells show later grip type encoding. We found that 31% of the cells where orientation tuned either during the first cue or the first planning period. From those cells, 59% showed grip type tuning during the second cue or the second planning period. This result shows that most of the early orientation encoding cells encode the grip type as well, but can nevertheless encode the orientation information alone. Furthermore, our results suggest that the instruction of grip type affects the representation of orientation. For the TO-task, there was only a moderate representation of the grip type during the presentation of the first cue. The two-proportion z-test revealed no significant increase in the representation of grip type during the first cue compared to the fixation period. The grip type representation significantly increased during the second cue. The orientation representation also appeared during the second cue presentation and stayed constant until movement execution (Figure 4.4C). We found that 35% of the cells where grip type tuned either during the second cue or the second planning period. From those cells, only 42% showed orientation tuning during the second cue or the second planning period as well. From this, we conclude that the grip type representation during the second cue was rather due to the visualization of the object and not to the instruction of the

orientation itself. This suggests that the cells in F5 need object information in order to have a full representation of the grip type.

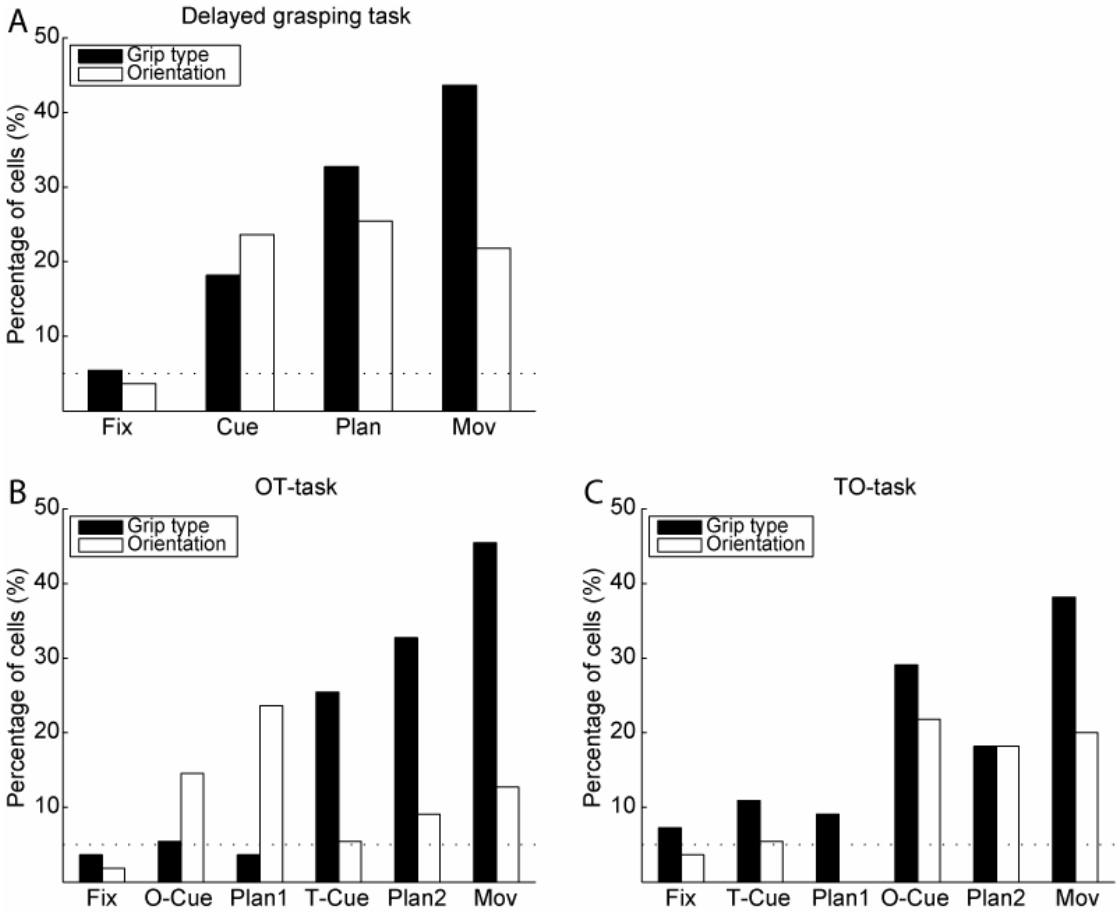

Figure 4.4 Grip type and orientation tuning during each task epoch during the delayed grasping task and the cue separation task (55 cells).
Percentage of cells that are grip type specific (black) and orientation specific (white) (two-way ANOVA, p = 0.05) during each task epoch. A) Results for the delayed grasping task. B) Same graph for the OT-task where the object orientation was presented first followed by the grip type. C) Same graph for the TO-task where the grip type was presented first followed by the object orientation.

To investigate the grip type and orientation representation over time, we performed a two-way ANOVA (p = 0.05) in small time windows (window size = 200 ms, step size = 50 ms) (Figure 4.5). During the OT-task, the number of orientation tuned cells increased during the first cue period and stayed constant during the following planning period (Figure 4.5A). The number of orientation tuned cells then decreased during the presentation of the second cue and increased again slowly until movement execution. For grip type, the number of tuned cells stayed around chance level during the first cue (orientation presentation) and the first planning period. It then increased

during the second cue (grip type presentation) and stayed at the same level during the following planning period. It finally increased again during the movement execution. In the TO-task, few cells became grip type tuned during the first cue (grip type presentation) and the following planning period (Figure 4.5B). This number increased during the second cue (orientation presentation), was maintained during the second planning period and further increased during movement execution. For orientation, the percentage of tuned cells was around chance level during the first cue and planning. It increased during the second cue and stayed constant for the rest of the task. The higher number of grip type tuned cells compared to the orientation tuned cells during the movement execution again suggests a more prominent role of F5 in controlling the shaping of the fingers compared to the wrist orientation.

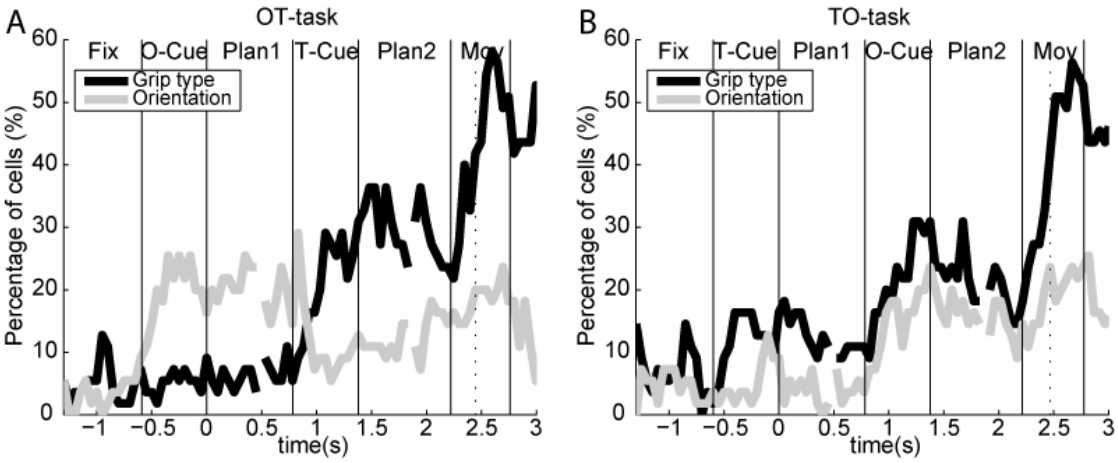

Figure 4.5 Percentage of grip type specific cells (black) and orientation specific cells (gray) determined by a two-way ANOVA in 200 ms time windows (p = 0.05, step = 50ms, centered in the middle of the 200ms window).
A) Results for the OT-task. B) Same graph for the TO-task.

4.2.2 Specific coding

In order to further investigate the differences in the grip type and the orientation encoding in area F5, we studied the representation of each particular grip type (Figure 4.6) and orientation during each task epoch (Figure 4.7). For power versus precision grip, our subset of neurons showed in the delayed grasping task similar results as for the whole population (Figure 3.5A). The precision grip representation increased during the task (cue: 5%, planning: 18%, movement: 29%) (Figure 4.6A). This

increase was not significant from one epoch to the following, but only between the cue and movement (one tail two-proportion z-test, p = 0.05). The representation of power grip was constant across the task (cue: 13%, planning: 15%, movement: 15%). Furthermore, we observed a higher representation of precision grip than power grip during planning and movement, but this difference was not significant (two tailed two-proportion z-test, p = 0.05). For the OT-task and the TO-task (Figure 4.6B-C), we also observed that more cells were encoding the precision grip compared to the power grip with the exception of the second planning period in the TO-task where the percentage of precision tuned cells was low. The difference between the precision and power representation was nevertheless not found significant. This result might be affected by the small number of cells recorded in that paradigm.

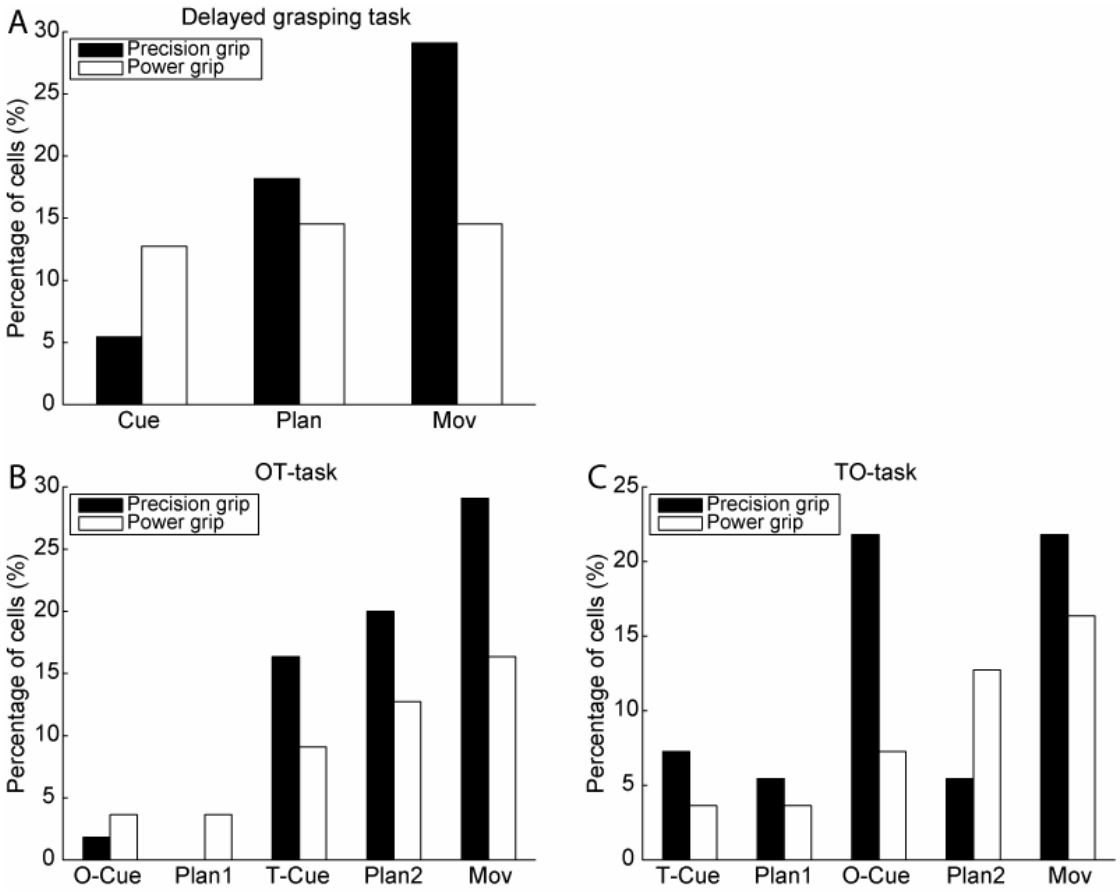

Figure 4.6 Preference for precision versus power grip in the cue separation task (n = 55).
A) Percentage of grip type specific cells preferring precision (black) versus power grip (white) during the different task epochs of the delayed grasping task. B) and C) Same percentages for the epochs of the OT-task and the TO-task respectively.

For the representation of each particular orientation, the results showed a higher representation of one of the extreme orientations (50 degrees to the right) in all task epochs of the delayed grasping task (Figure 4.7A). This result differs from the result of the total population where we found that both extreme orientations were more represented as the middle orientations (Figure 3.5B). When looking at the results for the individual monkeys, we found that this bias was present only in monkey J, the monkey that contributed the most to the subpopulation studied here (21 neurons from monkey L and 34 neurons from monkey J). For the OT-task and the TO-task (Figure 4.7B-C), we also observed that more cells were encoding the extreme orientation 50 degrees to the right. This bias was again found only in monkey J. These results might be accounted by the small number of neurons recorded in that task and the relatively high number of orientations studied (5 orientations).

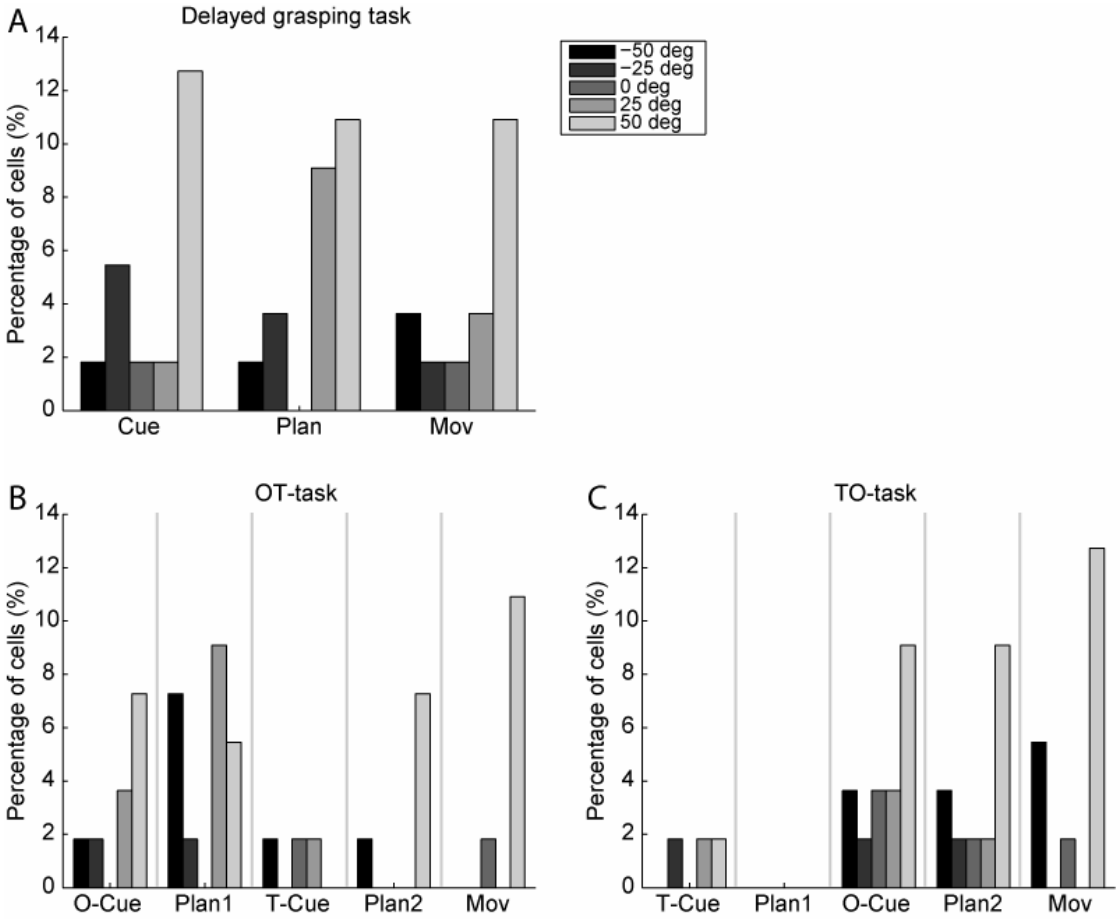

Figure 4.7 Preference for each orientation in each task epoch (n = 55).
A) Percentage of orientation specific cells preferring each of the 5 orientations (-50, -25, 0, 25, 50 degrees form the vertical) during the different task epochs (cue, planning and movement) of the delayed grasping task. B) Same graph for the OT-task. C) Same graph for the TO-task.

4.2.3 Tuning depth

The depth of encoding of the grip type and orientation was analyzed by calculating a tuning index (see Method). During the OT-task (Figure 4.8A-B), we found a higher tuning depth for orientation than for grip type during the first cue presentation as expected. It was followed by a decrease of the orientation tuning depth and an increase of the grip type tuning depth during the second cue period. During movement execution, the grip type tuning depth further increased and was higher than the orientation tuning depth. During the TO-task (Figure 4.8C-D), we found a very low tuning depth for grip type during the first cue presentation. This tuning increased across the task. This showed that even if some cells were significantly tuned for grip type during the first cue presentation of the TO-task, the tuning depth was nevertheless very low. The presence of an object seems to be necessary to the representation of grip type tuning.

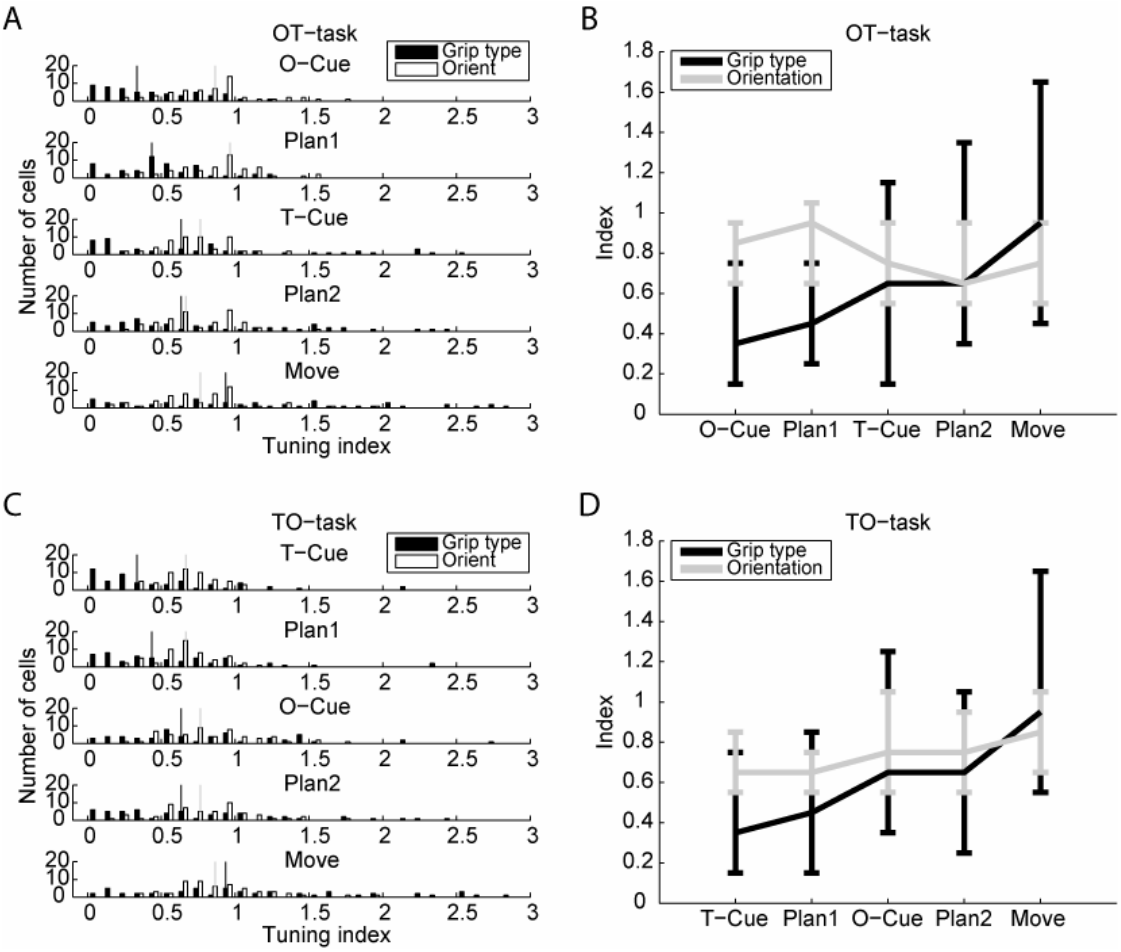

Figure 4.8 Normalized tuning index and median for grip type and orientation.
A) Number of cells in function of the normalized tuning index for grip type (black) and orientation (white) for all cells in the different task epochs of the OT-task. The median of the distribution for grip type is shown by the black vertical line and for orientation by a gray vertical line. B) Median, 25 percentile and 75 percentile of the distribution of the normalized tuning index during each task epoch of the OT-task. C) and D) Same graphs for the TO-task.

4.3 Summary

We developed a task in which the grip type and the object orientation were instructed in separate task epochs. We found that the orientation was represented in the population after the instruction of the orientation alone and that later, when the grip type was instructed, the grip type was also represented in the population. However, we found that the grip type was not encoded after the instruction of the grip type alone, but was represented with the orientation after the instruction of the orientation and the illumination of the object. These results suggest that the grip type

encoding requires the presentation of the object itself and the visualization of the features that are involved in the execution of the instructed grip type.

5. COMPARISON OF AIP AND F5

In the present chapter, we will compare the response of F5 neurons with the activity of neurons in the intraparietal area (AIP) in the parietal cortex that were tested in the same tasks. Results of AIP recordings were reported in a paper by Baumann, Fluet, and Scherberger (Baumann et al., 2009) and are presented in Appendix 9.1. Areas F5 and AIP are known to have strong interconnections and are part of a network responsible for visuomotor transformation for the control of hand grasping movements. A sample of AIP neurons has been recorded simultaneously with the sample of F5 neurons presented in the present thesis during the delayed grasping task and the cue separation task.

5.1 Tuning for grip type and orientation

One important aim of the present study was to investigate the specificity of the response of F5 neurons to grip type and object orientation during the delayed grasping task. The same question was also asked for neurons in AIP. There, sngle-unit activity was recorded from 571 neurons in the same animals and often simultaneously with the recordings in area F5 (489 neurons). The investigation of the grip type and orientation tuning during each task epoch of the delayed grasping task revealed that F5 and AIP encoded the grip type and the object orientation in similar ways. In AIP, the grip type showed a gradually increasing representation throughout the task from 25% during the cue to 58% during movement (two-way ANOVA performed in the same way as for F5, $p = 0.01$) while the orientation was found to be represented by a constant number of cells from cue instruction to movement execution (about 55% of the population). In F5, the representation of the grip type also gradually increased throughout the task and the percentages of grip type tuned cells were in the same range as for area AIP (F5: 23% during the cue and 39% during the movement). The orientation representation in F5 was also found to be constant, however at a lower level (approximately 20% of the F5 population in each task epoch). When comparing the tuning for grip type in both areas, we found that the increase in grip type representation was in both cases due to a group of neurons that became only tuned

during the movement execution. For orientation tuning, we found that a large proportion of the early tuned cells stayed tuned in AIP. In contrast, most of the early tuned cells in F5 lost their tuning during the course of the task. Nevertheless, the orientation information was maintained in the population of F5 by other cells that became tuned in subsequent epochs. These results suggest a similar representation of grip type in areas AIP and F5. In contrast, the stronger orientation representation and the encoding of orientation by the same neurons throughout the task in AIP and by different populations in F5 show important differences in the representation of the object orientation.

We also investigated the response in AIP and F5 to the separate instruction of grip type and orientation. The results were quite similar in both areas. When the object orientation was presented first, both areas represented the orientation alone before the grip type instruction was given. However, more cells were encoding the orientation in AIP than in F5 and the cells seemed to encode the orientation with a much higher tuning depth than in F5. When the grip type was presented first, only few neurons in AIP and F5 were modulated by the grip type before the presentation of the object and the modulation was weak. The grip type tuning increased dramatically after the object presentation. These results show that the grip type representation is strongly reduced in AIP and F5 in the absence of object information.

5.2 Cue processing and connectivity

We analyzed the grip type and orientation tuning in AIP and F5 within small window bins during the delayed grasping task (two-way ANOVA with $p = 0.01$, window width: 200 ms, step size: 50 ms) and found that the grip type and orientation representations increased rapidly after the beginning of the cue instruction (Figure 3.3 for F5 and Figure 3B in Appendix for AIP). In both areas, the orientation was represented earlier in the neural population than the grip type. The time delay between the orientation and grip type representations were 150 ms in AIP (time of half maximum, orientation: -0.492 s, grip type: -0.342 s) and 93 ms in F5 (time of half maximum, orientation: -0.466 s, grip type: -0.373 s). This delay could account for the different processing times that these two cues required. While the orientation required

a direct visuomotor mapping of the visual information, the grip type, which was instructed by a colored light, required an arbitrary visuomotor association. The orientation information is most probably propagated from the visual cortex to other parietal areas before being propagated to area AIP.

5.3 Cell classification

Grip type and orientation tuned cells presented differences in the tuning onset for these two parameters and thus revealed different populations of neurons in AIP and F5. Similar results were found in both areas (Figure 3.4 for F5 and Figure 4 in Appendix for AIP). The tuning onset distribution for grip type revealed two populations in both areas, one becoming tuned during the cue presentation and the other during the movement execution. The tuning onset distribution for orientation revealed a majority of cells becoming tuned during the cue presentation. The number of cells becoming orientation tuned during the cue presentation was however much higher in AIP then in F5. Furthermore, the investigation of the encoding combination of grip type and orientation revealed differences in these populations. In AIP, the early grip type tuned cells were found to be most likely also tuned by orientation, while most of the early orientation tuned cells were not tuned by the grip type. In contrary, most of the early grip type tuned cells in F5 were not tuned for orientation, and the early orientation tuned cells were most likely also tuned for grip type. These results show important differences in the early tuned populations in AIP and F5. In AIP, the orientation was encoded independently of the grip type, while in F5 the grip type was encoded independently of the orientation. For the late grip type tuned cells, the cells in AIP were either never tuned for orientation or showed early orientation tuning onset. In F5, the late grip type tuned cells were in large majority never tuned for orientation. The second type of late grip type tuned cells with early orientation tuning onset found in AIP was basically absent in F5 (2%).

5.4 Possible coding schemes

The representation of each specific grip type (precision vs power grip) and orientation (five possible orientations) was investigated in area AIP and F5 (Figure

3.5 for F5 and Figure 7 in Appendix for AIP). In AIP, the representation of each grip type was found to be equal during the cue presentation (precision vs power grip: 50% vs 50%). During the movement execution, the precision grip had a stronger representation than the power grip (precision vs power grip: 61% vs 39%). For the orientation, the representation of the extreme orientations (50 degrees to the left and to the right from vertical) was compared to the middle orientations (vertical, 25 degrees to the left and to the right). During the cue, the extreme orientations were equally represented than the middle ones (extreme vs middle orientations: 47% vs 53%) while during the movement execution, the extreme orientations had a stronger representation than the middle ones (extreme vs middle orientations: 59% vs 41%). In F5, the precision grip had a stronger representation than the power grip already during the cue presentation (precision vs power grip: 57% vs 43%) and this tendency further increased during the movement execution (precision vs power grip: 64% vs 36%). The extreme orientations were also found to have a stronger representation than the middle ones during the cue (59% vs 41%) and this tendency increased during the movement execution (extreme vs middle orientations: 81% vs 19%). These results suggest differences in the representation of grip type and orientation in area AIP and F5. In AIP, these representations seem to be more abstract during the cue presentation and more motor related during the movement whereas in F5 the grip type and the orientation seem to be represented in motor terms already during the cue. A possible reason for an overrepresentation of the precision grip could be the need for more neural resources to control this fine and precise movement. The overrepresentation of the extreme orientations could reflect a push-pull coding scheme of the clockwise/counterclockwise rotation of the hand.

The representation of each specific grip type and orientation was further extended to the different classes of cells found in AIP and F5 based on their tuning onset (Figure 3.6 for F5 and Figure 9 in Appendix for AIP). In AIP, we found that the early grip type tuned cells showed an equal representation of both grip types throughout the task but that the late grip type tuned population has a much stronger representation of precision grip. For the orientation, the early orientation tuned cells were encoding the five different orientations almost equally while the late orientation tuned cells had a much stronger representation of the extreme orientations. In F5, we found that the

early and late grip type tuned cells showed a stronger representation of precision grip. For the orientation, the early and late orientation tuned cells had a much stronger representation of the extreme orientations. Theses results show differences between the early and late tuned cells in AIP, but not in F5. While the early tuned cells in AIP seem to represent the grip type and the orientation in an abstract way, the late tuned cells in AIP and the cells in F5 seem to represent the grip type and the orientation in motor terms. Furthermore, we found that the tuned cells usually kept their tuning for the same grip type and orientation throughout the task or lost their tuning, but only very few cells changed their tuning preference. All together, we found that the increase in the representation of precision grip and the extreme orientations toward movement execution was mainly due to the late-tuned population that clearly showed a preference for precision and the extreme orientations, and partially caused by the loss of tuning of the power and the middle orientations in the early tuned cells.

6. GRASP DECODING

The aim of this chapter was to explore the possibility to decode grasp movement commands from higher order cortical areas for the control of hand prosthesis. Such a brain machine interface (BMI) would benefit to paralyzed patients that can still plan movements, but are unable to move their limbs. We used a maximum likelihood estimation technique to predict the grip type and the object orientation from the spiking activity of a population of neurons recorded in area F5 during a delayed grasping task. We first provide an introduction to decoding and maximum likelihood estimation followed by the results about the performance of the decoding simulations in function of the number of neurons used for the decoding.

6.1 Introduction to decoding

The successful decoding of a motor plan from neural activity in cortical motor areas is an important step in the development of a brain machine interface for paralyzed patients. The neural activity can be recorded using various techniques that can either be invasive or non invasive. Some of these techniques are electroencephalography (EEG), functional magnetic resonance imaging (fMRI), electrocorticography (ECoG), and chronically implanted electrode arrays. Different type of signals can also be recorded like blood oxygenation level-dependent (BOLD) signal, spiking activity, and local field potential (LFP). The planned movement should be decoded in real-time from the recorded signal and feed back to a prosthetic hand for movement execution as presented in Figure 6.1.

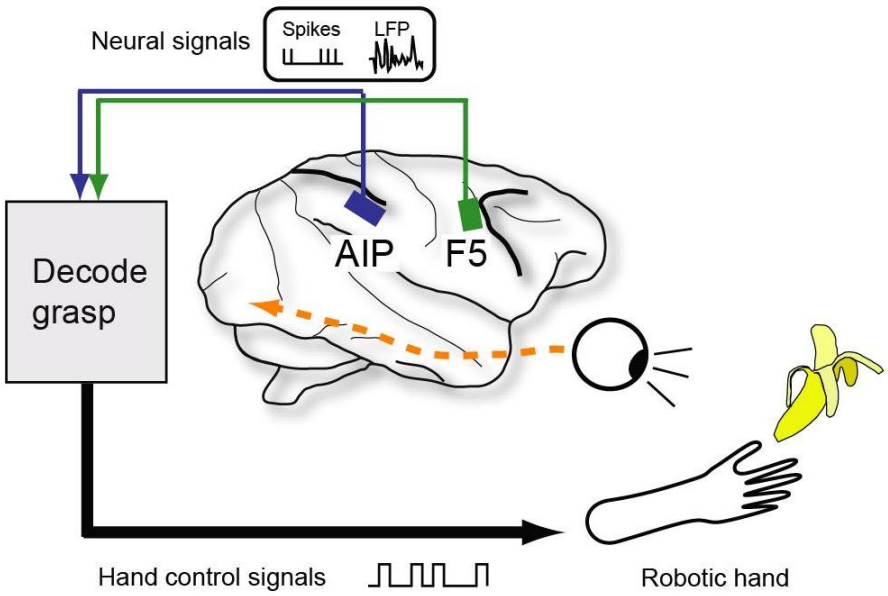

Figure 6.1 Grasp decoding.
Schematic of electrode arrays implanted in two high-order motor planning areas (parietal area AIP and frontal area F5). The neural activity, either the spiking activity or the local field potential (LFP), is recorded and the movement plan is decoded. A control signal is then generated and used to control a prosthetic hand.

In the present study, we recorded the spiking activity with movable electrodes over many recording sessions. However, in order to simulate a decoding session, we assumed that the activity of all neurons was recorded simultaneously. We used the same dataset recorded during the delayed grasping task and presented in Chapter 3. In that task, the monkey had to perform one of 2 grip types, either power or precision grip, in one of five possible orientations (upright, and 25 or 50 degrees to the left and to the right) for a total of 10 different grasping conditions. The neurons were recorded during each conditions for a least 7 repetitions. The goal of this study was to predict the grasping condition for a specific trial separately for each task epoch (cue, planning, and movement) based on the neural population activity. We assumed statistical independence between the cells and a Poisson distribution of the firing rate in each condition and each epoch. By experimental design, the probability for the occurrence of each condition was the same ($p(c) = 0.01$). We defined the scalar $c \in \{1,2,\ldots,10\}$ to be the grasping conditions and N the number of recording sites. For each neuron, we calculated the probability density of the firing rate from the repeated trials for each condition as shown schematically in Figure 6.2. We then calculated

$p_i(c|f)$, the probability for neuron i that the firing rate of the trial that we wanted to decode corresponded to the condition c, using the Bayes rule:

$$p_i(c|f) = \frac{p_i(f|c) \cdot p(c)}{p_i(f)}$$

The value p(c) is known and is uniform while the value $p_i(f)$ is a normalization factor which reduces the previous equation to the following:

$$p_i(c|f) = p_i(f|c)$$

We know $p_i(f|c)$ from our measurements and it corresponds to the probability of observing the rate f in condition c. The likelihood function L(c) of each condition was then obtained by multiplying the probability $p_i(c|f)$ of each condition c of all the neurons as expressed in the following equation:

$$L(c) = \Pi^{N}_{i=1}\, p_i\,(c|f)$$

The maximum likelihood can also be obtained from the sum of the logarithm of all $p_i(c|f)$ as expressed by the following expression:

$$LL(c) = \log\,(L(c)) = \Sigma^{N}_{i=1}\, \log\,(p_i\,(c|f))$$

Finally, the estimated grasp movement condition for the trial to be decoded corresponds to the condition with the highest likelihood.

$$C = \text{argmax}(LL(c)) = \text{argmax}(L(c))$$

In brief, maximum likelihood estimation allows to estimate unknown parameters, like the grasping movement condition, based on known outcomes, in the present application the activity of a population of neurons.

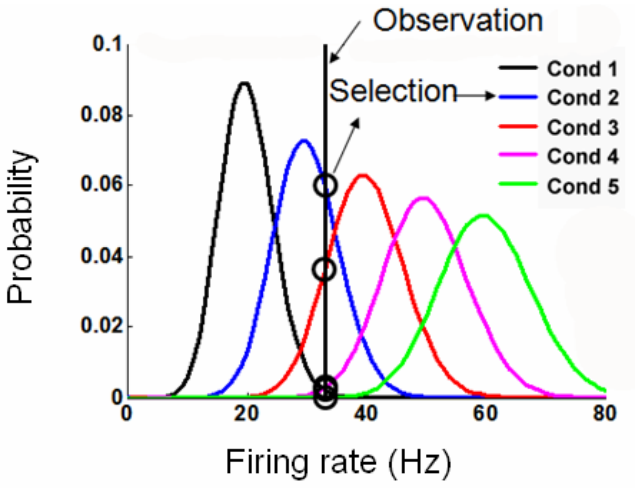

Figure 6.2 Schematic of maximum likelihood estimation.
Probability density of a neuron for each grasping condition (only five conditions are shown with different colors) estimated from the trial repetitions of each condition. The observed firing rate of that neuron during the trial is illustrated by the black vertical line and each condition has a probability to be the correct decoded condition (black circles along the black vertical line). The condition with the highest probability is most likely the intended condition.

6.2 Results

6.2.1 Decoding performance

We used the maximum likelihood estimation method to simulate the decoding of the grip type and the orientation from neural activity in area F5 during the different epochs of the delayed grasping task (cue, planning, and movement). We performed the decoding simulation based on the sequentially recorded population of neurons as described in Chapter 3 (182 neurons in monkey L, 307 neurons in monkey J). We repeated the decoding process 1000 times for each condition and in each task epoch of the delayed grasping task in order to have a more accurate estimation of the prediction performance (for more details refer to (Scherberger et al., 2005)). We calculated the percentage of accurately decoded grasp conditions by comparing the decoded condition with the instructed condition of successful trials. The correct decoding and the decoding errors are displayed in confusion matrices presented in Figure 6.3A-C for monkey L and Figure 6.4A-C for monkey J. For this analysis, we only used neurons that showed significantly different activity across conditions for each time epoch (one way ANOVA with factor condition, $p = 0.05$). Using this selection

criterion, from the 182 neurons recorded in animal L, 80 cells were selected for the decoding during the cue, 97 cells during the planning, and 83 cells during the movement epoch. From the 307 neurons recorded in animal J, the number of neurons with a significantly different activity across conditions was 119 during the cue, 124 during planning and 169 during movement. The decoding performance for each epoch corresponds to the mean of the diagonal of the confusion matrices. The values of the diagonals are shown in Figure 6.3D-F for monkey L and Figure 6.4D-F for monkey J. Overall, the decoding performance during the cue was 87.5%, during planning 87.6% and during movement 66.4% from animal L and for animal J, 93.0% during the cue, 90.1% during planning, and 83.9% during movement. This is similar to the performance of monkey L except for better performance during the movement epoch. This difference is probably due to the large variability in the numbers of cells available for each analysis. For both animals, we found better performances during the cue and the planning periods compared to the movement period. By looking more closely at the confusion matrices, we found that most of the mistakes were due to the decoding of a false orientation (orientation decoding error for monkey L: cue: 12.4%, planning: 13.4%, movement: 34.6%; monkey J: cue: 7.0%, planning: 10.9%, movement: 17.2%). There was rarely an error in decoding of the grip type as indicated by the dark blue color in the upper left and the lower right quadrant. Only 0.1% grip type decoding errors occurred during the cue period in monkey L. In any other period and in the other animal, no grip type mistake occurred. The results presented in Chapter 3 have shown that the representation of object orientation was only weak during the movement execution. This low representation and the low tuning depth both contribute to the reduced orientation decoding performance during the movement period.

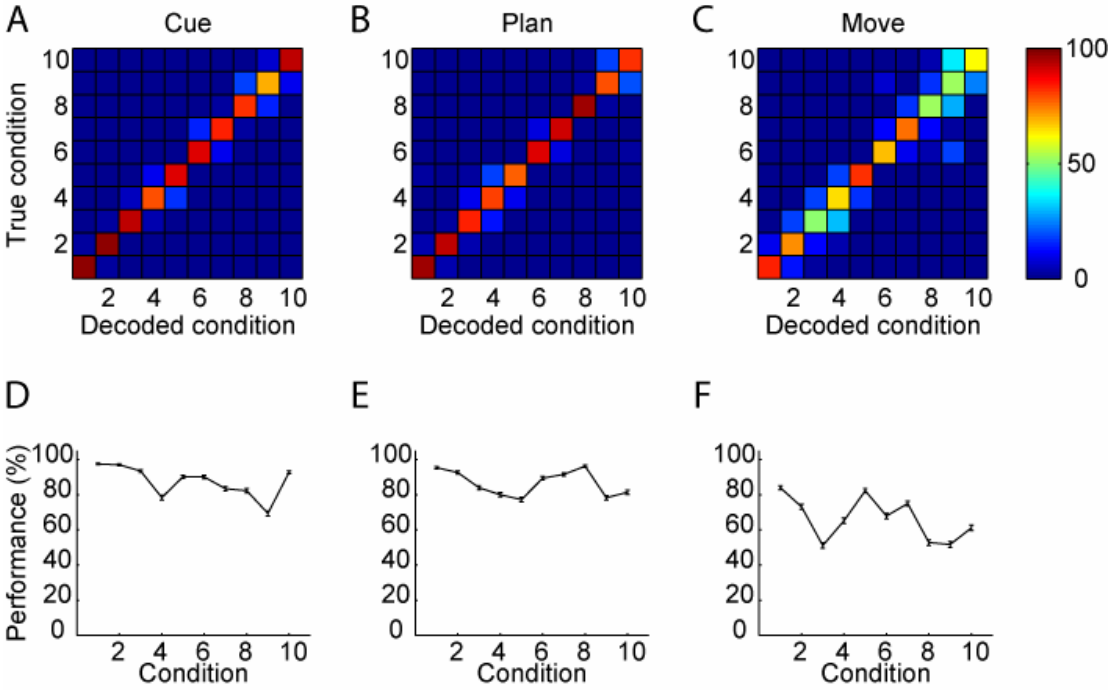

Figure 6.3 Decoding performances for monkey L.
A) Confusion matrices show for each true condition (along the y axis) the percentage with which all ten conditions had been decoded (along the x axis) during the cue period (n = 80). The numbers ranging from one to ten correspond to the 10 conditions with the five first conditions corresponding to the precision trials with the orientations -50, -25, 0, 25, 50 degrees and the five following conditions correspond to the power trials with the same orientations order. Percentages are colored scaled according to the color bar on the right. Correct decoding performances are aligned on the diagonal. B) Results for the planning period (n = 97). C) Results for the movement period (n = 83). D) Decoding performances for each condition are indicated in percentage by a black line and error bars indicate the standard error. Performances during the cue period. E) Performances during the planning period. F) Performances during the movement period.

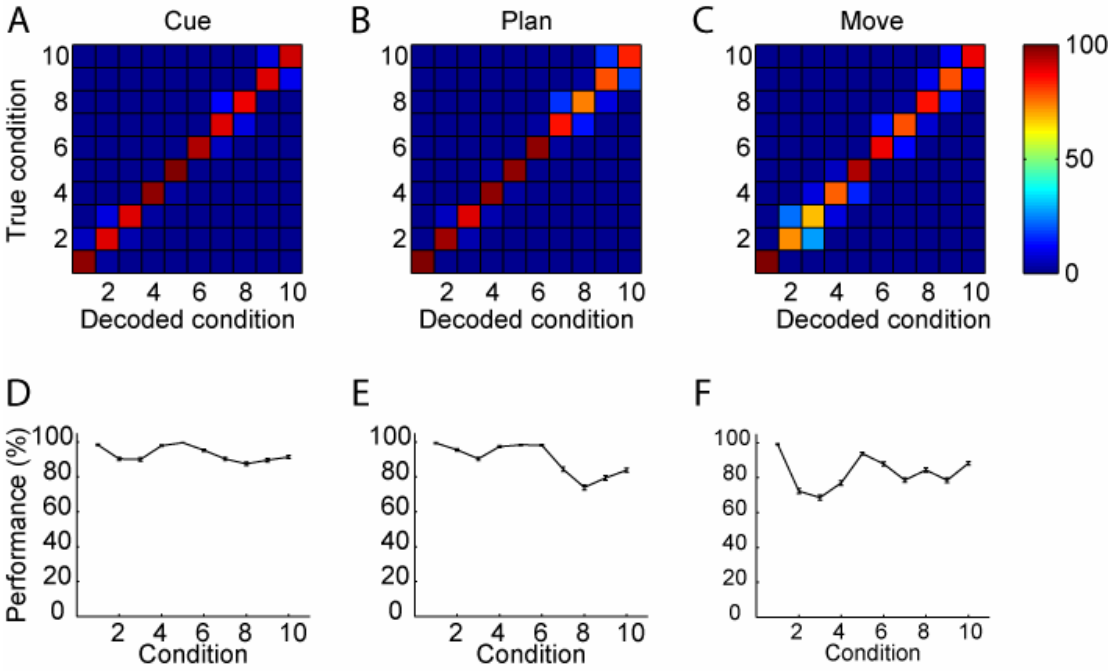

Figure 6.4 Decoding performances for monkey J.
A) Confusion matrices show for each true condition (along the y axis) the percentage with which all ten conditions had been decoded (along the x axis) during the cue period (n = 119). Percentages are colored scaled according to the color bar on the right. Correct decoding performances are aligned on the diagonal. B) Results for the planning period (n = 124). C) Results for the movement period (n = 169). D) Decoding performances for each condition are indicated in percentage by a black line and error bars indicate the standard error. Performances during the cue period. E) Performances during the planning period. F) Performances during the movement period.

We further investigated the orientation decoding errors during each task epoch for both monkeys separately in order to find the most common type of error. For this, we calculated the orientation shift between the decoded condition and the true condition. We found that most of the decoding errors were not simply random but occurred mostly to the immediate neighboring orientation (orientation shift of 25 degrees) as shown in Figure 6.5A for monkey L and Figure 6.5B for monkey J. These two graphs also clearly show that for both monkeys more orientation decoding errors occurred during the movement period as compared to the cue and the planning periods.

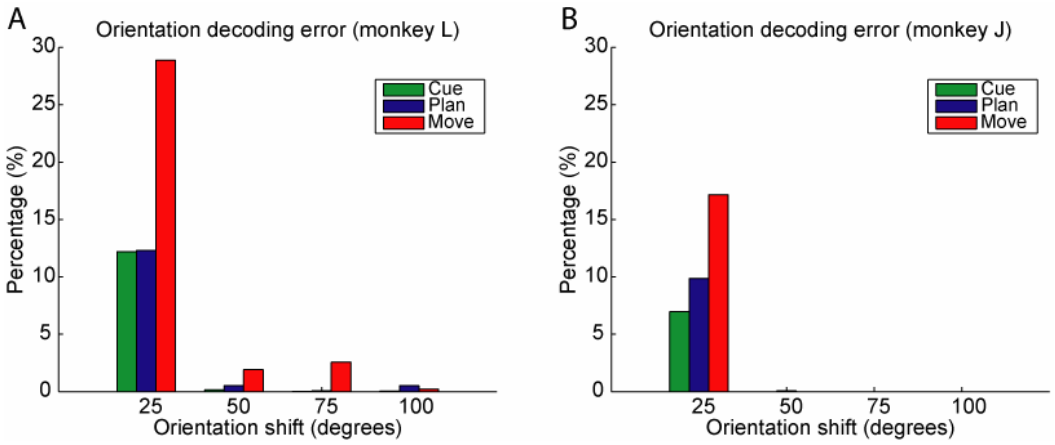

Figure 6.5 Orientation decoding errors.
Percentage of error in decoding the orientation as a function of the orientation difference between the true and the wrongly decoded condition for each task epoch (cue in green, planning in blue, and movement in red). A) Results for monkey L. B) Results for monkey J.

6.2.2 Neuron dropping analysis

Decoding performances vary in function of the number of neurons available for the decoding. This relationship is very important to know in order to estimate the size and number of electrode arrays that should be implanted for simultaneous recording. We investigated this relationship by retrieving random subsets of neurons from the total neural population recorded in the delayed grasping task. We performed the decoding analysis in the same way as described in the previous section for each task epoch, but with 100 repetitions instead of a 1000. The decoding performances for each subpopulation of neurons (all values between 1 and 30, and steps of 5 from 35 to the total number of significant neurons in the one-way ANOVA with factor condition) are presented in Figure 6.6A for monkey L and Figure 6.6B for monkey J during the different task epochs (cue in green, planning in blue, and movement in red). We found that the decoding performances rapidly increased and then saturated. In order to obtain decoding performances of 80%, 50 to 60 units would be necessary when decoding during the cue and the planning periods, while approximately 140 units would be necessary when decoding during the movement period. In practice, the decoding should most probably be performed during the planning period, as patients cannot execute the movement. It would then be feasible to record simultaneously

from 50-60 units with the actual technology. Electrode arrays can have up to hundred electrodes in only few millimeters surface.

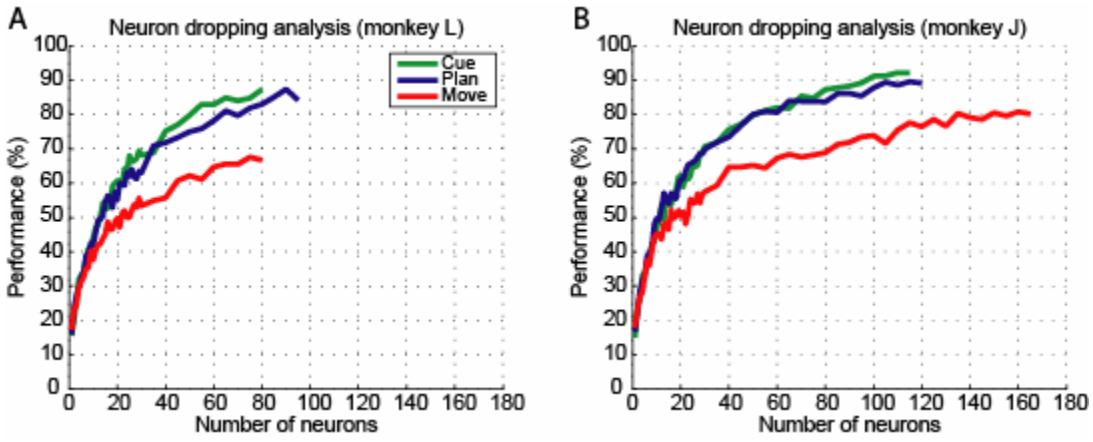

Figure 6.6 Neuron dropping analysis.
Decoding performance as a function of the number of cells in the different task epochs of the delayed grasping task (cue, planning, and movement). A) Results from monkey L. B) Results from monkey J.

6.3 Summary

Using a decoding simulation, we could decode between two different grip types (power versus precision grip) and five different orientations from the neural activity in area F5. Almost no errors were done in decoding the grip type and most of the errors in decoding the orientation were caused by mistaking the true condition with neighboring orientations. Furthermore, the performances were found to be slightly better during the cue and the planning period compared to the movement execution. The lower performance during the movement execution could be due to the lower tuning depth of the cells for the orientation during that period. Finally, the performances increase exponentially with the increase of the number of units used for the decoding before it saturates.

7. ANATOMY

The first aim of this section is to attest the correct location of the electrical recordings by analyzing the position of lesions performed during a terminal experiment. We first provide the description of the lesion protocol and the histology protocol. We further describe the recording technique used to perform the experiments in this thesis and investigate the extent of the tissues damages caused by this technique. A description of the recording electrodes will also be provided, followed by images of brain tissue where tens of electrode penetrations have been performed. Finally, we present the activity of the cells that were found to be recorded outside of area F5.

7.1 Brain lesions

In a terminal experiment, small electrolytic brain lesions were performed in area F5 of one animal (right hemisphere). Lesions were performed using a DC current of 20μA of a duration of 30 seconds. Figure 7.1A shows the planned locations of the lesions (red dots) and all the penetration sites (black dots, regardless whether useful cells had been recorded at that location or not) superimposed on an MRI of the brain. Lesions were performed at two locations (first: anterior 3 and lateral 7, second: posterior 3 and lateral 2; in chamber coordinates) and at two different depths for each location (first at 6000μm and second at 2000μm). The locations of the lesion have been chosen in order to be approximately at the edges of the recording area. Figure 7.1B shows the distance of the planned lesions relative to some anatomical markers that where used to assess the correct position of the lesions. According to the planned locations, the most anterior lesion should be found 1.5 mm lateral to the inferior limb of the arcuate sulcus (iAS). The planned locations have to be later confirmed by studying the real positions in the histology slides (see section 7.3).

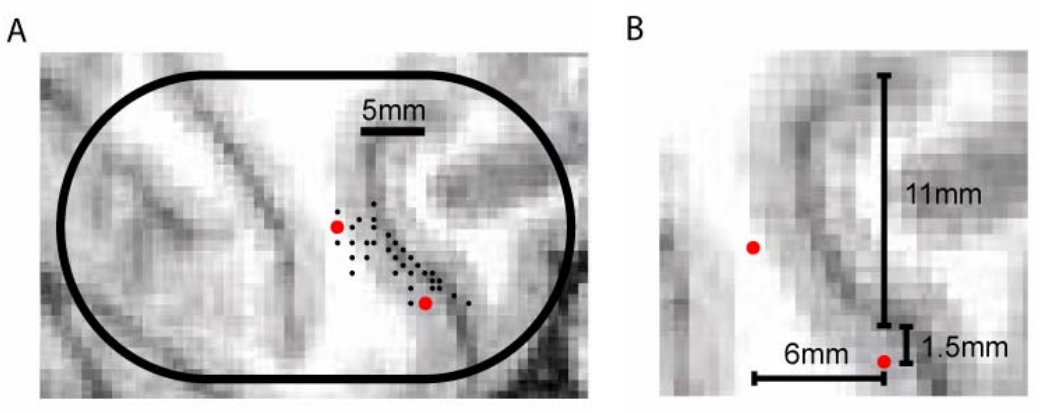

Figure 7.1 Lesions locations and recording penetrations.
A) MRI section of the right hemisphere of monkey L in the plane of the recording chamber. Superimposed to the MR image are all penetration sites in area F5 (black dots), the lesion sites (red dots), and the recording chamber (black ellipse). B) Zoomed image of the lesions and distances relative to the sulcus and between the lesions.

7.2 Histology protocol

The aim of our neurohistology study was to investigate the cells and the neuronal tissues in the light microscope. For this, it is important to prepare and stain the structures to be studied appropriately. The main steps are the following: fixation of the tissue, processing, sectioning, mounting of sections, and staining. Fixation of the tissue is crucial in order to preserve the cytoarchitecture of the biological structures. The best technique in order to minimize the diffusion artifacts of structures that are not bound to solid structures is to perform the fixation in vivo. The monkey was then perfused three days after the lesions. The animal was first anaesthetized using ketamin (150 mg) and valium (7.5mg) followed by a dose of pentobarbital (1000 mg) which was administrated intravenously. When all reflexes were gone, the chest was opened and the animal transcardially perfused with a 0.9% NaCl solution in order to flush out the blood, followed by the fixative solution of paraformaldehyde (4%), glutaraldehyde (0.3%) and picric acid (15%) in 0.1M phosphate buffer (PB) pH7.4. Importantly, the perfusion pressure was maintained constant in order to avoid artifacts by air infusion. Finally, the animal was perfused with solutions of successively increasing concentration of sucrose (10% and 20%) in 0.1M PB. The brain was stereotaxically cut into blocks, with one block containing area F5. All blocks were then put in a sucrose solution of 20% in 0.1M PB until they sunk and then placed in a 30% sucrose

solution. This step provided cryoprotection to the tissue. The brain was further processed using a freeze-thaw technique. It was frozen using nitrogen liquid and then put in PB (0.1M) for two hours in order to reverse the shrinkage caused by the soaking in the sucrose solution. The brain was cut into sections of 80µm in the coronal plane using a vibratome and then washed with PB (0.1M) and tris buffered saline (TBS, pH 7.4) in order to remove leftover fixative. It was kept over night in an avidin biotin complex (ABC) solution in the refrigerator, washed with PB (0.1M) and TBS (pH 7.4) and incubated with diaminobenzidine tetrahydrochloride (DAB and Ni-DAB) solutions. Peroxydase was added to trigger the staining reaction. The tissue was stained with cresyl violet. Sections were dehydrated using solution with progressively increasing concentration of ethanol and then fixed on glass slides using DPX Mountant (Fluka). We obtained 124 brain slices, each one having a thickness of 80µm, for a total of 9.92mm.

7.3 Observations

The lesions and the entrance points were localized on the slices. The lesions looked like circular brown colored areas while the entrance points were located by the presence of microglia on the pia mater, presumably caused by damages from the use of sharp guide tubes. Because the electrode penetration angle and the coronal sections where not perfectly aligned, the lesions were found in different slices. Two slices for the posterior lesions have been superimposed and are presented in Figure 7.2B on the left and two slices for the anterior lesions have been superimposed and are presented in Figure 7.2C. The lesions are indicated by black arrows. A line passing through the lesions was traced (red line). The distances between the lesions were found to be around 4 mm for the two posterior lesions and the two anterior lesions, as it was expected. However, the lesions were found slightly deeper than expected (approximately 1mm deeper). As mentioned above, sharp guide tubes were used in order to perform the lesions. After touching the surface, the guide tubes were moved three millimeters down until the dura could be penetrated. This was necessary because a layer of granulation tissues had grown over the dura at the time of the terminal experiment. Consequently, the sharp guide tubes (penetrating the dura) were located deeper than the blunt guide tubes (not penetrating the dura) used during the recording

sessions. The entrance point of the electrode for the anterior lesion was found approximately 1.5 mm lateral to the inferior limb of the arcuate sulcus, as predicted from Figure 7.1B. The anterior-posterior locations of the lesions were more difficult to attest because this axis is perpendicular to the sections. According to the locations of the lesions, the distance between the anterior and posterior lesions should be situated 6 mm apart in the anterior-posterior direction. The posterior entrance point was found around the 27th brain slice while the anterior entrance point was found around the 100th brain slice which represents 73 slices of 80um thick and corresponds to a total of 5.84 mm. In the slice containing the entrance point of the anterior lesion (Figure 7.2D), the distance between the superior and the inferior limb of the arcuate sulcus was found to be around 11 mm as shown in Figure 7.1B. The rapid decrease of this distance measured in the more posterior slides support the correct position of the lesions. Based on the study of the locations of the lesions, we can consider the location of the recordings as being accurate. The penetration map shown in Figure 7.1A nevertheless suggest that some recording locations situated in the sulcus might not be situated in area F5 but in the anterior bank of the inferior arcuate sulcus (iAS). These cells were not included in the analysis presented in the previous chapters. The activity of those cells was analyzed separately and is briefly reported in section 7.5.

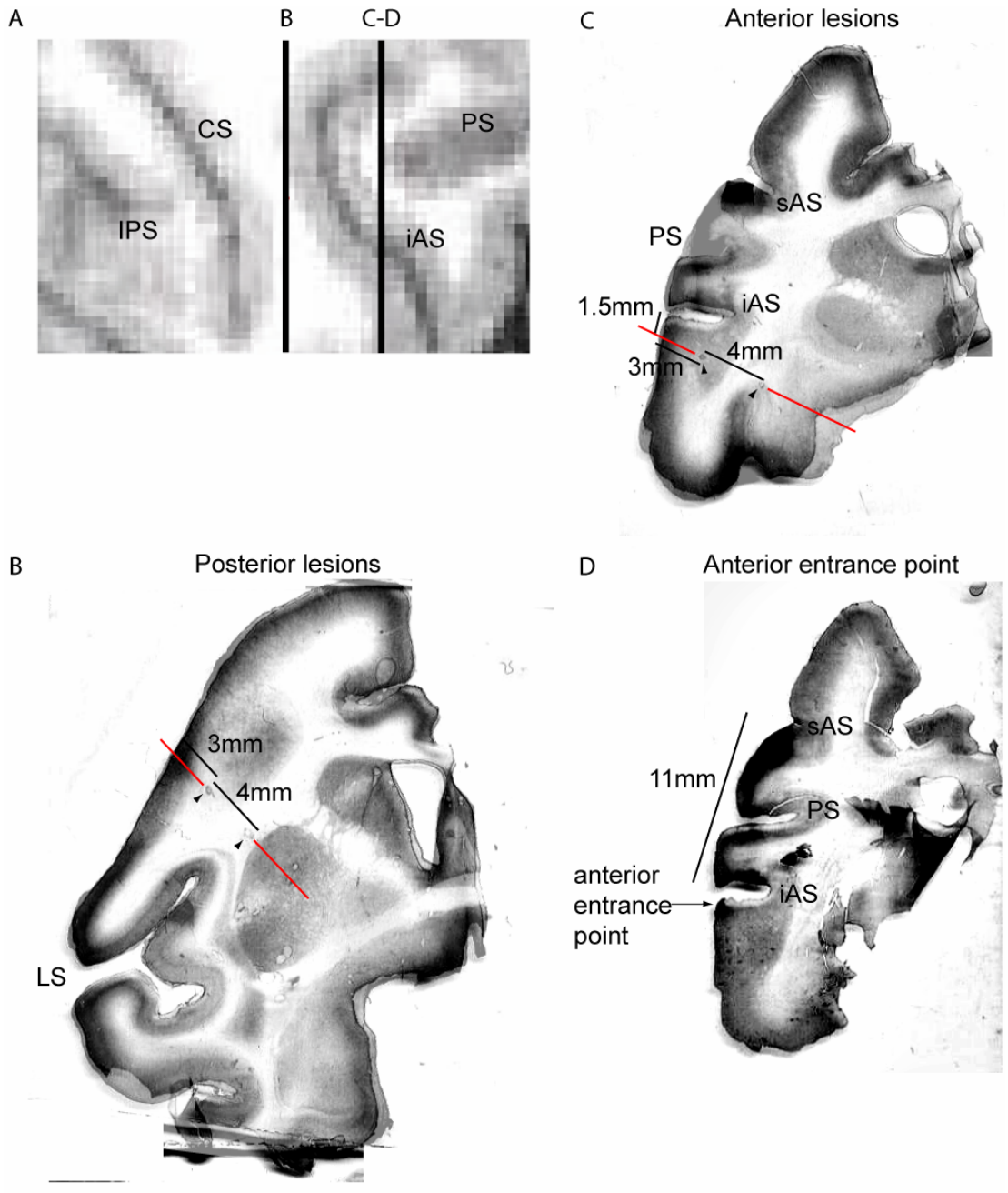

Figure 7.2 Superimposed images of the two posterior, the two anterior lesions and the entrance point of the anterior lesion.
A) Approximate positions of the sections containing the lesions and presented in B-D. Abbreviations: CS: central sulcus, IPS: intraparietal sulcus, iAS: inferior arcuate sulcus, PS: principal sulcus. B) The positions of the two posterior lesions are indicated by the black arrows. A projection line passing through the two lesions is drawn in red. The depth of the shallow lesion is 3mm while the depth of the deepest lesion is 7 mm. Abbreviations: LS: lateral fissure. C) The positions of the two anterior lesions are indicated by the black arrows. The depth of the shallow lesion is 3mm while the depth of the deepest lesion is 7 mm. Abbreviations: sAS: superior arcuate sulcus,. D) Distance between the inferior and superior limbs of the arcuate sulcus at the level of the entrance point of the anterior lesion.

7.4 Electrodes and tissue damages

Quartz/platinum-tungsten electrodes (Thomas Recording, Germany) were used for extracellular recording of single-units. These electrodes are made of a metal core and a quartz mantle. The tip is exposed using a specialized grinding technique and the impedance of the electrode varies in function of the size of the exposed tip. We used impedance values in the range of 1-2 MΩ measured at 1 kHz. A picture of the electrode tip is presented in Figure 7.3. The electrodes are strong enough to penetrate through the dura giving the possibility to keep the dura intact and thus reducing substantially the risk of infections. The small dimensions of the electrodes (diameter 80μm) combined with a smooth transition between the glass and the core of these microelectrodes contribute to reduce the tissue damage during electrode penetration. It has been reported that the brain shows inflammatory responses following chronic implantation of electrodes (Shain et al., 2003). In long term, an increasing number of microglia surrounding the electrodes can be seen. For the acute system used in the present thesis, the manufacturer nevertheless claims that electrode tracks cannot be seen with standard histological techniques. We verified that claim with the slices of one animal (monkey L). All slices were examined carefully under the light microscope and no electrode tracks could be found in any of the slices. We concluded that the damages caused to the brain tissue by the penetration of this type of electrodes are very limited despite the high number of penetrations in this tissue (about 110 penetrations had been performed).

However, we found a broken electrode tip as shown in Figure 7.4. Indeed, one of the major problems encountered during the months following the bone trephination was a problem of tissue growing on the dura. These tissues made the dura thicker and therefore more difficult to penetrate. The use of 5 Fluorouracil helped slowing down the growth of those tissues (Spinks et al., 2003), but did not completely prevent that electrodes were breaking during the penetration of the dura.

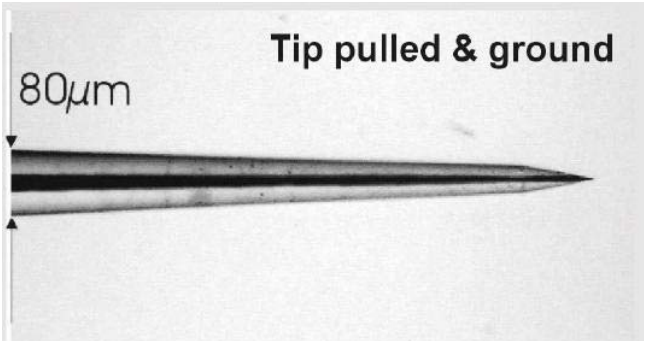

Figure 7.3 Tip of a recording electrode.
The metal core can be seen in black while the quartz coating situated around the core can be seen in lighter shades of gray. The electrode has very smooth sides and a maximum diameter of 80um.

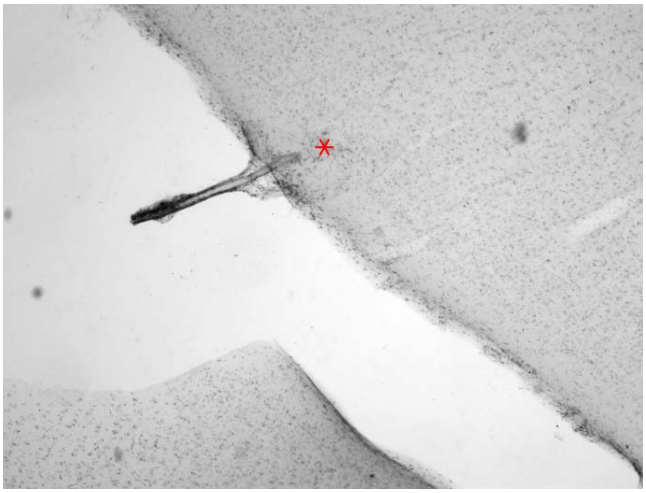

Figure 7.4 Broken electrode tip in brain tissue.
Broken electrode tip (red star) covered with tissue in the superior bank of the superior arcuate sulcus. Tissues growing on top of the electrode tip can be seen.

7.5 Neurons outside of F5

In animal L, some cells were found to have been recorded too close to the arcuate sulcus and were thus probably situated on the anterior side of the inferior arcuate sulcus. These cells were excluded from our analysis presented in the previous chapters. The following objective criteria were used to determine which cells would be rejected. Cells had to have been recorded in the sulcus and at a depth lower than 5000µm. With these criteria, 90 cells were rejected. These cells were mainly active during the cue presentation and had a low firing rate during the movement period (Figure 7.5A). This type of activity is very atypical for area F5, but could well

correspond to neurons from the frontal eye field (FEF, area 8). FEF was found to discharge before and during contraversive fixation and saccades (Schall, 1991). When investigating the preference for power versus precision grip, we found that the cells preferring power grip (47 cells) were firing much more than the cells preferring precision grip (43 cells) (Figure 7.5B). By looking closely at the experimental design, we noticed that the green LED coding for the power grip was situated on the left of the red fixation light and therefore contralateral to the recording chamber. This could then explain the stronger response that we found for the power grip instruction cue in that population. This kind of response was not observed in the database presented in Chapter 3 and 4.

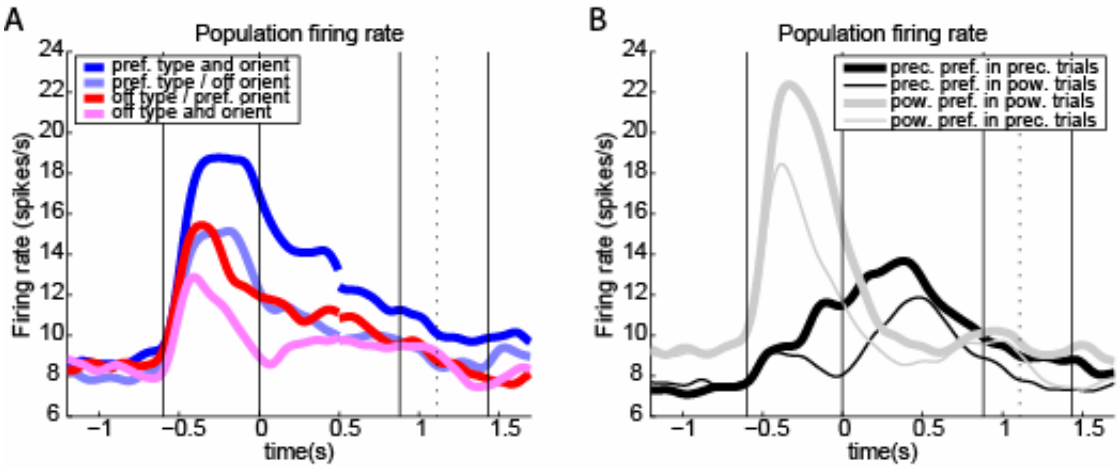

Figure 7.5 Population firing rate histogram of the neurons presumably anterior of the iAS (n = 90) during the delayed grasping task and population histogram of the cells preferring precision grip and power grip during the conditions with preferred versus non preferred grip type.
A) Population firing rate histogram for the 90 cells during the preferred and non preferred conditions (grip type and orientation). The cells show high visual activity and little activation during the movement period. B) The population preferring precision grip is drawn in black while the population preferring power grip is drawn in gray. The trials with the preferred condition are drawn with a thick line while the trials with the non preferred condition are drawn with a thin line. The power preferring cells were increasing much more their firing rate during the cue period compared to the precision preferring cells.

7.6 Summary

We performed the histology with one animal and the examination of the slices under the microscope allowed us to verify that the technique that we used to plan the recording positions and based on MRI sections of the recording chamber together with the brain rotated in the plane of the recording chamber was accurate and matched our estimation. With this technique, the histology would not necessarily be required for all animals to determine the recorded locations. Furthermore, the recording technique that we used caused only minimal damages to the brain tissues as no traces from the microelectrodes penetration could be seen. We nevertheless found a broken electrode tip which is due to a problem of growth of granulation tissues on the dura that makes the penetration of the dura more difficult.

8. DISCUSSION

The aim of the present thesis was to investigate the specificity of the response of F5 neurons for grip type and object orientation as well as the representation interaction of these two parameters. In order to answer these questions, we trained macaque monkeys to perform a delayed grasping task in which the animal had to perform one of two grip types (power or precision grip) in one of five orientations (vertical, 25 or 50 degrees to the left or right). The results were presented in Chapter 3. Another aim of the present thesis was to investigate the representation of partial instruction by training the monkeys to perform a cue separation task. Results were reported in Chapter 4. A comparison of the results in AIP and F5 were presented in Chapter 5. Furthermore, we evaluated the possibility of using the activity from a higher order planning area, like F5, to control a prosthetic hand. Results were presented in Chapter 6. Finally, the recording locations and the damages caused by the recording technique were discussed in Chapter 7. In the present chapter, we will further discuss our results. Furthermore, we will discuss the limitations and shortcomings of the experimental design and expose suggestions for future work.

8.1 Functional properties of F5

8.1.1 Tuning for grip type and orientation

One of the aims of the present study was to investigate the specificity of the response of F5 neurons to grip type and object orientation during a delayed grasping task. The results showed that area F5 encodes both parameters. The orientation was encoded in a constant way across the task by approximately 20% of the population. These results showed that area F5 plays a role in rotating the hand in the correct orientation but the low percentage of orientation tuned cells suggests that area F5 might only play a minor role. Others studies have shown that the orientation is represented in other areas. One of those studies report orientation representation in the medial posterior parietal area V6A (Fattori et al., 2009). This area is known to project to other areas in the medial lobe of the intraparietal sulcus like MIP, PRR and PEc

(Gamberini et al., 2009) which in turn project to dorsal premotor areas. These areas are commonly thought to be involved in the control of more proximal limbs. Nevertheless, area V6A is also known to be connected with area AIP (Borra et al., 2008) in the lateral lobe of the intraparietal sulcus which project to area F5. The traditional view of completely distinct pathways for reaching and for grasping in view of these results is then questionable (Stark et al., 2007). For the grip type, it was found to be encoded early during the task by one population of neurons while another population of neurons started to encode the grip type only during movement execution. This led to an increase of the grip type representation from about 20% during the cue to almost 40% during movement execution. These results support the idea that area F5 plays a significant role during planning and in shaping the fingers for grasping.

8.1.2 Tuning onset

The analysis of the tuning onset revealed different populations of neurons. For the orientation specific cells, we found a large population of early tuned cells. For the grip type specific cells, we also found a large population of early tuned cells, but also a second population of late tuned cells. In a study by Murata et al. (Murata et al., 1997), two types of neurons were reported, visuomotor and motor neurons. The visuomotor neurons are coding the grip type already during the cue while the motor neurons become grip type specific during movement execution. These motor cells correspond to our late grip type tuned cells while the visuomotor cells could correspond to our early grip type tuned cells. However, our results showed that most of the early grip type tuned cells did not remain tuned for the complete task. In a study by Hoshi (Hoshi and Tanji, 2006), it was suggested that the premotor cortex might be composed of two populations of neurons. One population would be connected to the input while the other one is connected to the output. The first population would respond at the beginning of the trial during the cue while the other one would be active at the end of the trial during movement. These two populations could be directly connected to each other or they could be bridged by cells that respond during the complete task. Our results seem to support this hypothesis due to the loss of tuning at the single cell level, but the maintaining of tuning at the population level.

The simultaneous encoding of the grip type and the orientation was hardly studied. In a study by Raos (Raos et al., 2006), monkeys were required to grasp a plate and a ring in a vertical and a horizontal position. As the neurons responded specifically to one object in one orientation, they proposed that the grip type and the wrist orientation are encoded in a combined fashion. This study nevertheless had some limitations. Only cells with grip type specificity were reported and the orientation was not studied alone. Our results showed different levels of dependency in different type of neurons depending on their tuning onset. We found a strong dependency of the orientation representation with the grip type in early orientation tuned cells, while early grip type tuned cells showed a moderate dependency with the orientation and late grip type tuned cells showed a complete independence with the orientation.

8.1.3 Specific coding

Detailed analysis of the preference for each grip type and orientation during each task epoch revealed differences in the encoding of the different grip types and the different orientations. For the two tested grip types, we found a constant representation of power grip across the task and a significant increase of precision grip representation from planning to movement. The increased representation of precision grip was due to the late tuned cells, but a significantly higher representation of power grip and precision grip was found in both the early and the late grip type tuned cells. We hypothesized that the precision grip needs to recruit more cells for accurate execution due to its higher complexity and the higher need for coordination. Furthermore, our results showed that grip type specific cells usually keep the same grip type preference from one period to the other. For the five tested orientations, we found that the extreme orientations (-50 and 50 deg) were more represented than the middle orientations (-25, 0, 25 deg). The representation of the extreme orientations remained constant across the task while the representation of the middle orientations decreased significantly from planning to movement. A significant decrease of tuning for the middle orientations was found in the early tuned cells. Only few cells became lately tuned for orientation. The tuning consistence of the orientation also revealed that the extreme orientations tend to keep their tuning across epochs while the middle orientations tend to loose their tuning. This higher representation of the extreme

orientations could be a consequence of the small range of orientations that we tested (100 degrees). The neuron preferring an orientation above the one tested would then show a preference for one of the extreme orientations tested. Another hypothesis would suggest that this result is due to a push-pull encoding of the wrist rotation in one dimension.

8.1.4 Visual response

F5 neurons have been shown to respond during the presentation of an object. This activity first seemed a contradiction knowing that area F5 has direct projections to the spinal cord and strong connections to primary motor cortex and is mainly known for playing a role in movement execution. The nature of this response during object presentation is still under debate. This response could either reflect the characteristics of the object presented in visual terms or it could reflect the upcoming movement in motor terms. In a study by Murata (Murata et al., 1997), six different objects were presented to a monkey in four different conditions: grasping in light, grasping in dark, object fixation and LED fixation. One type of neurons, referred to as visuomotor neurons, responded selectively to one object or a subgroup of objects during the visual presentation and the movement execution. The visuomotor neurons responded even in the absence of a subsequent movement. The authors concluded that the visual response of F5 neurons represents a potential motor action. However, in that study, no dissociation between the grasp and the object was possible as each object could be grasped only in one specific way. In the present study, the monkeys had to grasp the same object in two different manners, meaning that the object characteristics remained the same for all trials while the grip type could either be precision or power grip. We studied the response to precision trials versus power trials of the population that we divided into cells preferring precision grip and the cells preferring power grip. These two populations showed an early grip type tuning during the cue period, but otherwise similar activation for their respective preferred and non preferred grip type. These results support the idea that the response during object presentation reflects the upcoming movement. During movement execution, the precision preferring cells had a higher firing rate than the power preferring cells during their respective preferred trials. This observation was also reported by Umilta (Umilta et al., 2007), where they

reported that some types of grasp (e.g., precision grip) were associated with a higher mean level of activity, whereas others grips (hook grip with the index finger) evoke far lower discharge rates in area F5. For the non preferred trials, each population showed some activation during movement execution although lower than for the preferred grip type. This suggests that there might be something common between these two grip types, possibly a subset of activated muscles, which is encoded with different amplitude.

8.1.5 Cue separation task

The aim for developing the cue separation paradigm was to investigate the neural response of F5 neurons to the individual instructions of grip type and object orientation. In the OT-task, we found that cells were encoding the orientation alone after the instruction of the orientation and that later these cells were encoding the grip type after the instruction of the grip type. Therefore, the orientation and the grip type can be both encoded in the same cells, but the orientation can be expressed individually when the grip type is still ambiguous. In the TO-task, we found that the grip type encoding was not present or was hardly represented after the instruction of the grip type only. However, the representation of the grip type significantly increased after the instruction of the orientation and the illumination of the object. From the cells that were grip type tuned during the orientation instruction, only a low percentage of cells were also tuned for orientation. This suggests that grip type encoding is not due to the instruction of the orientation, but most likely to the presentation of the object itself and the visualization of the features that are involved in the execution of the instructed grip type.

Our detailed analysis of the preference for each grip type and orientation during each task epoch support the finding reported in Chapter 3, which revealed differences in the encoding of the different grip types and the different orientations. For the two tested grip types, we found a constant representation of power grip across the task and an increase of precision grip representation. This difference in the representation of power versus precision grip suggests that the precision grip requires a stronger activated population in order to generate an accurate and precise movement. For the

five tested orientations, we found a strong representation of one of the extreme orientations (50 degrees to the right). This result is nevertheless not contradicting the previous results presented in Chapter 3. As suggested earlier, this higher representation could be a consequence of the small number of neurons recorded in this paradigm and the relatively high number of different orientations tested.

8.2 Comparison of AIP and F5

We compared the specificity of the response of AIP and F5 neurons to grip type and object orientation during the delayed grasping task. We found that F5 and AIP encoded the grip type and the orientation in very similar ways with the difference that AIP showed a much higher representation of the orientation. Based on the tuning onset, we identified three populations of neurons in each area: early orientation tuned, early grip type tuned and late grip type tuned cells. The investigation of the combined encoding of grip type and orientation in these three populations revealed that in AIP, the orientation was most likely encoded independently of the grip type, while in F5 the grip type was most likely encoded independently of the orientation. This suggested that the intrinsic characteristics of the object represent the dominant feature encoded in AIP while in F5 the motor representation of the movement is the predominant feature. A study of area F5 by Murata et al. (Murata et al., 1997) reported two types of neurons, motor and visuomotor neurons. The motor neurons became grip type specific during movement execution while the visuomotor neurons were coding the grip type already during the cue. These motor cells correspond to our late grip type tuned cells while the visuomotor cells could correspond to our early grip type tuned cells. Our study provides further information about the orientation tuning of theses classes of neurons. The late grip type tuned cells showed a complete independence of the orientation while the early grip type tuned cells showed a partial dependence. A study of area AIP by Sakata et al. (Sakata et al., 1995) reported three types of neurons based on their activity during object manipulation and fixation in the light and in the dark. Motor-dominant cells were equally active in grasping in the light and in the dark and consequently not modulated by the object characteristics but only by the action. Visual-dominant cells were only active during grasping in the light and then only modulated by the object characteristics. Finally, visual and motor cells were

preferentially active in the light and then modulated by the object characteristics and the action. The last two classes were further divided in object type and non-object type depending on whether they were active during object fixation or not. Our classification can be compared to the classification of the study by Sakata et al. The late grip type tuned cells with no orientation tuning found in the delayed grasping task correspond to the motor-dominant cells and non-object type visual and motor dominant cells. This would suggest that the late grip type tuned cells are either equally activated during manipulation in the light and in the dark, or preferentially active during manipulation in the light. The early tuned cells in the delayed grasping task correspond to the object type visual-dominant and the object type visual and motor cells. Our results showed that these cells are either modulated by the orientation alone or by the orientation and the grip type.

The representation of each specific grip type (precision vs power grip) and orientation (five possible orientations) was investigated in area AIP and F5. The results showed differences in the representation of grip type and orientation. In AIP, these representations seemed more abstract in the early tuned cells and more motor related in the late tuned cells. In F5, the grip type and the orientation tended to be represented in motor terms in all classes of cells that encoded preferentially the precision grip compared to the power grip and the extreme orientations compared to the middle orientations. An overrepresentation of the precision grip could be explained by the need for more neural resources to coordinate this fine movement, while the overrepresentation of the extreme orientations could reflect a push-pull coding scheme of the rotation of the hand. Furthermore, we found that the tuned cells usually kept their tuning for the same grip type and orientation throughout the task or lost their tuning. Only very few cells changed their tuning preference.

We also investigated the response in AIP and F5 to the separate instruction of grip type and orientation. The results showed that the orientation is encoded in both areas in the absence of information about the grip type. In contrast, the grip type representation is strongly reduced in the absence of object information. These results suggest that the motor plan emerges only in these two areas when it can be matched to an object.

In both areas, the investigation of the grip type and the orientation revealed that the orientation was represented earlier than the grip type. This is most probably due to the different nature of the two cues: while the orientation required a direct visuomotor mapping of the visual information, the grip type, which was instructed by a colored light, required an arbitrary visuomotor mapping. We also found that the orientation representation was present in AIP slightly earlier than in F5. Possibly, the orientation information is processed by the visual cortex and projected to parietal areas before being further propagated to the premotor areas. Thus, the orientation representation in F5 could originate from AIP. Some studies have indeed shown that the orientation is represented in the medial posterior parietal area V6A (Fattori et al., 2009), which projects to areas in the medial lobe of the intraparietal sulcus like MIP, PRR and PEc, but also to area AIP in the lateral lobe of the intraparietal sulcus (Borra et al., 2008). Due to the strong interconnections between AIP and F5, the orientation could be further propagated to F5. A monosynaptic connection could well explain the slightly earlier representation in AIP as compared to F5 (time delay = 26 ms). For arbitrary visuomotor mapping, the cortical areas known to be involved consist in the prefrontal and premotor cortex (Murray et al., 2000). There is also evidence pointing to a role of the inferior temporal cortex for arbitrary visuomotor mapping, most specifically area TE on the middle temporal gyrus and the perirhinal cortex on the inferior temporal gyrus in interaction with the prefrontal cortex. The circuit processing the abstract grip type cue could then consist in the temporal cortex, followed by the prefrontal cortex and then the premotor cortex, among which area F5 that is known to receive projections from the prefrontal cortex (Matelli et al., 1986). This multisynaptical pathway involving many cortical areas could then explain the longer delay in processing the abstract grip type compared to the directly mapped orientation. Furthermore, the grip type representation could be propagated to AIP through either its connections with F5 or with the prefrontal cortex (Borra et al., 2008). The slightly longer time required for the grip type representation in AIP compared to F5 (time delay = 31 ms) suggest that a slightly longer path might connect AIP to the areas performing the abstract visuomotor mapping than F5.

8.3 Decoding

We performed a decoding simulation in order to verify whether grasping movements could be decoded from area F5. Up to now, most of the attempts to decode movement plans have been performed using the firing activity from the primary motor cortex in intact animals (Serruya et al., 2002; Taylor et al., 2002). It was however not known until recently whether the primary motor cortex undergoes changes following spinal cord injury that would compromise the usability of this area for brain machine interface. A recent study has shown that paralyzed patients could still modulate the activity of neurons in primary motor cortex many years after a spinal cord injury or stroke (Hochberg et al., 2006). However, the use of high-order areas for the control of a prosthetic might still have advantages over the primary motor cortex. The representation of movements in such areas might be simpler to decode as it represents the movement goal rather than the movement trajectory and dynamics that are strongly encoded in the primary motor cortex. Our results show that it is possible to decode two different grip types (power versus precision grip) and five different orientations from a planning area like area F5. The decoding of the grip type nevertheless achieved better performances as compared to the orientation. Decoding errors for grip type were almost zero while decoding orientation errors were above 10% in each task epoch using between 80 and 170 tuned neurons. Most of the decoding errors for the orientation were caused by mistaking the true condition with neighboring orientations. These errors were most probably due to a low tuning depth for the orientation, with a better tuning depth during the cue period and a decrease of the tuning in the movement period. The orientation decoding errors cannot be due to differences in the number of tuned cells used for the decoding because the comparison of performances in different epochs for the same number of neurons still revealed lower performance during movement. Finally, our results showed that it would be feasible with the actual technology to implant electrode arrays in area F5 and record from a sufficient amount of neurons in order to achieve acceptable performance for the control of a prosthetic hand. One of the principal limitations of this recording technique is to maintain the isolation of neurons over a long period of time. In this respect, new electrodes have to be developed with a higher biocompatibility or other signals have to be used for decoding, for example the local field potential (LFP),

which can be recorded over a longer period that the single unit activity. Finally, the possibility of decoding more than two grip types should be explored as well as the possibility of generating arbitrary hand movements from the neural activity.

8.4 Recording technique

We examined the histology results for two major purposes. One purpose was to attest the correct location of the recordings and the second to determine the extent of the tissues damages caused by the electrodes. Concerning the first aim, we measured the positions of electrical lesions performed in a terminal experiment which allowed us to confirm that the planned recording positions were accurate and matched our estimation based on MRI data. We think that the technique employed in the present study to use MR imaging of the recording chamber together with the brain that can subsequently be rotated in the plane of the recording chamber is a very accurate method and that the histology is not necessarily required for all animals to determine the recorded locations. When observing carefully the recording locations, some recordings situated in the inferior limb of the arcuate sulcus were found to be located outside of area F5 on the anterior bank of the iAS. These cells had a strong visual response to the contralateral light instruction (LED cue for power grip) and very little activity during the movement. We presume that these cells are located in area FEF. Concerning our second aim, we found no penetration traces of the microelectrodes, which suggest that tissues damages caused by the penetration of the electrodes were minimal. We nevertheless found a broken electrode tip which is due to a problem of growth of granulation tissues on the dura that makes the penetration of the dura more difficult. In order to solve this problem, sharp guide tubes could be used in every recording sessions. However, the use of sharp guide tubes for dura penetration could lead to strong scarring reaction on the dura and to damage of the underlying cortex, as observed in our lesion experiment. There is also an additional drawback that the electrodes could be situated deeper than expected. We believe that the technique that we used combined with a regular removal of excessive granulation tissue on top of the dura (dura scraping) result in very limited damages.

8.5 Future work

One of the future projects that could be realized in order to extend the findings of the present project would be to explore the decision making process in area AIP and F5. In a decision making task, the monkey is free to decide with which grip type he/she would like to grasp the object. The neural response in AIP and F5 could then be analyzed during this process and compared with the response during the delayed grasping task. This investigation would represent a step forward in the development of a brain-machine interface for hand grasping in more realistic conditions where the grip type is not instructed by an external cue but by internal decision processes. Another step toward a beneficial hand prosthetic for patients would require the decoding of many more grip types. In the present experiment, only two grip types have been studied. In order to fully understand the mechanisms of grip type encoding, neural recording should be performed during the execution of many more grip types. We have seen that most of the cells showing a preference for a certain grip type were not completely silent during the execution of another grip type. This might reveal that something might be common to the two grip types. These cells might encode hand movements broadly, i.e. in a distributed sense with each neuron contributing potentially to more than one grip type. It will be interesting to see how the brain generates the large multitude of possible grasp movements from sensory input, and it is unlikely that high-order grasp intentions already entail all the details of the movement, like the movement kinematics and dynamics.

9. APPENDIX

9.1 Publication

Behavioral/Systems/Cognitive

Context-Specific Grasp Movement Representation in the Macaque Anterior Intraparietal Area

Markus A. Baumann,[1] Marie-Christine Fluet,[1] and Hansjörg Scherberger[1,2]

[1]Institute of Neuroinformatics, University of Zürich and Eidgenössische Technische Hochschule Zürich, CH-8057 Zürich, Switzerland, and [2]Deutsches Primatenzentrum GmbH, D-37077 Göttingen, Germany

To perform grasping movements, the hand is shaped according to the form of the target object and the intended manipulation, which in turn depends on the context of the action. The anterior intraparietal cortex (AIP) is strongly involved in the sensorimotor transformation of grasping movements, but the extent to which it encodes context-specific information for hand grasping is unclear. To explore this issue, we recorded 571 single-units in AIP of two macaques during a delayed grasping task, in which animals were instructed by an external context cue (LED) to perform power or precision grips on a handle that was presented in various orientations. While 55% of the recorded neurons encoded the object orientation from the cue epoch on, the number of cells encoding the grip type increased from 25% during the cue epoch to 58% during movement execution. Furthermore, a classification of cells according to the time of their tuning onset revealed differences in the function and anatomical location of early- versus late-tuned cells. In a cue separation task, when the object was presented first, neurons representing power or precision grips were activated simultaneously until the actual grip type was instructed. In contrast, when the grasp type instruction was presented before the object, type information was only weakly represented in AIP, but was strongly encoded after the grasp target was revealed. We conclude that AIP encodes context specific hand grasping movements to perceived objects, but in the absence of a grasp target, the encoding of context information is weak.

Introduction

Humans and other primates are able to perform a wide range of complex hand movements and shape their hands both according to the target object, as well as depending on the intended manipulation. Since grasping movements are typically made to visually perceived targets, their neural control can perhaps be most easily understood in the framework of visuomotor transformations. However, such a framework needs to incorporate the fact that the same object, depending on internal goals or external context cues, can lead to different types of actions.

It has long been known that the parietal lobe plays an important role for the generation of hand grasping movements. Lesions in human parietal cortex lead to optic ataxia, a deficit in hand movement coordination (Balint, 1909; Jeannerod et al., 1984), while in the monkey, single-unit activity in the parietal lobe has been associated with the generation of hand movements (Hyvärinen and Poranen, 1974; Mountcastle et al., 1975). More recently, the group of Sakata described a region of the macaque parietal lobe, the anterior intraparietal area (AIP), which contains neurons that specifically encode the shape of the hand during grasping (Taira et al., 1990; Sakata et al., 1995, 1997; Murata et al., 2000). Moreover, the functional relevance of AIP for hand grasping was shown by inactivation (Gallese et al., 1994) and strong direct and reciprocal connections have been demonstrated between AIP and the ventral premotor area F5 (Luppino et al., 1999; Borra et al., 2008), an area that is also involved in hand movement control (Rizzolatti et al., 1988; Murata et al., 1997; Raos et al., 2006; Stark et al., 2007). Finally, there is evidence for a human homolog of AIP (Binkofski et al., 1998; Culham et al., 2003; Shikata et al., 2008).

In all these electrophysiological studies of AIP, a particular object was always grasped with the same grip. However, in everyday situations, several grip types are often possible for the same object, and we select an appropriate grip according to the intended goal of the manipulation. Such a goal-dependent grip selection can be regarded as a rule-based sensorimotor transformation, which has been attributed to the frontal cortex (White and Wise, 1999; Hoshi et al., 2000; Wallis et al., 2001; Amemori and Sawaguchi, 2006). However, signals representing action selection and task rules for eye and arm movements have also been found in the parietal cortex (Gottlieb and Goldberg, 1999; Kalaska et al., 2003; Gail and Andersen, 2006; Scherberger and Andersen, 2007).

In this study, we recorded single-unit activity in AIP while monkeys were instructed by an external context cue to grasp a handle either with a power or a precision grip. Additionally, we systematically varied a parameter of the object shape, by presenting it in five different orientations. The majority of neurons in AIP encoded the object orientation as well as the instructed grip type. We classified neurons according to the time of their tuning

Received Nov. 12, 2008; revised April 1, 2009; accepted April 6, 2009.

This work was supported by the Swiss National Science Foundation (108323/1 and 120652/1), the Swiss National Center for Competence in Research "Neural Plasticity and Repair," the European Commission (International Reintegration Grant 13072 "NeuroGrasp"), the University of Zurich (FK2004), the Zurich Center for Integrative Human Physiology (fellowship to M.C.F.), and the Swiss Association of Medical Sciences (fellowship to M.A.B.). We thank B. Disler and G. Stichel for animal care, K. Aguilar, D. Lawrence, P. Lieb, and S. Schumacher for administrative assistance, and P. Berthier and S. Rickauer for technical support.

Correspondence should be addressed to Hansjörg Scherberger, Institute of Neuroinformatics, University of Zürich and Eidgenössische Technische Hochschule Zürich, CH-8057 Zürich, Switzerland. E-mail: hjs@ini.phys.ethz.ch.

DOI:10.1523/JNEUROSCI.5479-08.2009

 0270-6474/09/296436-13$15.00/0

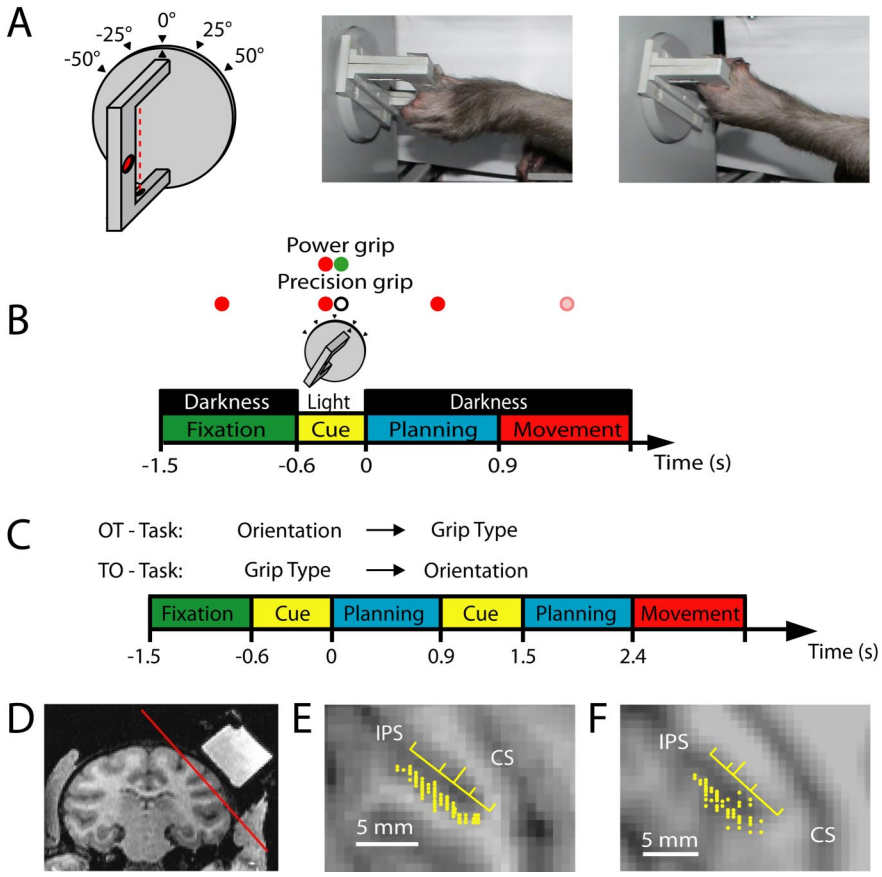

Figure 1. Task paradigm and recording penetrations. ***A***, Sketch of the handle (left) and photographs of a monkey performing a precision grip (middle) and a power grip (right). In the drawing, the red dotted line indicates a light barrier for detecting power grips, and the red oval indicates a touch sensor in a groove for sensing precision grips (a second sensor is located on the opposite side of the handle). The handle was presented in five different orientations. ***B***, Delayed grasping task. Trials were divided into four epochs: fixation, cue, planning, and movement. Monkeys initiated trials by placing both hands on rest sensors and fixating a red LED in the dark. After a variable delay (fixation, 700–1100 ms), the handle was illuminated for 600 ms (cue), revealing its orientation. At the same time, a second colored LED ("context cue") was illuminated, which instructed the animal about the required grip type (power or precision). After a variable delay (planning, 700–1100 ms), the dimming of the fixation light served as the go signal to initiate movement execution. All trial conditions were randomly interleaved. ***C***, Cue separation task. Modified task from ***B***, with the cues for grip type and orientation presented consecutively and with each cue followed by a separate planning period. In one version of this task (OT task), the orientation information preceded the grip type information, while in the other version the cue sequence was reversed (TO task). ***D***, Coronal MRI section (monkey J) with the recording chamber on the right hemisphere filled with contrast medium. The red line indicates the position of the oblique section in ***E***. ***E***, ***F***, Maps of recording electrode penetrations (yellow dots) in monkeys J and L, respectively. The yellow ruler indicates the median (long tick mark) and quartiles of the recording distribution along the intraparietal sulcus (IPS). CS, Central sulcus.

onset and found differences in function and anatomical distribution of early- and late-tuned cells.

Materials and Methods

Experimental setup. Two female rhesus monkeys (*Macaca mulatta*) participated in this study (animals L and J). Procedures and animal care were in accordance with the regulations set by the Veterinary Office of the Canton of Zurich and the Guidelines for the care and use of mammals in neuroscience and behavioral research (National Research Council, 2003).

Animals were habituated to comfortably sit upright in individually adjustable primate chairs with the head post rigidly fixed to the chair. A grasp target was located at a distance of ~30 cm in front of the animal at the level of its chest. The target consisted of a handle that could be grasped with two different grip types, either with a precision grip with index and thumb in opposition or a whole-hand power grip (Fig. 1*A*). To detect the contact of the animal's thumb and index finger during precision grips, two touch sensors were placed in small recessions. Their locations were well visible. Power grips were sensed by a light barrier. The handle was rotatable and 5 different handle orientations were tested in this experiment (upright and tilted 25 or 50° to the left or right). To illuminate the handle in the dark, two dedicated spotlights were positioned to the left and right of the handle (outside of the animal's reach). A halfway mirror was placed horizontally between the monkey's eye and the grasp target, such that the LED light stimuli used for eye fixation and task instructions (see below) were projected on the center of the handle. The mirror also ensured that the grasp target was only visible when illuminated by the spotlights. Two capacitive touch sensors (model EC3016NPAPL, Carlo Gavazzi) were fixed to the chair in front of the animal's hips to monitor the hand resting position for both hands. An optical eye tracking system (model AA-ETL-200; ISCAN) was used to monitor the animal's eye position. The animal's behavior and all stimulus presentations were controlled in LabView Realtime (National Instruments) with a time resolution of 1 ms using custom-written software. Finally, an infrared camera was used to monitor the monkey's behavior continuously throughout the entire experiment.

Tasks. Monkeys were trained to perform a delayed grasping task, in which they were required to grasp a single object (handle) in one of five possible orientations with either a power grip or a precision grip. This led to a combination of 10 task conditions that were presented randomly interleaved. While the orientation of the handle became immediately apparent after illumination, the grip type was instructed by the color of an additional LED next to the fixation light that was green for a power grip and white for a precision grip.

The monkey initialized each trial by fixating a red LED and placing both hands on the hand rest sensors while otherwise sitting in the dark (Fig. 1*B*). The trial started with a baseline epoch (fixation) of variable length (700–1100 ms, mean: 900 ms), during which the animal had to maintain its resting position in the dark. The following cue epoch (length 600 ms) was dominated by visual input: the grasp target was illuminated, hence revealing the handle orientation, and the additional LED was shown, which informed the animal about the required grasp type (power grip or precision grip). Then, during the planning epoch of variable length (700–1100 ms, mean: 900 ms), the animal could plan, but was not allowed to execute the movement, until the dimming of the fixation light gave the go signal to reach and grasp (movement epoch). Planning and movement epochs were again in complete darkness except for the red LED light that the animal had to keep fixating. Only left-hand movements (contralateral to the right recording chamber) were allowed. All correctly executed trials were rewarded with a fixed amount of juice, and the animal could initiate the next trial after a short intertrial interval (1500 ms). Error trials were immediately aborted without giving a reward. To maintain a high motivation for reward, animals were restricted from access to water up to 24 h before the training and recording sessions.

Animals were also trained in a modified version of this task, in which the instructions regarding the grip type (colored LED) and the handle orientation (spotlight) were presented sequentially in two distinct cue periods (Fig. 1*C*). In this cue separation task, each cue epoch (duration 600 ms) was followed by its own planning period (length 600–1000 ms,

mean: 800 ms) before the movement was executed. Animals were trained to perform this cue separation task in two variations: either with the object orientation shown in the first cue epoch and the grip type instruction in the second (OT task), or with the grip type instruction presented first and the object orientation in the second cue epoch (TO task). When testing neurons in this cue separation task, trials of both versions (OT and TO task) were always run randomly interleaved with each other and with trials of the (standard) delayed grasping task.

Surgical procedures. To prepare for the recording experiments, a titanium head post was secured in a dental acrylic head cap, and a custom made oval-shaped recording chamber (material PEEK; outer dimensions: 40 × 25 mm) was implanted over the right hemisphere on top of AIP with the skull bone removed underneath the chamber. This allowed the insertion of recording microelectrodes through the dura in subsequent recording sessions without discomfort to the animal. The recording chamber and head post were fixed on the skull with bone cement (Refobacin Plus, Biomet Orthopaedics) and reinforced with titanium (Synthes) and ceramic bone screws (Thomas Recording).

All surgical procedures were performed under sterile conditions and general anesthesia (induction with ketamine 10 mg/kg, i. m., atropine 0.05 mg/kg, s.c., followed by intubation, isoflurane 1–2%, and analgesia with 0.01 mg/kg buprenorphine, s.c.). Heart and respiration rate, electrocardiogram, O_2 saturation, and body temperature were continuously monitored, and systemic antibiotics and analgesics were administered for several days after each surgery. Animals were allowed to recover for at least 1 week before behavioral training or recording experiments recommenced.

MRI scans. Before surgical procedures, a structural magnetic resonance image (MRI) of the brain and skull was obtained from each animal to help guide the chamber placement. For this, animals were sedated (ketamine 10 mg/kg, i. m., atropine 0.05 mg/kg, s.c., and xylazine 0.5 mg/kg, i. m.), supplemented with O_2 (1 L/min), and their heart rate, O_2 saturation, and end-tidal CO_2 level continuously monitored. After placing in the scanner (GE Healthcare 1.5T) in a prone position, T1-weighted volumetric images of the brain and skull were obtained (3D IR-SPGR sequence, acquired voxel size 0.7 mm isometric, TR 7.6 ms, TE 3.16 ms, flip angle 12°, 400 ms inversion time) and realigned off-line in stereotaxic coordinates using AFNI 3.0 (for details see: Scherberger et al., 2003). The stereotaxic location of the tip of the right intraparietal sulcus was then obtained (approximate location: 8 mm anterior, 22 mm lateral) to guide the placement of the recording chamber over AIP.

Weeks after chamber implantation, a second MRI scan was obtained with the recording chamber filled with an MRI sensitive contrast medium (Gadolinium solution diluted in saline 1:2000). This allowed the mapping of cortical structures in the coordinates of the chamber, which greatly facilitated to target AIP with subsequent electrode penetrations (Fig. 1*D–F*).

Neural recording. Single unit (spiking) activity was recorded using glass-coated tungsten electrodes (impedance: 1–2 MΩ at 1000 Hz) that were positioned by a 5-channel micromanipulator (MiniMatrix, Thomas Recording) that was directly attached to the recording chamber. Neural signals were amplified (400×), digitized with 16 bit resolution at 30 kS/s using Cerebus Neural signal processor (Bionics), and stored to disc together with the behavioral data. To coarsely monitor the tuning properties of the recorded neurons during data acquisition, spike detection was performed in real-time (Cerebus hardware) and analyzed for various task conditions using Matlab (MathWorks). However, all quantitative analysis reported here was performed off-line as described below.

Data analysis. Raw data traces were bandpass filtered (600–8000 Hz) using Matlab and spikes were extracted and sorted using Offline Sorter (Plexon). The quality of single unit isolation was assessed with the following criteria: (1) the separation of waveform clusters in projections onto the first three principle component axes, (2) the homogeneity of waveforms, and (3) the presence of a refractory period in the interspike interval (ISI) distribution. A retrospective analysis revealed that <0.26% of all ISIs were shorter than 1 ms. Single units were included in our database if they were stably recorded for at least 7 trials per condition in the delayed grasping task (total of 70 trials) and at least 5 trials per condition in the cue separation task (total of 150 trials).

Peristimulus time histograms (PSTH) for the visualization of spike rates were generated by replacing each spike with a kernel function and then averaging all such functions across all spikes and trials. To obtain PSTHs that are continuous as well as causal (i.e., the PSTH at any given time point is not influenced by spikes that occur in the future), we chose the kernel to be a gamma-distribution function, hence replacing each spike at time t_s with the following time-shifted function:

$$R(t) = \begin{cases} (t - t_s)^{\alpha-1} * \beta^{\alpha} * \exp(-\beta(t - t_s))/\Gamma(\alpha) & \text{if } t \geq t_s \\ 0 & \text{if } t < t_s \end{cases}.$$

The shape ($\alpha = 1.5$) and rate parameter ($\beta = 30$) were chosen to achieve little delay (kernel peak at 16 ms) and an SD of ~40 ms. It is important to note that PSTHs were only used for illustration; all quantitative analysis was based on exact spike counts. To obtain population averaged PSTHs, individual histograms were averaged across the cell population. For this, preferred and nonpreferred conditions were defined as follows:

For each neuron, the preferred grip type and orientation were determined from the mean firing rates in the delayed grasping task taken in the time interval from the cue onset to the end of the movement epoch, which was then averaged across all trials of the same grip type or the same object orientation, respectively. The preferred grip type was then defined as the grip for which the mean rate was largest while the off type was defined as the other grip. Likewise, the preferred orientation was defined as the object orientation for which the firing rate was maximal, while the off-orientation was taken as the object orientation at 75° angular distance from the preferred one. For neurons with preferred orientation of 0°, we randomly chose +50° or −50° as the off-orientation, since no 75° condition existed. This definition was chosen to select the off-orientation not exclusively from the two extreme orientations (±50°). However, all results stayed essentially the same if the off-orientation was defined as the orientation with maximal angular distance to the preferred orientation, or as the orientation with the lowest firing rate.

To test whether neurons were significantly tuned for grip type and/or orientation in a particular task epoch (fixation, cue, planning, or movement), we first determined in each trial the mean firing rate (spike count/length of epoch) and then applied a two-way ANOVA with group factors grip type and orientation. This compared the rate variance within conditions to across conditions. Neurons were considered to be significantly tuned for grip type or orientation for p values <0.01, and if they fired at least 5 spikes/s in the preferred condition.

In addition, tuning significance for grip type and orientation was tested at multiple time points *t* using a 2-way ANOVA on the spike count in a 200 ms window centered around *t*. This test was repeated in time steps of 50 ms (sliding window ANOVA). Due to the variable length of the planning period, trials were first aligned to cue offset up until 0.6 s after cue offset; after that they were aligned to movement start (release of the hand rest button). Criteria for significant tuning were the same as for the ANOVA analysis of the fixed time epochs.

For the tuning analysis in the cue separation task, we applied the same 2-way ANOVA as in the (standard) delayed grasping task, but with a significance level of $p < 0.05$ due the lower number of trials per condition (minimum 5, average 6.8; standard task: minimum 7, average 9.8). Since the cue separation task contained 2 planning periods of variable length, trials were aligned to the cue offset of the first and second cue as well as to the movement start (hand rest release), and realignments were placed 0.6 s after each cue offset.

To estimate the time when the number of significantly tuned cells for grip type or orientation sharply increased (during the cue and movement epoch), we determined the time in each epoch when the increase became half-maximal. For this, we first computed a linear interpolation of the number of significantly tuned cells (as obtained from the sliding window ANOVA) in steps of 2 ms (using Matlab command interp). We then determined, for each epoch, the time when this curve became half-maximal with respect to a baseline level. This baseline was set to 0 for the cue epoch and to the value of the curve at the time of the go signal for the movement epoch. To assess significance of possible time shifts in the increase of grip type and orientation tuning, we used a Monte Carlo procedure, in which 1000 repetitions of the same analysis were per-

formed with random shuffling of the labels "grip type tuned" and "orientation tuned," to determine the null distribution and its associated significance level.

Furthermore, we quantified the time in the task when each neuron first became significantly tuned for grip type or orientation. We called this the tuning onset of grip type and orientation tuning, and defined it as the first time when a neuron was significantly tuned in the sliding window ANOVA in at least five consecutive steps. If this occurred, tuning onset was set to the center of the first window; if not, it was set to infinity. Using this quantitative measure, we classified each neuron, separately for grip type and orientation, in one of the four categories: (1) early, (2) middle, (3) late, or (4) no tuning onset, corresponding to the tuning onset falling in the cue, planning, or movement epoch, or never occurring.

Furthermore, we quantified the number of cells preferring each of the two grip types and five grip orientations separately for the different task epochs. For this, the same definition of preferred grip type and orientation was used as for the calculation of population PSTHs, except it was restricted to the task epoch in consideration.

Finally, we applied a receiver operating characteristic (ROC) analysis (Britten et al., 1992) to various task epochs to assess for each individual cell, how well its firing rates during precision grip trials could be discriminated from those during power grip trials. We calculated the area between the ROC curve and the no-discrimination (diagonal) line as a measure of discriminatory power. To remove interaction effects of superimposed orientation tuning, we computed this measure separately for each orientation and averaged the five results. Significance levels were assessed by performing a Monte Carlo analysis for each cell as explained above, this time with random shuffling of the labels for power and precision grip between trials. The 95th percentile of the resulting distribution was then taken as the significance level.

Results

We recorded a total of 571 single cells in two monkeys (monkey L: 299 cells, monkey J: 272 cells) while the animals performed the delayed grasping task. Results were essentially the same for both animals and are therefore reported together.

Both monkeys performed the task with high accuracy. Errors due to the execution of the wrong grip type occurred only in ~5% of all trials. Observation of the animals via infrared camera during task performance revealed that the handle was approached with the hand preshaped and in the matched orientation. Analysis of the movement times also suggested that the animals did not approach the target in a "standard" orientation and then adjusted the hand orientation based on sensory (tactile) feedback information: the influence of the object orientation on the movement time was quite small to allow for such feedback adjustments. The median movement times for precision grips/power grips were 0.53 s/0.22 s (−50° orientation), 0.47 s/0.21 s (−25°), 0.46/0.21 s (0°), 0.47/0.21 s (+25°), and 0.53 s/0.21 s (+50°). Monkeys kept holding the object on average for 0.36 s. No preshaping occurred before the go signal, and the hands were kept motionless on the sensor pads.

Tuning for grip type and orientation

A large majority of cells were modulated by the delayed grasping task. Three typical neurons are shown in Figure 2. Neuron A showed a sharp increase of its firing rate immediately after the movement instruction was given (cue epoch), in particular for objects oriented to the right (+25/+50°), and more strongly for power grips than for precision grips. This activity pattern was preserved throughout the task until the movement was executed. The example neuron was therefore modulated by grip type and orientation in all three task epochs (cue, planning, and movement). Note that the timing of the early rise for trials with rightward orientations of the handle was identical for both grip types (left and right panel), before the curves separated shortly afterward.

A second type of neuron is depicted in Figure 2*B*. It showed a clear modulation of its firing rate with object orientation immediately after cue presentation, while throughout the cue and planning epoch its activity was identical for power and precision trials. However, during movement execution (starting immediately after handrest release) the firing rate of precision trials increased with respect to power trials. Therefore this neuron represented the object orientation from the object presentation onward, while grip type modulated the neuron only during movement execution.

Finally, neuron C in Figure 2 did not respond at all after cue presentation, neither for the grip type nor for the object orientation. However, it responded vigorously during movement execution with a strong peak for precision grips while being indifferent to object orientation.

These examples illustrate the variety in our dataset. As a summary, Figure 2*D* shows the population firing rate across all 571 neurons for each neuron's preferred and nonpreferred grip type and orientation. Both grip type and object orientation were well represented in the population during cue presentation and remained so until the movement was finished. Importantly, this was true even if the definition of the preferred and nonpreferred condition was based on the activity during the movement epoch alone, indicating that this finding is not a selection artifact.

To quantify the number of cells with a particular tuning in each task epoch, we performed, for each cell, a two-way ANOVA with factors grip type and orientation on the firing rates within each task epoch (Table 1). We found that in the course of the trial, these two variables behaved distinctively (Fig. 3*A*). During the cue period the fraction of neurons showing specificity for the object-cued factor, i.e., the object orientation, accounted for 55% of all cells, and this ratio stayed approximately constant throughout the planning and movement epochs. In contrast, only ~25% of the cells showed selectivity for the context-cued variable (grip type) during the cue period; however this value increased to 37% during the planning epoch and 58% during movement execution, reaching a level that was eventually similar to the number of orientation-tuned cells.

Of the cells which did not show tuning for either grip type or orientation, more than half (cue: 57%, planning: 62%, movement: 68%) displayed significant rate variations (increase or decrease) when compared with the baseline activity in the fixation epoch (2-tailed t test, $p = 0.01$). Presumably, some of these neurons could be tuned for other objects or grip types than the ones we tested in this study.

To further investigate grip type and orientation tuning over time, without constraining the analysis to predefined epochs, we extended the 2-way ANOVA on a sliding window (window width: 200 ms, step size: 50 ms), which revealed marked differences between the two variables (Fig. 3*B*). First, the number of orientation-selective cells after cue presentation rose considerably earlier than for grip type-selective cells. By measuring the time at half height of this increase during the cue epoch, this time difference was found to be ~150 ms in the population ($p \ll 10^{-3}$, Monte Carlo procedure). This time difference was also observed in individual neurons (e.g., see: Fig. 2*A*), perhaps indicating that the processing of an abstract cue took longer than processing of an object cue. During the planning epoch, both fractions of tuned neurons stayed on a plateau, with the orientation fraction slightly larger than type; while during movement execution, the number of grip type specific neurons further in-

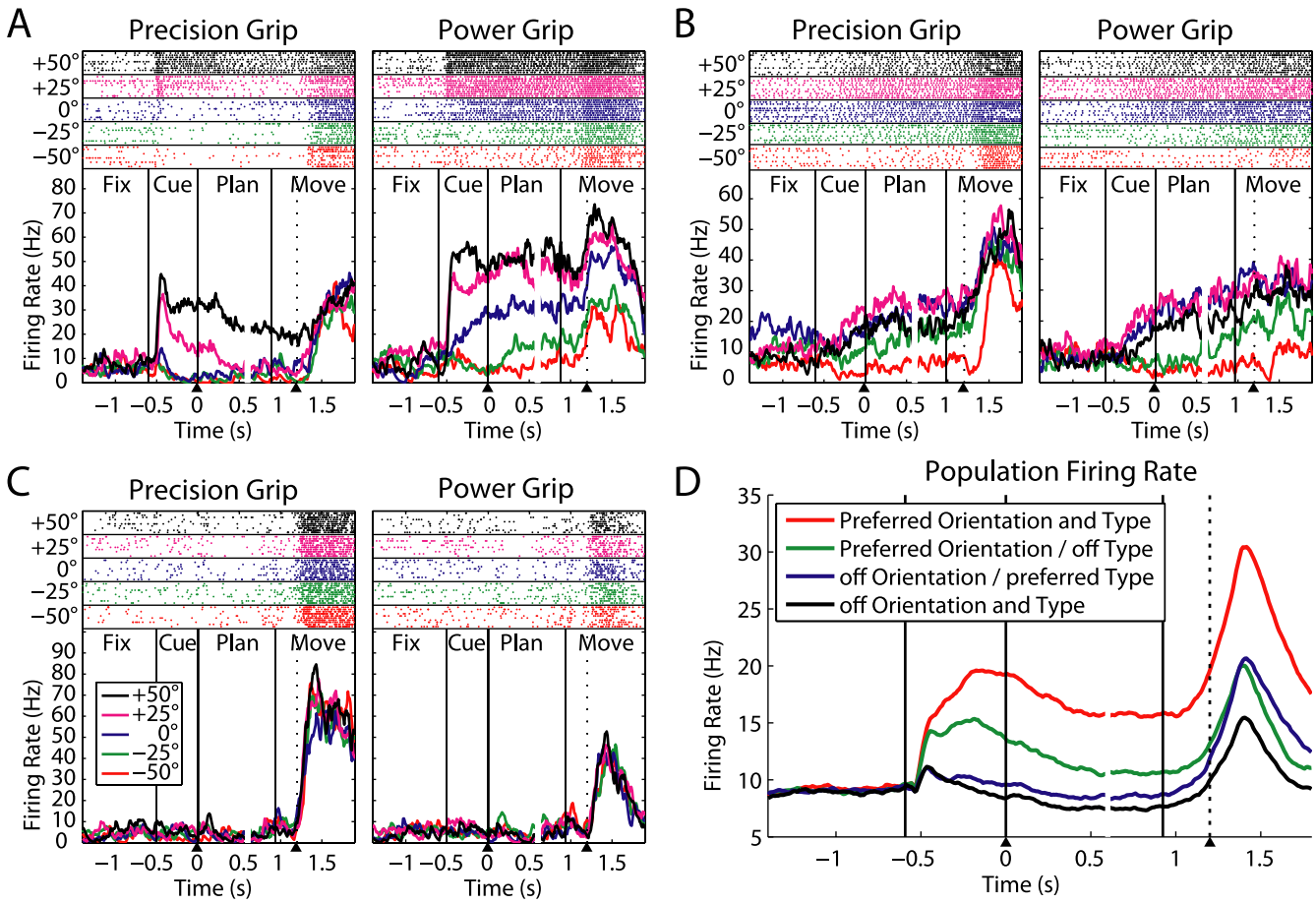

Figure 2. Three example neurons with different tuning onsets. For each neuron, precision grip trials are shown on the left panel and power grips on the right panel. Different colors indicate various handle orientations, for which spike rasters (on top) and averaged firing rates (at bottom) are shown individually. The dotted line within the movement epoch indicates the release of the hand rest button (movement start). All trials are aligned to both the end of the cue epoch and the start of the movement (arrow heads below); gaps in the curves (at ~0.6 s) indicate the realignment. ***A***, Neuron that exhibits tuning for the handle orientation and the instructed grip type starting in the cue period and extending until movement execution. ***B***, Neuron with tuning for the handle orientation starting in cue, but with significant grip type modulation only during movement execution. ***C***, Neuron showing no response during cue presentation and movement planning, but with a strong selectivity for precision grips during movement execution without significant orientation tuning. ***D***, Population firing rate across all 571 neurons for each combination of the cells' preferred and nonpreferred grip type and orientation.

Table 1. Cell classification by tuning in task epochs

Orientation tuning				Grip type tuning			
Cue	Plan	Move	Percentage	Cue	Plan	Move	Percentage
+	+	+	30%	+	+	+	12%
+	+	−	11%	+	+	−	4%
+	−	+	6%	+	−	+	3%
+	−	−	8%	+	−	−	6%
−	+	+	7%	−	+	+	15%
−	+	−	3%	−	+	−	6%
−	−	+	12%	−	−	+	28%
−	−	−	23%	−	−	−	26%

Left, List of cell classes (different rows) according to the presence (+) or absence (−) of significant orientation tuning in the task epochs: cue, planning, and movement (2-way ANOVA, see Materials and Methods). Percentages indicate the fractional size of each class in our population ($n = 571$). Right, Corresponding classification for grip type tuning.

creased and actually exceeded the number of orientation-selective cells, which was due to neurons that became type specific only during the movement epoch (e.g., as in Fig. 2*B*,*C*). However, no significant time difference was found between the two fractions in this second increase ($p > 0.3$).

In summary, the population analysis showed that the representation of grip type, while already present in the cue period shortly after the instruction was given, strongly increased toward movement execution, both in absolute terms (number of tuned cells) and in relation to the number of cells coding for orientation. These different roles of AIP for the encoding of an object-cued factor (orientation) and a context-cued factor (grip type) are further analyzed in the next section.

Tuning onset

As we have seen in the example neurons (Fig. 2*A*–*C*), some cells were grip type modulated already in the cue period, while others were tuned only during movement execution. Similarly, cells ex-

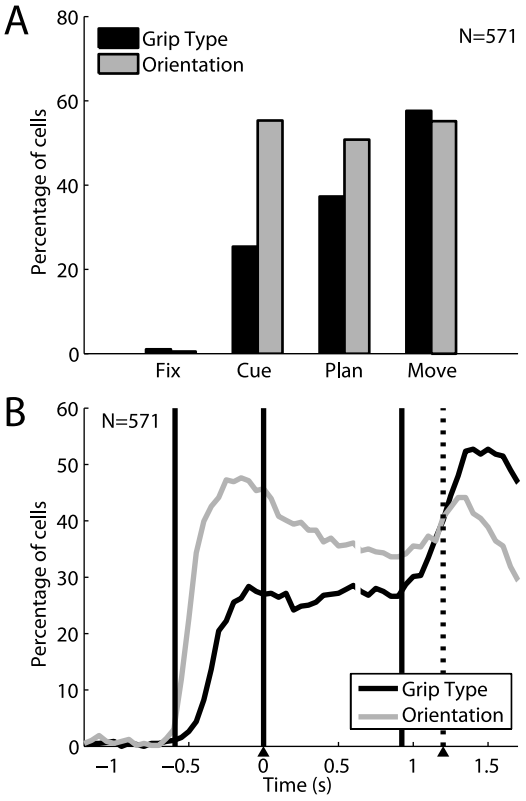

Figure 3. Orientation and grip type tuning in the neuronal population ($n = 571$). ***A***, Fraction of cells showing tuning for grip type (black) and handle orientation (gray) in the different task epochs (two-way ANOVA; see Materials and Methods). Tuning for object orientation was constant from cue to movement, while grip type tuning increased over time. ***B***, Percentage of tuned cells in a sliding window (width: 200 ms, centered on each data point). During cue, tuning for orientation started ~150 ms earlier than for grip type. Grip type tuning increased in two steps: one during cue and one during the movement epoch. Trials are aligned on cue offset and movement onset (as in Fig. 2).

hibited different onset times for the tuning of orientation. To quantify this effect, we determined each cell's tuning onset for grip type and object orientation, respectively (see Materials and Methods). Figure 4 (top row) shows, separately for grip type (left panel) and object orientation (right panel), the time periods when neurons were significantly tuned (black lines). Each neuron is represented by one row, and neurons were sorted (along the *y*-axis) according to their tuning onset. The graph emerging from the white–black transition depicts the cumulative distribution of the tuning onset, which is shown below in its derivative (histogram) form (bottom panels). For grip type (left panels), the tuning onset distribution was clearly multimodal with a first peak during cue presentation followed by a second peak of similar size after the go signal, and only a small fraction of cells located in between. For object orientation, the majority of cells had a tuning onset during cue presentation and only a few cells became tuned late in the task.

To describe the relationship between the onset of grip type and orientation tuning, we classified neurons into four groups according to their tuning onset (early, middle, late, and none), separately for grip type and orientation tuning. Early, middle, and late onset corresponded to the cue, planning, and movement epochs. Table 2 shows a 4×4 contingency table of the combined tuning onset for grip type and object orientation. As can be readily seen, this contingency table is not statistically independent (Pearson's $\chi^2 = 88.5$, df $= 9$, $p \ll 10^{-3}$).

During the cue period, neural responses were dominated by the object feature orientation. While approximately half of the recorded cells (278/571, 49%) showed an early onset of orientation tuning, only 152 cells (27%) signaled the grip type. A considerable part of the orientation-sensitive group was also modulated by the instructed grip (108/278, 39%), leading to the largest class of cells (for an example, see Fig. 2*A*). However, neurons that were orientation tuned during the cue period were not always grip type tuned at the same time. In fact, many of these cells only became tuned for the grip type during planning (40) or movement (53) (e.g., Fig. 2*B*), and others not at all (77). In contrast, cells that were grip type tuned in the cue period were very likely also orientation tuned (108/152, 71%), while the other groups with early type tuning were small. Together, these results suggest that during the cue period, grip type coding is only modulating the primary coding of object features.

Only a few neurons had their tuning onset during the planning period. Some cells that were already orientation tuned in the cue became additionally grip type tuned in the planning epoch (40). All other groups were very small. Therefore, most of the activity during the planning period (Fig. 3*A*,*B*) was a continuation of the activity already present during the cue epoch, which is consistent with a role of AIP, and of the parietal cortex in general, in working memory (Mountcastle et al., 1975; Sakata et al., 1995; Murata et al., 2000; Andersen and Buneo, 2002).

Neurons whose tuning began during the movement epoch behaved quite differently from those with early tuning onset. Late onset tuning was directed primarily to the grip type rather than the object orientation. The largest group of these neurons was selective for the grip type but lacked orientation tuning (75) (see also Fig. 2*C*). A second large group consisted of cells that had developed orientation selectivity during the cue period and now additionally expressed a late onset tuning to grip type (53) (see Fig. 2*B*). A third group of neurons developed tuning to both the grip type and the orientation during the movement period (37). These latter neurons accounted for the majority of cells with late orientation tuning. In contrast, neurons that became orientation tuned during the movement period, without tuning to grip type, were very rare (12).

Note that cutaneous tactile information could not have been the major source of input for late-onset cells, because the movement epoch ended when the hand had grasped the object. Also, previous studies found little or no neurons in AIP with somatosensory responses (tactile or joint-related) (Taira et al., 1990; Murata et al., 2000). Therefore, these cells are most likely related to motor output. Together, our findings indicate that neurons with a late tuning onset, in contrast to early-tuned cells, primarily encode the grip type, and only secondarily (and optionally) the object orientation.

Cue separation task

Given these asymmetries between the coding of grip type and orientation in AIP, we also tested a subset of 120 neurons in the cue separation task, in which the two task instructions were presented in two cue epochs that were separated by an additional planning period (Fig. 1*C*). This cue separation task was run in two versions, with either the object orientation presented in the first cue epoch and the type instruction in the second (OT task), or the type instruction in the first cue epoch and the orientation in the second (TO task). In addition, all neurons were also tested in the standard delayed grasping task, where similar results were obtained as in the full dataset. This indicated that our subset was representative. An example neuron tested in the cue separation

task is shown in Figure 5. For clarity of presentation, only 4 task conditions are shown: the preferred (−25°) and the nonpreferred orientation (50°) for the two grip types. In the standard task (Fig. 5*A*), the neuron was tuned for orientation and grip type in all three epochs, with the highest activity for power grips and the object tilted to −25°. When only the object orientation was revealed during the first cue (OT task) (Fig. 5*B*), the cell showed a clear response to the preferred orientation, independent of grip type. Then later, starting with the second cue, the firing rate was additionally modulated with respect to the instructed grip type. In contrast, when the grip type was instructed first (TO task) (Fig. 5*C*), the cell's firing rate did not reflect this information, but stayed low for all conditions. Only when the object orientation was revealed during the second cue did the neuron respond vigorously and with preference for power grips in the preferred orientation, obviously combining the newly presented orientation information with the grip type information that was given before.

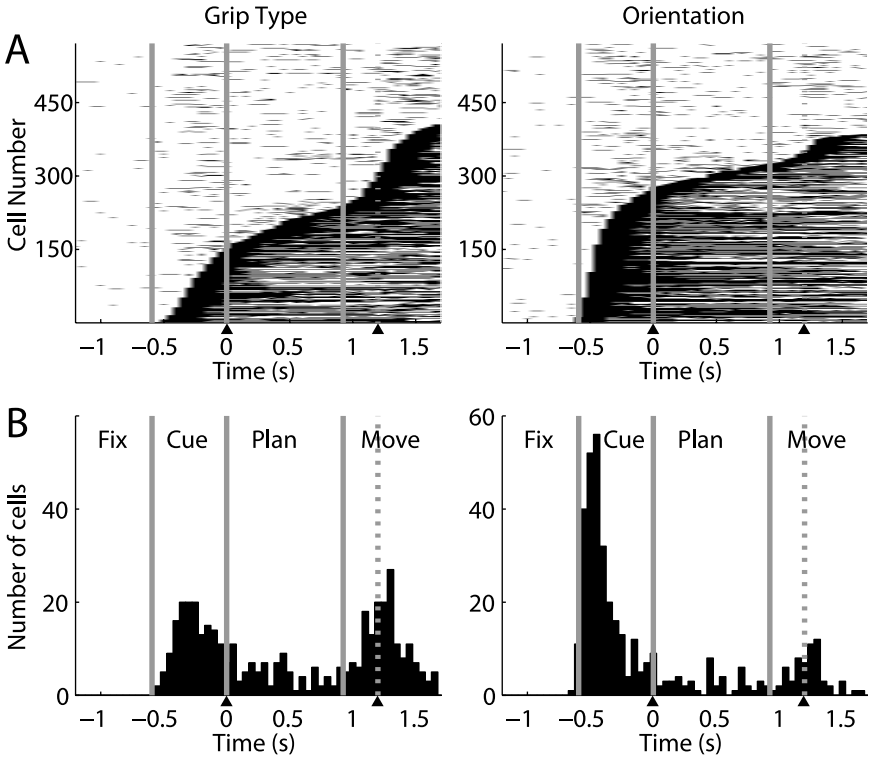

Figure 4. Times with significant tuning in the neuronal population. ***A***, Sliding window analysis (two-way ANOVA) for each cell (*y*-axis) at each time step (*x*-axis). Significant grip type (left) and orientation tuning (right) is indicated by black squares ($p < 0.01$). Cells are ordered by tuning onset (first occurrence of five consecutive significant steps). ***B***, Histogram of tuning onset for grip type (left) and orientation (right) across the population.

Such a response pattern, with a strong modulation for orientation when presented first, and a delayed modulation for grip type that kicked in only after the orientation cue was revealed, was typical for many cells, as shown in our population analysis (Fig. 6). The top panels show the firing rate of the population in 4 conditions (preferred and nonpreferred type and orientation). In the first cue of the OT task (left panel), the population activity increased strongly for both conditions in which the handle was presented in the preferred orientation. This orientation modulation persisted despite some decrease in activity during the first planning period. When the grip type information was subsequently provided in the second cue, the population response decreased for the nonpreferred grip type, but remained constant for the preferred grip type instruction. This activity pattern suggests that the neural population in AIP encodes movement plans for both types of actions simultaneously, until the ambiguity between the two grip types is resolved by the type instruction.

The activity pattern in the OT task also became apparent in the sliding window ANOVA (Fig. 6*B*, left). Object orientation was maximally encoded at the end of the first cue. After the second cue, grip type was represented in ~35% of all cells, similar to the planning phase of the delayed grasping task. A second increase in grip type selectivity then occurred during movement execution.

The population activity in the TO task showed a quite different pattern (Fig. 6*A*, right panel). Neurons responded weakly to the grip type instruction (first cue), but when the object orientation was presented in the second cue, the population activity became tuned for the object orientation and the grip type at once, similar to the population response in the delayed grasping task (Fig. 2*D*). The sliding window analysis (Fig. 6*B*, right) showed a reduced number of cells, ~20%, that displayed grip type selectivity before the object presentation. This selectivity is reflected in the slight increase in population activity of the preferred grip type conditions (red and blue curves) during the first planning epoch (Fig. 6*A*, right). Overall however, this modulation was weak; only after the presentation of orientation information in the second cue was there an increase in the number of grip type-tuned neurons to a similar level to that observed in the OT task.

Given the weak modulation in the population activity during the first planning of the TO task, the amount of grip type selectivity in the sliding window ANOVA seems surprisingly high, especially when compared with the level found in the second planning epoch. This could in part be explained by an increased sensitivity of the ANOVA for grip type effects in the absence of orientation information before the second cue, due to a reduction of within-group variance in the power and precision groups.

To compare grip type effects at different task phases of the TO task without being influenced by the presence or absence of orientation information, we performed ROC analyses separately for each orientation and averaged the five results (see Materials and Methods). This allowed us to compute, for each individual cell and any task epoch, how well the firing rates during precision grip trials could be discriminated from those during power grip trials. The result of this analysis showed that only 24 cells (20%) significantly discriminated between power and precision trials before the object cue, while this value rose to 62 (52%) after object presentation, confirming that many more cells displayed a grip type effect after object presentation. These findings indicate that the representation of grip type is strongly reduced in AIP in the absence of object information, which corresponds well with our cell classification in the full dataset (Table 2), where grip type-selective neurons during cue were usually orientation tuned as well.

Table 2. Cell classification by tuning onset

	Grip type				
Object orientation	Cue	Planning	Movement	None	Sum
Cue	108[A]	40	53[B]	77	278 (49%)
Planning	11	14	9	8	42 (7%)
Movement	9	7	37	12	65 (11%)
None	24	18	75[C]	69	186 (33%)
Sum	152 (27%)	79 (14%)	174 (30%)	166 (29%)	571 (100%)

Contingency table of tuning onset for type (columns) and orientation (rows) for all neurons in our population ($n = 571$). Example neurons for the marked classes (A–C) are shown in Figure 2*A–C*.

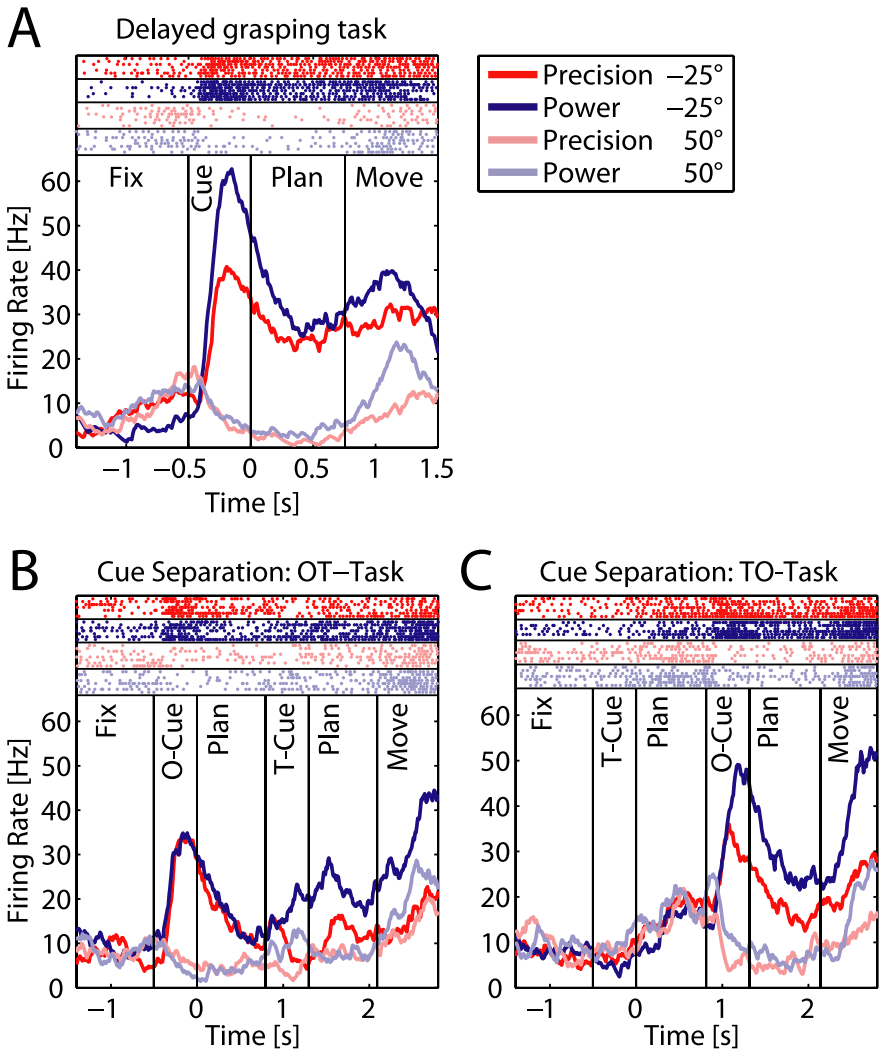

Figure 5. Neural activity in the cue separation task. Panels show one example neuron during the delayed grasping task (***A***) and the cue separation task: OT task (***B***), TO task (***C***). Different grip types are shown in red (precision) and blue (power), while the two grip orientations are shown in light and dark color. ***A***, The neuron was early tuned for both parameters, showing highest activity for power grips at −25° orientation. ***B***, In the OT task, presentation of the object in the −25° orientation evoked a strong response, which was then differentially modulated for the two grip types after the second cue. ***C***, In the TO task, the cell did not respond to the type cue when presented in the absence of the object. However, the cell responded vigorously after the orientation cue with a preference for power grips in the preferred orientation.

Coding schemes

As we have shown, many neurons in AIP represent the object orientation or the grip type in one or several trial epochs. Here we explore, which grip types and object orientations are preferred in the population, and how these representations change over time. Figure 7*A* shows the ratio of cells that prefer precision vs power grip. During the cue period, half of the grip type specific cells preferred precision grip and the other half power grip. However, later on in the trial, this ratio shifted in favor of precision-preferring cells, such that during movement execution, the ratio of precision- to power-grip-preferring cells was ~60 to 40.

A somewhat similar development became apparent when looking at the preferred orientation (Fig. 7*B*). During cue presentation, the preferred orientations were fairly evenly distributed with only a slight overrepresentation of the extreme (±50°) orientations (47% vs 40% expected from uniform distribution), while during movement execution, the fraction of neurons preferring extreme orientations increased to 59%.

These shifts of preference in the population were not caused by preference changes of individual neurons. Figure 8*A* illustrates the consistency of grip type preference between consecutive epochs. Between adjacent task epochs, only 2% (cue to planning) and 4% (planning to movement) of the cells tuned in one epoch changed their grip type preference between power and precision (gray bars), while the overwhelming majority of cells remained either tuned for the same grip (black bars; 64% and 70%, respectively) or were no longer significantly tuned (white bars; 34% and 26%). This indicates that in general, the preferred grip type did not change across task epochs but remained constant throughout the task. Similarly, the cell's preferred orientation usually did not change systematically between task epochs, but stayed the same or shifted by one step at most (Fig. 8*B*,*C*). Note that a shift by one is usually not meaningful, since the cell's firing rate was often not significantly different between neighboring orientations.

We demonstrated that the tuning of individual neurons remained largely constant during the task whereas the population tuning shifted at later task epochs toward an overrepresentation of precision grips and extreme orientations. This apparent discrepancy suggests that different populations of cells with diverse coding schemes might be active at different task epochs. To explore this further, we determined the preferred grip type and preferred orientation separately for the three cell groups of early, intermediate, and late tuning onset. We found, in fact, that the cell group with early-onset grip type tuning preferred precision grips and

power grips equally likely throughout the task (in the cue, planning, and movement epoch); in contrast, the cell group with a late tuning onset for grip type (in the movement epoch) had a preference ratio for precision and power grips of 70 to 30 (Fig. 9*A*). Similarly, the cell group with the orientation tuning onset during the cue epoch had a fairly constant rate of neurons preferring terminal orientations (±50°) during the course of the task (cue: 49%, planning: 52%, movement: 54% of cells), while neurons with a late onset of orientation tuning mainly preferred extreme orientations (76% of cells) (see Fig. 9*B*). Moreover, for both grip type and orientation, the middle group behaved similarly to the early group, suggesting that they followed the same scheme as early-tuned neurons. Such tuning differences between cells with early and late tuning onset suggest that these cell groups encode different entities earlier in the task during movement instruction, compared with later during movement execution. During movement instruction, similar numbers of neurons are allocated for the representation of the two grip types and for the various object orientations. However, later in the task, this coding scheme seems to change in favor of a motor representation, in which the precision grip (being more difficult) requires more cortical resources than the power grip while the preponderance of neurons preferring extreme orientations could indicate a push–pull representation for hand rotation in the pronation–supination direction.

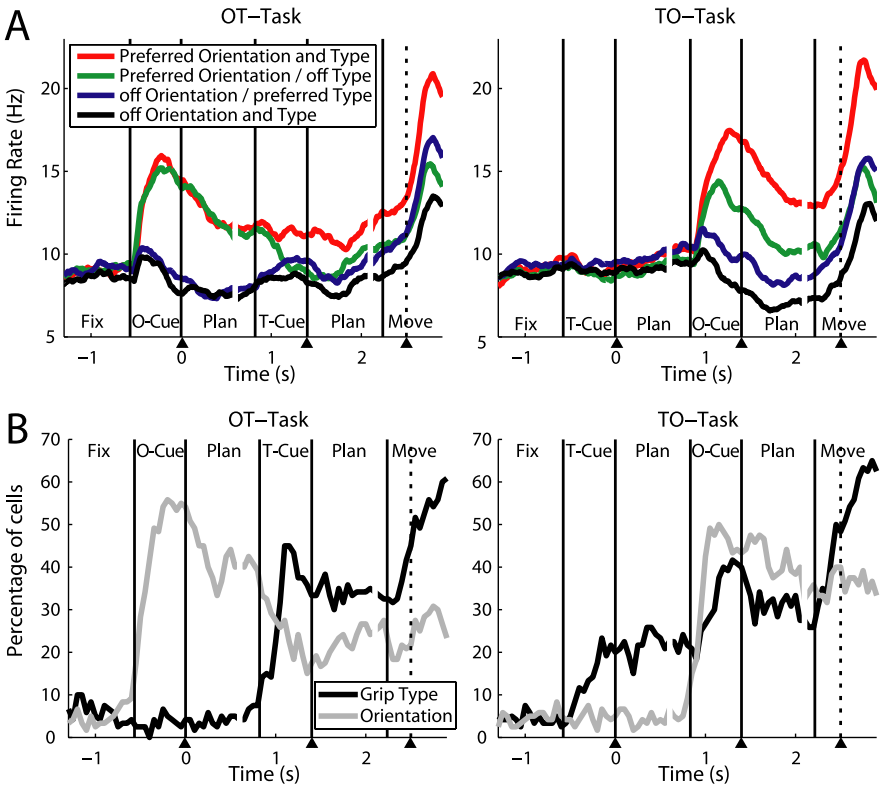

Figure 6. Population analysis of the cue separation task. ***A***, Population firing rates in the cue separation task ($N = 120$) with OT task on the left and TO task on the right panel. For each cell, its preferred type and orientation was established in the delayed grasping task (data not shown). ***B***, Fraction of cells that were significantly tuned by grip type and orientation in the course of the OT and TO task (sliding window ANOVA as in Fig. 3*B*).

Anatomical organization

Finally, we analyzed whether there is a correlation between the reported functional classification (Table 2) and the location along the intraparietal sulcus (IPS) where the cells were recorded. For this we projected the recording coordinates of each neuron onto an axis parallel to the IPS and then split the cell population into eight bins, according to the cells' posterior-anterior position on that axis, such that each bin contained the same number of cells. This allowed us to calculate, separately for each bin along the IPS, the fraction of cells that belonged to a particular cell class (e.g., early onset orientation-tuned cells). Figure 10 displays the result for orientation and grip type-tuned cells with early and late tuning onset, respectively. Although all cell classes were present in all bins, the distributions were clearly nonuniform, but instead showed steady gradients. Cells with an early tuning onset (orientation or grip type) were found with a higher probability in the posterior recording sites. In contrast, cells with late tuning onset (orientation or grip type) occurred more frequently in the more anterior segments. To assess the significance of these effects, we compared the occurrence of cell classes in the anterior half of the recordings to those in the posterior half (i.e., to the left and the right of the dashed lines in Fig. 10; for the anatomical location of the median, see Fig. 1 *E*,*F*). For a cell class that was evenly distributed along the anterior–posterior axis, one would expect to see an even distribution of neurons between the anterior and posterior halves. Instead we found that 60% of all cells with early onset of

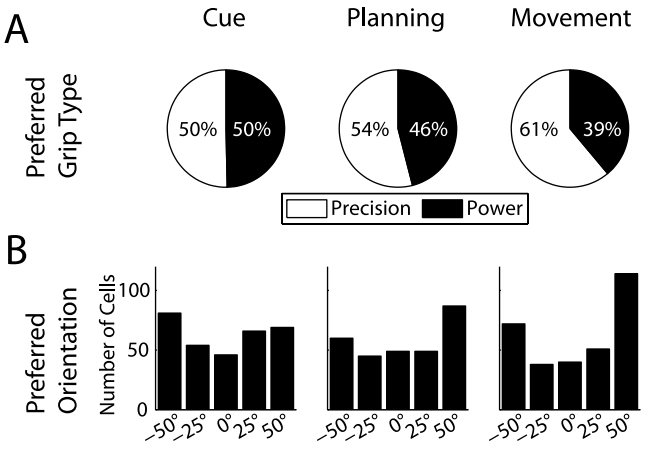

Figure 7. Distribution of preferred grip type and orientation in various task epochs. ***A***, Ratio of cells preferring precision (white) or power grip (black). From cue to movement, the fraction of cells encoding precision grip increased substantially. ***B***, Number of cells preferring each of the five orientations. In the movement epoch, the distribution shifts in favor of terminal orientations (±50°).

orientation tuning and 61% of the cells with early onset of grip type tuning were located in the posterior half of the neural population, while 66% of the cells with late onset of orientation tuning and 67% with late onset of type tuning were located in the anterior half. All of these findings were significantly different from the null hypothesis of a uniform distribution (binomial test, $p < 0.01$). Additionally, cells that displayed early orientation tuning but late tuning for grip type (as the example cell in Fig. 2*B*) did not show such a gradient but were evenly distributed among

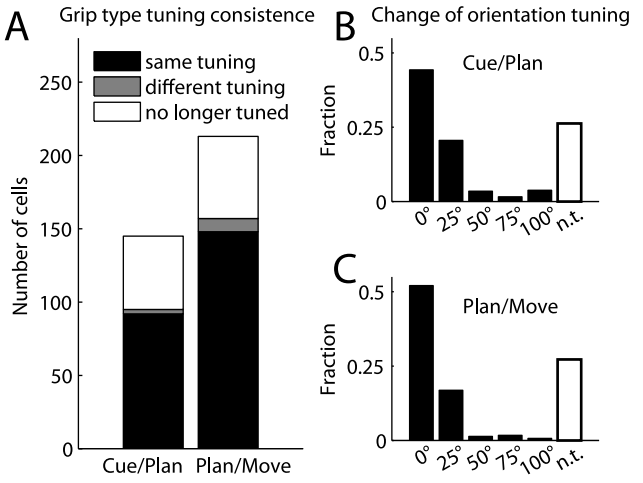

Figure 8. Tuning consistency across task epochs. ***A***, Grip type tuning. Histogram bars indicate the number of cells that stay tuned for the same grip (black), change preference to the opposite grip (gray), or lose their tuning (white) when transitioning between consecutive task epochs (cue–planning and planning–movement). ***B***, ***C***, Change of orientation tuning in consecutive task epochs: cue–planning (***B***) and planning–movement (***C***). Histograms show the fraction of cells for which the preferred orientations in the two epochs were the same (0° shift), neighboring orientations (25°), or further apart (50–100°), and of cells that lost their tuning (white bars). Preferred orientation shifts of >25° were rare. In general, cells were tuned consistently over time.

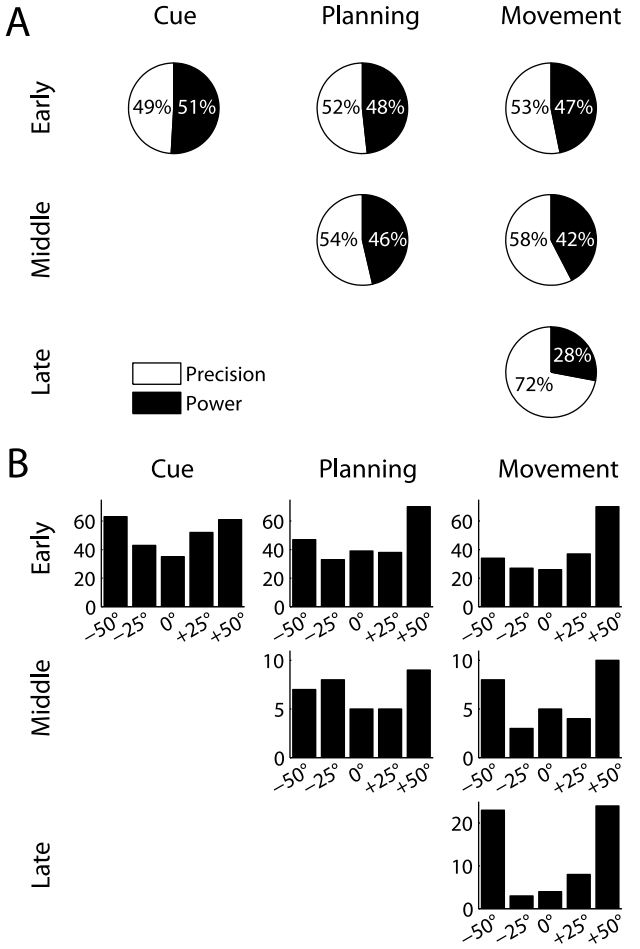

Figure 9. Distribution of preferred grip type and orientation in different cell classes. ***A***, Ratio of precision and power preference in cell groups with early (top row), intermediate (middle), and late (bottom) tuning onset for grip type. In all three task epochs, early-tuned cells preferred power grips and precision grips approximately equally often. In contrast, ~70% of late tuning cells preferred precision grips. ***B***, Number of cells with a particular orientation preference for the three cell classes. In early orientation-tuned cells, the portion of cells that preferred extreme orientations (±50°) changed little from cue (49%) to movement (53%), while 78% of cells with a late onset of orientation tuning preferred extreme orientations.

the different bins. These results suggest the presence of a visuomotor gradient along the IPS, with cells that show strong responses during the cue epoch being more frequently found in the posterior part of AIP, and cells with predominantly motor responses occurring more frequently toward the tip of the IPS. This fits well with anatomical data of neurons projecting from AIP to F5 that seem to be more frequently located in the anterior part of AIP, as Figure 1 of Borra et al. (2008) suggests. Finally, the presence of cells with sensory and motor representations in one area might facilitate sensorimotor transformation (Cisek and Kalaska, 2005; Optican, 2005; Buneo and Andersen, 2006).

Discussion

We investigated neural activity in AIP during a delayed grasping task, in which monkeys grasped a single object in various orientations with one of two possible grip types (Fig. 1). AIP neurons represented the object orientation and the instructed grip type immediately after cue presentation, indicating that AIP integrates 3D features of graspable objects with contextual information (Fig. 2, Table 1). The representation of grip type was stronger during movement execution than in the cue and planning epochs (Fig. 3) due to grip type-selective cells that became specifically active during movement (Fig. 4). Furthermore, grip type selectivity in the cue epoch was mainly found in cells that were also orientation selective, while the opposite was true in the movement epoch (Table 2).

In the TO task, the grip type was only weakly encoded in response to the grip type cue alone. In contrast, in the OT task, neurons preferring either grip type were activated simultaneously, after object presentation but before the type was instructed (Figs. 5, 6).

Individual cells generally kept the same preference for grip type and object orientation across task epochs (Figs. 7, 8). However, at the population level, neurons with early and late tuning onset had different distributions of preferred conditions (Fig. 9) as well as different anatomical distributions within AIP (Fig. 10).

Anatomical connectivity of AIP

Our findings are compatible with known anatomical connections of AIP. AIP receives input from parietal visual areas (in particular LIP, CIP, and V6a) and from the inferior temporal cortex (TEa, TEm) (Nakamura et al., 2001; Borra et al., 2008). These areas represent spatial and object orientation information of visible objects (Sakata et al., 1997; Tsutsui et al., 2001, 2002; Galletti et al., 2003). Also, AIP receives connections from the prefrontal cortex (areas 46v and 12l) (Borra et al., 2008), which might convey contextual information, as we have observed in AIP. Furthermore, AIP is reciprocally connected to area F5 in the ventral premotor cortex (Luppino et al., 1999) which exhibits similar activity related to hand movements (Rizzolatti et al., 1988; Murata et al., 1997; Raos et al., 2006; Stark et al., 2007) and is considered to be part of the cortical output structures for controlling the hand due to its projections to primary motor cortex and the spinal cord (Rizzolatti et al., 1988; Luppino et al., 1999; Lemon, 2008). Together these previous studies locate AIP at the interface between sensory and motor areas related to hand movement control.

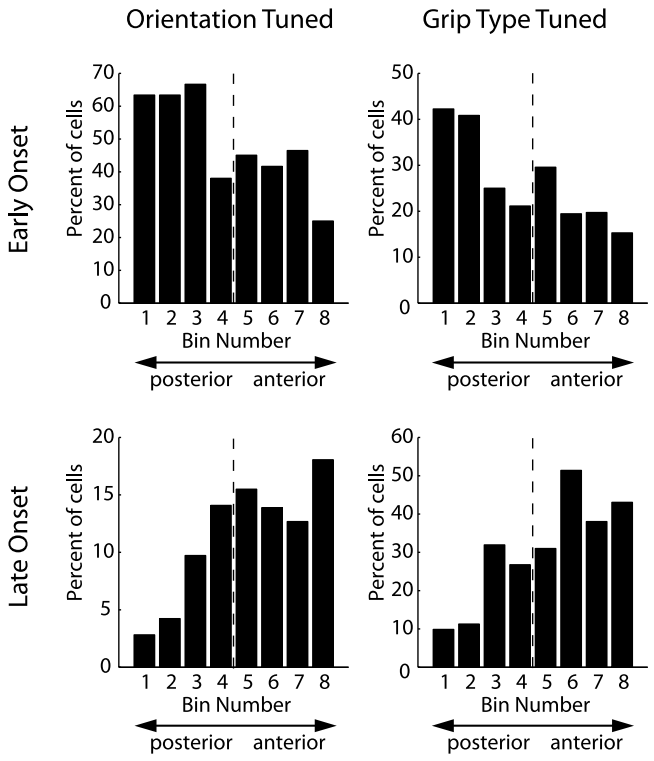

Figure 10. Anatomical distribution of different cell classes. Cells ($N = 571$) were distributed into eight bins according to their location along the intraparietal sulcus, such that each bin contained the same number of cells. Bin 1 contained the most posterior and bin 8 the most anterior cells (*x*-axis). Individual panels show the distribution along the intraparietal sulcus (IPS) for a particular cell class (left: orientation tuned, right: grip type tuned, top: early onset, bottom: late onset). Histograms display the fraction of cells in each bin that belonged to the respective cell class. Early onset cells showed a decreasing, late onset cells an increasing gradient from posterior to anterior. Dashed line, Median of the population.

Functional classification of AIP neurons

The group of Sakata described three cell classes in AIP based on their activity during grasping in the light and in the dark (Taira et al., 1990; Sakata et al., 1995, 1997): visual-dominant cells were only active when grasping in the light, visuomotor cells were preferentially active in the light, and motor-dominant cells were equally active for grasping in the light or dark. Furthermore, visually responsive cells were labeled "object type" if they were active in a separate object fixation task, and otherwise classified as "non-object type" (Sakata et al., 1995; Murata et al., 2000).

Our results confirm and extend this classification. Neurons active in the cue period of the delayed grasping task correspond to Sakata's object-type cells (visual dominant and visuomotor). These neurons fall in two subcategories: some are tuned to object orientation without selectivity for grip type, while others are modulated by grip type instruction. Most of these cells remain active during the planning epoch, suggesting a role for working memory or movement planning. Neurons active exclusively during the movement epoch correspond to Sakata's motor-dominant or non-object type/visuomotor classes.

In contrast to the previous categorization, our classification is based on the tuning onset for object orientation and grasp type during the entire course of the task, not just during the movement execution, and therefore quantifies the temporal appearance of object features and actions. This might allow us to draw inferences about the functional role of these cells during sensorimotor transformation.

Sensorimotor transformation and context dependency

The parietal cortex has long been known for its role in sensory–motor transformation (Mountcastle et al., 1975; Andersen, 1997; Scherberger and Andersen, 2003). Different subregions are specialized for particular types of actions, like the lateral intraparietal area for eye movements and the parietal reach region for arm reaching. Neurons in these areas are continuously active from stimulus presentation to action execution (Barash et al., 1991; Snyder et al., 1997). Furthermore, they represent not only the target object, but also context information, to select an appropriate action for that target (Gottlieb and Goldberg, 1999; Kalaska et al., 2003; Gail and Andersen, 2006; Scherberger and Andersen, 2007).

AIP fits well into this scheme. It is specialized for hand grasping, and its function can be well described within the framework of sensorimotor transformation (Taira et al., 1990; Sakata et al., 1995, 1997; Murata et al., 2000). Using a delayed grasping task, we found a strong visual component of AIP activity, with 55% of the cells distinguishing a spatial property of the grasp target—its orientation—already in the cue epoch (Fig. 3*A*). The activity of the majority of these cells extended to planning and execution (Table 1). Furthermore, 25% of the cells discriminated between power and precision grips already in the cue epoch, although the applicable grip type was not provided by the grasp target but by context information from the LEDs. This demonstrates that AIP represents not only the target object but also context information for action selection.

Our results suggest that upcoming hand movements are initially encoded as an object representation that is modulated by the action context, rather than a representation of a particular hand and finger configuration in purely motor terms. Such a context-dependent enhancement of motor-relevant object features has previously been described as a crucial step in visuomotor transformation: the remapping from a visual object description onto a representation that is more meaningful in motor terms (Allport, 1987; Rizzolatti et al., 1987; Gail and Andersen, 2006). This view is compatible with several aspects of our findings.

First of all, the neural response during cue was dominated by the spatial object feature. Orientation-selective neurons outnumbered the grip type-selective ones more than twofold during cue. In addition, 71% of all grip type-selective neurons were also selective for the object feature orientation during cue.

Second, in the cue separation task we found no increased activity for an abstract grip type instruction in the absence of an object to be grasped (TO task), while neural activity in the OT task was increased immediately after the object orientation cue for all neurons preferring either grip type. AIP neurons therefore seem to represent visual object features together with the ambiguities of the grip type until they are resolved by further instructions.

Finally, neural activity during the cue epoch was consistent with a coding scheme that is possibly more suitable for a uniform representation of object features, whereas late onset cells are probably more motor related, as we discuss in the following section.

Possible coding schemes

It has been argued that activity in cortical areas related to sensorimotor transformation reflects the sensory stimuli and context cues during the instruction phase of the task, while during movement execution these areas represent the movement plan independent of the sensory stimuli. This becomes evident in decision experiments for eye and arm movements (Platt and Glimcher, 1999; Gold and Shadlen, 2000; Scherberger and Andersen, 2007)

and in anti-saccade and anti-reaching tasks (Everling et al., 1999; Zhang and Barash, 2000; Gail and Andersen, 2006).

Our study supports this view. Neurons with a tuning onset during cue were stimulus-driven and represented the different object features and potential movement plans roughly in a uniformly distributed manner. In contrast, neurons with tuning onset during movement execution encoded the grasp type independently of the object orientation, and were more frequently tuned for precision grips and for extreme orientations. These neurons therefore seemed to use a different coding scheme than the visually responsive cells.

We consider late-onset neurons to be closely related to movement execution based on the following arguments: the overrepresentation of precision grips could be explained by the need of increased neural resources for controlling fine precision grips as opposed to power grips, as observed in other cortical areas (e.g., M1 and F5) (Muir and Lemon, 1983; Lemon et al., 2004; Umilta et al., 2007). Likewise, the overrepresentation of extreme object orientations could be explained by a motor-related encoding, namely a push–pull representation in pronation/supination coordinates. In contrast, visually responsive cells seem to use a coding which is closer to the visual input, as discussed above.

In summary, AIP neurons are modulated by contextual information about upcoming grasp movements when multiple grip types are possible. The encoding of a motor plan in AIP depends on the presence of knowledge about a target object, suggesting that hand movements are initially encoded by a goal-dependent modulation of the object representation, while during movement execution neurons seem to represent the grip type as such, independent of the target object.

References

Allport DA (1987) Selection for action: some behavioral and neurophysiological considerations of attention and action. In: Perspectives on perception and action (Heuer H, Sanders AF, eds), pp 395–419. Hillsdale, NJ: Erlbaum.

Amemori K, Sawaguchi T (2006) Rule-dependent shifting of sensorimotor representation in the primate prefrontal cortex. Eur J Neurosci 23:1895–1909.

Andersen RA (1997) Multimodal integration for the representation of space in the posterior parietal cortex. Philos Trans R Soc Lond B Biol Sci 352:1421–1428.

Andersen RA, Buneo CA (2002) Intentional maps in posterior parietal cortex. Annu Rev Neurosci 25:189–220.

Balint R (1909) Seelenlähmung des "Schauens", optische Ataxie, räumliche Störung der Aufmerksamkeit. Monatsschr Psychiatr Neurol 25:51–81.

Barash S, Bracewell RM, Fogassi L, Gnadt JW, Andersen RA (1991) Saccade-related activity in the lateral intraparietal area. I. Temporal properties; comparison with area 7a. J Neurophysiol 66:1095–1108.

Binkofski F, Dohle C, Posse S, Stephan KM, Hefter H, Seitz RJ, Freund HJ (1998) Human anterior intraparietal area subserves prehension: a combined lesion and functional MRI activation study. Neurology 50:1253–1259.

Borra E, Belmalih A, Calzavara R, Gerbella M, Murata A, Rozzi S, Luppino G (2008) Cortical connections of the macaque anterior intraparietal (AIP) area. Cereb Cortex 18:1094–1111.

Britten KH, Shadlen MN, Newsome WT, Movshon JA (1992) The analysis of visual motion: a comparison of neuronal and psychophysical performance. J Neurosci 12:4745–4765.

Buneo CA, Andersen RA (2006) The posterior parietal cortex: sensorimotor interface for the planning and online control of visually guided movements. Neuropsychologia 44:2594–2606.

Cisek P, Kalaska JF (2005) Neural correlates of reaching decisions in dorsal premotor cortex: specification of multiple direction choices and final selection of action. Neuron 45:801–814.

Culham JC, Danckert SL, DeSouza JF, Gati JS, Menon RS, Goodale MA (2003) Visually guided grasping produces fMRI activation in dorsal but not ventral stream brain areas. Exp Brain Res 153:180–189.

Everling S, Dorris MC, Klein RM, Munoz DP (1999) Role of primate superior colliculus in preparation and execution of anti-saccades and pro-saccades. J Neurosci 19:2740–2754.

Gail A, Andersen RA (2006) Neural dynamics in monkey parietal reach region reflect context-specific sensorimotor transformations. J Neurosci 26:9376–9384.

Gallese V, Murata A, Kaseda M, Niki N, Sakata H (1994) Deficit of hand preshaping after muscimol injection in monkey parietal cortex. Neuroreport 5:1525–1529.

Galletti C, Kutz DF, Gamberini M, Breveglieri R, Fattori P (2003) Role of the medial parieto-occipital cortex in the control of reaching and grasping movements. Exp Brain Res 153:158–170.

Gold JI, Shadlen MN (2000) Representation of a perceptual decision in developing oculomotor commands. Nature 404:390–394.

Gottlieb J, Goldberg ME (1999) Activity of neurons in the lateral intraparietal area of the monkey during an antisaccade task. Nat Neurosci 2:906–912.

Hoshi E, Shima K, Tanji J (2000) Neuronal activity in the primate prefrontal cortex in the process of motor selection based on two behavioral rules. J Neurophysiol 83:2355–2373.

Hyvärinen J, Poranen A (1974) Function of the parietal associative area 7 as revealed from cellular discharges in alert monkeys. Brain 97:673–692.

Jeannerod M, Michel F, Prablanc C (1984) The control of hand movements in a case of hemianaesthesia following a parietal lesion. Brain 107:899–920.

Kalaska JF, Cisek P, Gosselin-Kessiby N (2003) Mechanisms of selection and guidance of reaching movements in the parietal lobe. Adv Neurol 93:97–119.

Lemon RN (2008) Descending pathways in motor control. Annu Rev Neurosci 31:195–218.

Lemon RN, Kirkwood PA, Maier MA, Nakajima K, Nathan P (2004) Direct and indirect pathways for corticospinal control of upper limb motoneurons in the primate. Prog Brain Res 143:263–279.

Luppino G, Murata A, Govoni P, Matelli M (1999) Largely segregated parietofrontal connections linking rostral intraparietal cortex (areas AIP and VIP) and the ventral premotor cortex (areas F5 and F4). Exp Brain Res 128:181–187.

Mountcastle VB, Lynch JC, Georgopoulos A, Sakata H, Acuna C (1975) Posterior parietal association cortex of the monkey: command functions for operations within extrapersonal space. J Neurophysiol 38:871–908.

Muir RB, Lemon RN (1983) Corticospinal neurons with a special role in precision grip. Brain Res 261:312–316.

Murata A, Fadiga L, Fogassi L, Gallese V, Raos V, Rizzolatti G (1997) Object representation in the ventral premotor cortex (area F5) of the monkey. J Neurophysiol 78:2226–2230.

Murata A, Gallese V, Luppino G, Kaseda M, Sakata H (2000) Selectivity for the shape, size, and orientation of objects for grasping in neurons of monkey parietal area AIP. J Neurophysiol 83:2580–2601.

Nakamura H, Kuroda T, Wakita M, Kusunoki M, Kato A, Mikami A, Sakata H, Itoh K (2001) From three-dimensional space vision to prehensile hand movements: the lateral intraparietal area links the area V3A and the anterior intraparietal area in macaques. J Neurosci 21:8174–8187.

National Research Council (2003) Guidelines for the care and use of mammals in neuroscience and behavioral research. Washington, DC: National Academies.

Optican LM (2005) Sensorimotor transformation for visually guided saccades. Ann N Y Acad Sci 1039:132–148.

Platt ML, Glimcher PW (1999) Neural correlates of decision variables in parietal cortex. Nature 400:233–238.

Raos V, Umiltá MA, Murata A, Fogassi L, Gallese V (2006) Functional properties of grasping-related neurons in the ventral premotor area F5 of the macaque monkey. J Neurophysiol 95:709–729.

Rizzolatti G, Riggio L, Dascola I, Umilta C (1987) Reorienting attention across the horizontal and vertical meridians: evidence in favor of a premotor theory of attention. Neuropsychologia 25:31–40.

Rizzolatti G, Camarda R, Fogassi L, Gentilucci M, Luppino G, Matelli M (1988) Functional organization of inferior area 6 in the macaque monkey. II. Area F5 and the control of distal movements. Exp Brain Res 71:491–507.

Sakata H, Taira M, Murata A, Mine S (1995) Neural mechanisms of visual guidance of hand action in the parietal cortex of the monkey. Cereb Cortex 5:429–438.

Sakata H, Taira M, Kusunoki M, Murata A, Tanaka Y (1997) The TINS

Lecture. The parietal association cortex in depth perception and visual control of hand action. Trends Neurosci 20:350–357.
Scherberger H, Andersen RA (2003) Sensorimotor transformations. In: The visual neurosciences (Chalupa LM, Werner JS, eds), pp 1324–1336. Cambridge, MA: MIT.
Scherberger H, Andersen RA (2007) Target selection signals for arm reaching in the posterior parietal cortex. J Neurosci 27:2001–2012.
Scherberger H, Fineman I, Musallam S, Dubowitz DJ, Bernheim KA, Pesaran B, Corneil BD, Gilliken B, Andersen RA (2003) Magnetic resonance image-guided implantation of chronic recording electrodes in the macaque intraparietal sulcus. J Neurosci Methods 130:1–8.
Shikata E, McNamara A, Sprenger A, Hamzei F, Glauche V, Büchel C, Binkofski F (2008) Localization of human intraparietal areas AIP, CIP, and LIP using surface orientation and saccadic eye movement tasks. Hum Brain Mapp 29:411–421.
Snyder LH, Batista AP, Andersen RA (1997) Coding of intention in the posterior parietal cortex. Nature 386:167–170.
Stark E, Drori R, Asher I, Ben-Shaul Y, Abeles M (2007) Distinct movement parameters are represented by different neurons in the motor cortex. Eur J Neurosci 26:1055–1066.
Taira M, Mine S, Georgopoulos AP, Murata A, Sakata H (1990) Parietal cortex neurons of the monkey related to the visual guidance of hand movement. Exp Brain Res 83:29–36.
Tsutsui K, Jiang M, Yara K, Sakata H, Taira M (2001) Integration of perspective and disparity cues in surface-orientation-selective neurons of area CIP. J Neurophysiol 86:2856–2867.
Tsutsui K, Sakata H, Naganuma T, Taira M (2002) Neural correlates for perception of 3D surface orientation from texture gradient. Science 298:409–412.
Umilta MA, Brochier T, Spinks RL, Lemon RN (2007) Simultaneous recording of macaque premotor and primary motor cortex neuronal populations reveals different functional contributions to visuomotor grasp. J Neurophysiol 98:488–501.
Wallis JD, Anderson KC, Miller EK (2001) Single neurons in prefrontal cortex encode abstract rules. Nature 411:953–956.
White IM, Wise SP (1999) Rule-dependent neuronal activity in the prefrontal cortex. Exp Brain Res 126:315–335.
Zhang M, Barash S (2000) Neuronal switching of sensorimotor transformations for antisaccades. Nature 408:971–975.

9.2 List of figures and tables

9.3 Technical drawings

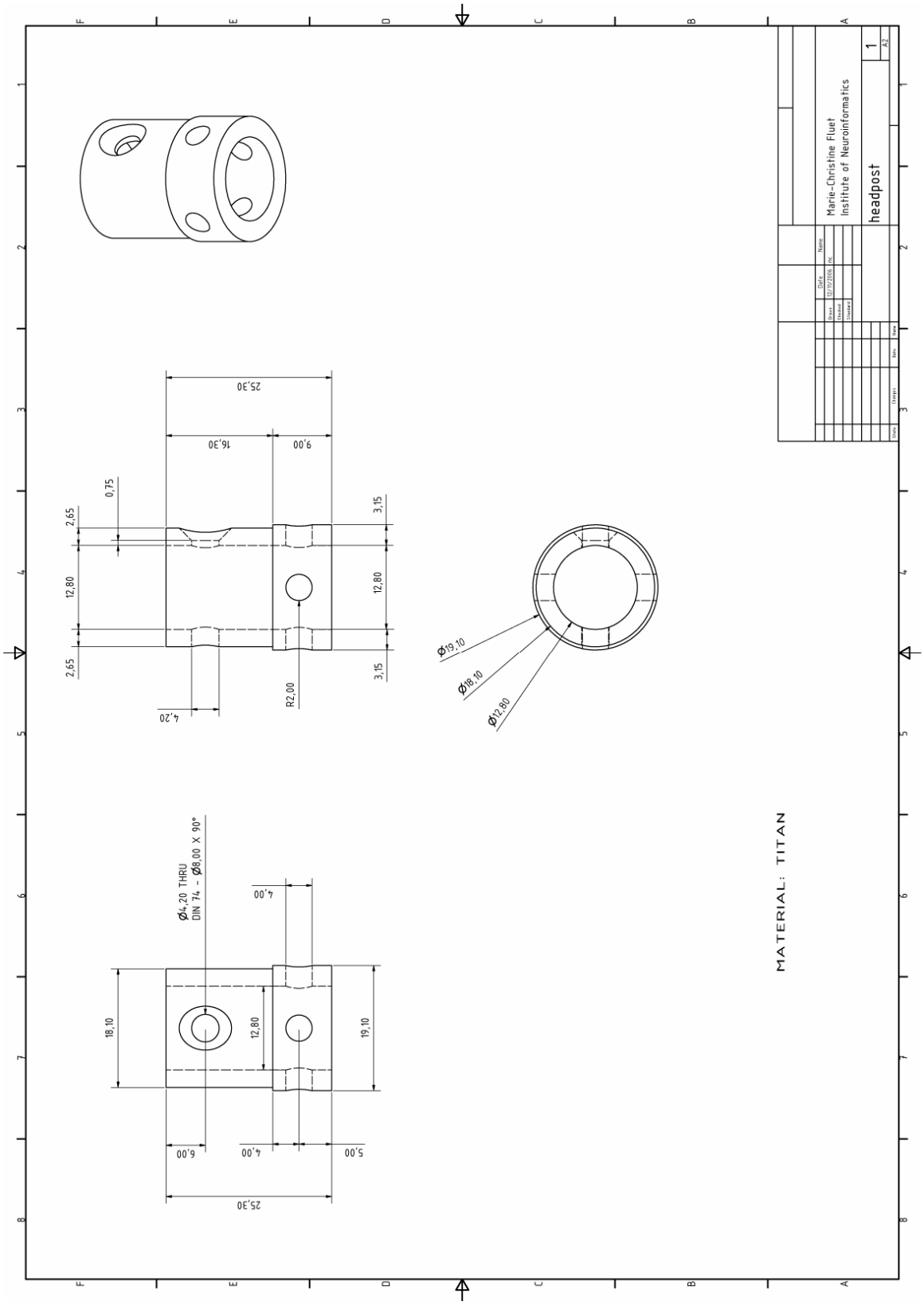

Figure 9.1 Head post.
The head post has a cylindrical shape (diameter: 18mm) and is made of titanium. It was fixed to the skull using bone cement and was used to immobilize the head of the animal during recordings.

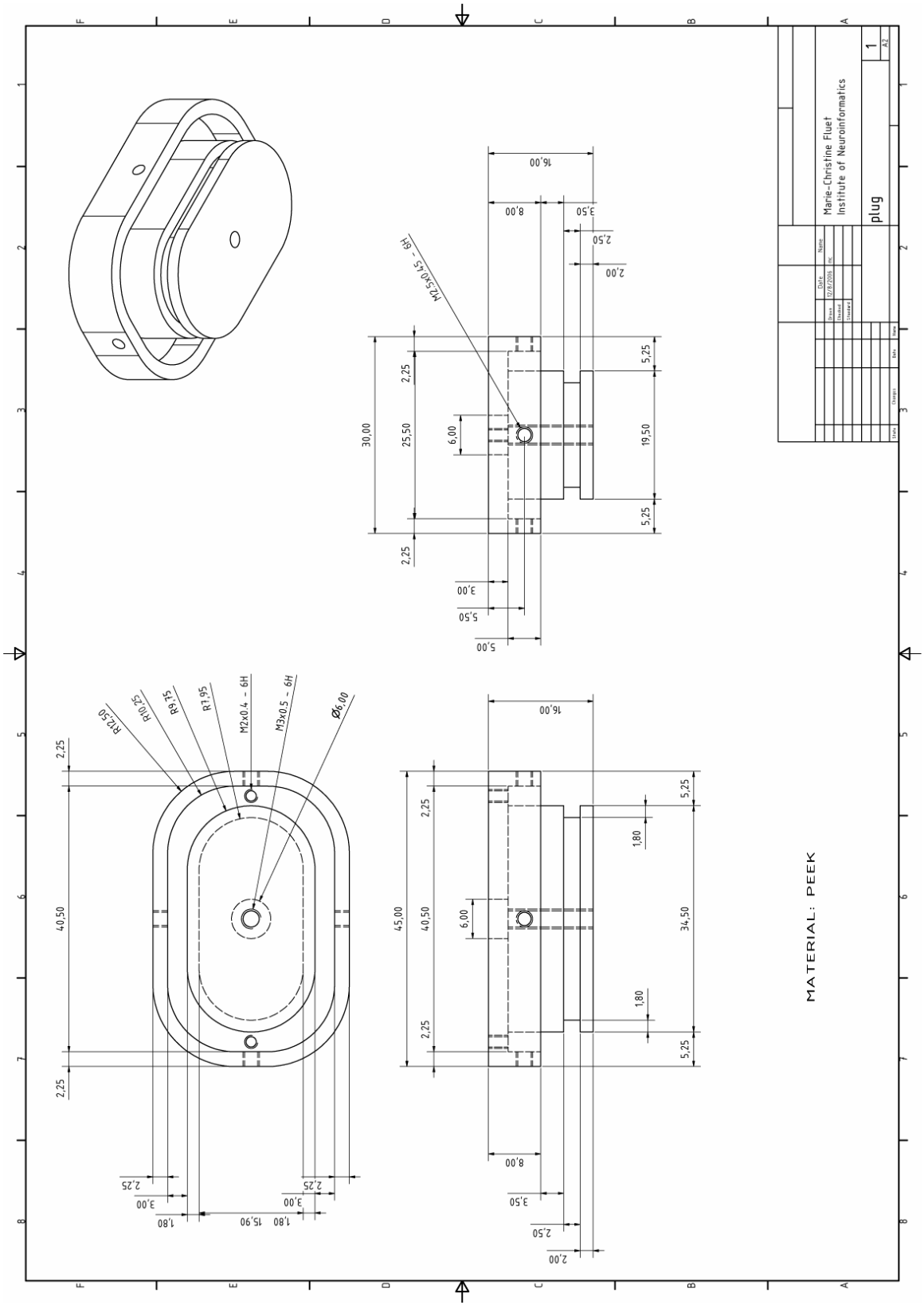

Figure 9.2 Cover of the recording chamber.
The cover of the recording chamber is made of PEEK (polyetheretherketone), which is MRI compatible. It fills almost completely the chamber thus sealing it properly.

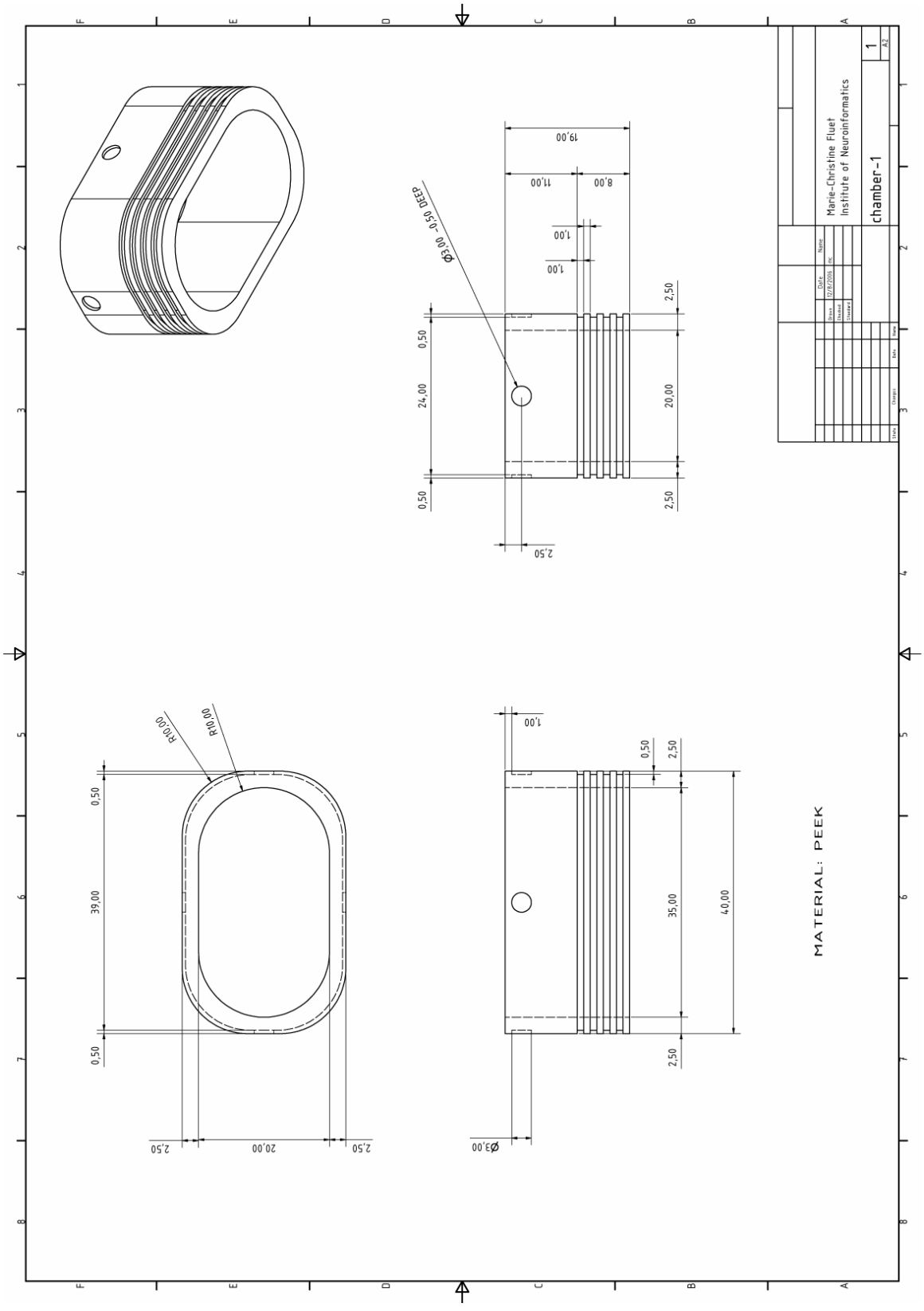

Figure 9.3 Recording chamber.
The recording chamber is made of PEEK, which is MRI compatible. It was fixed to the skull using bone cement. The recording electrodes were mounted directly on the chamber.

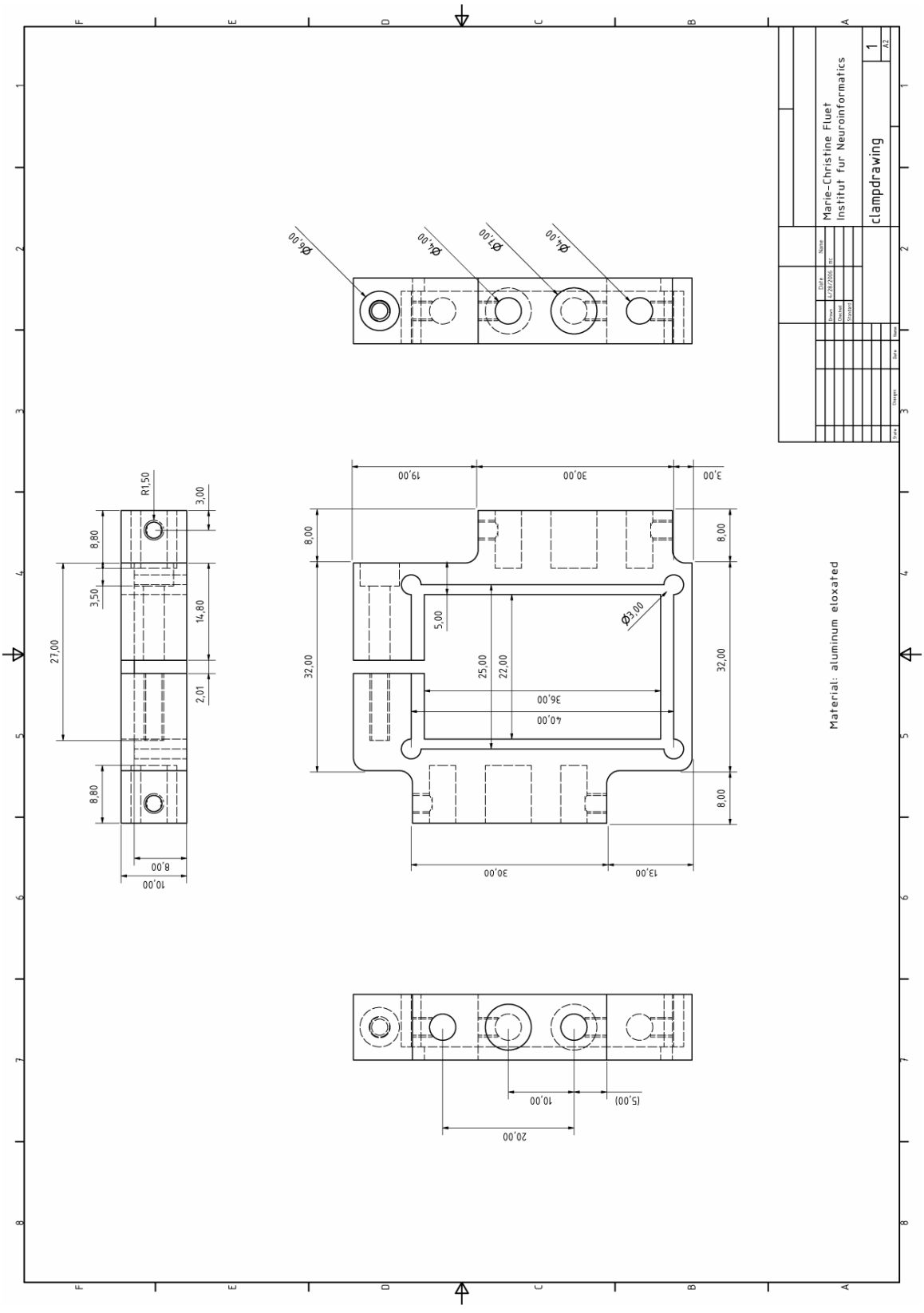

Figure 9.4 Chamber clamp.
The chamber clamp was fixed on the recording chamber. Two xyz-manipulators and microelectrode drives could be mounted on the clamp.

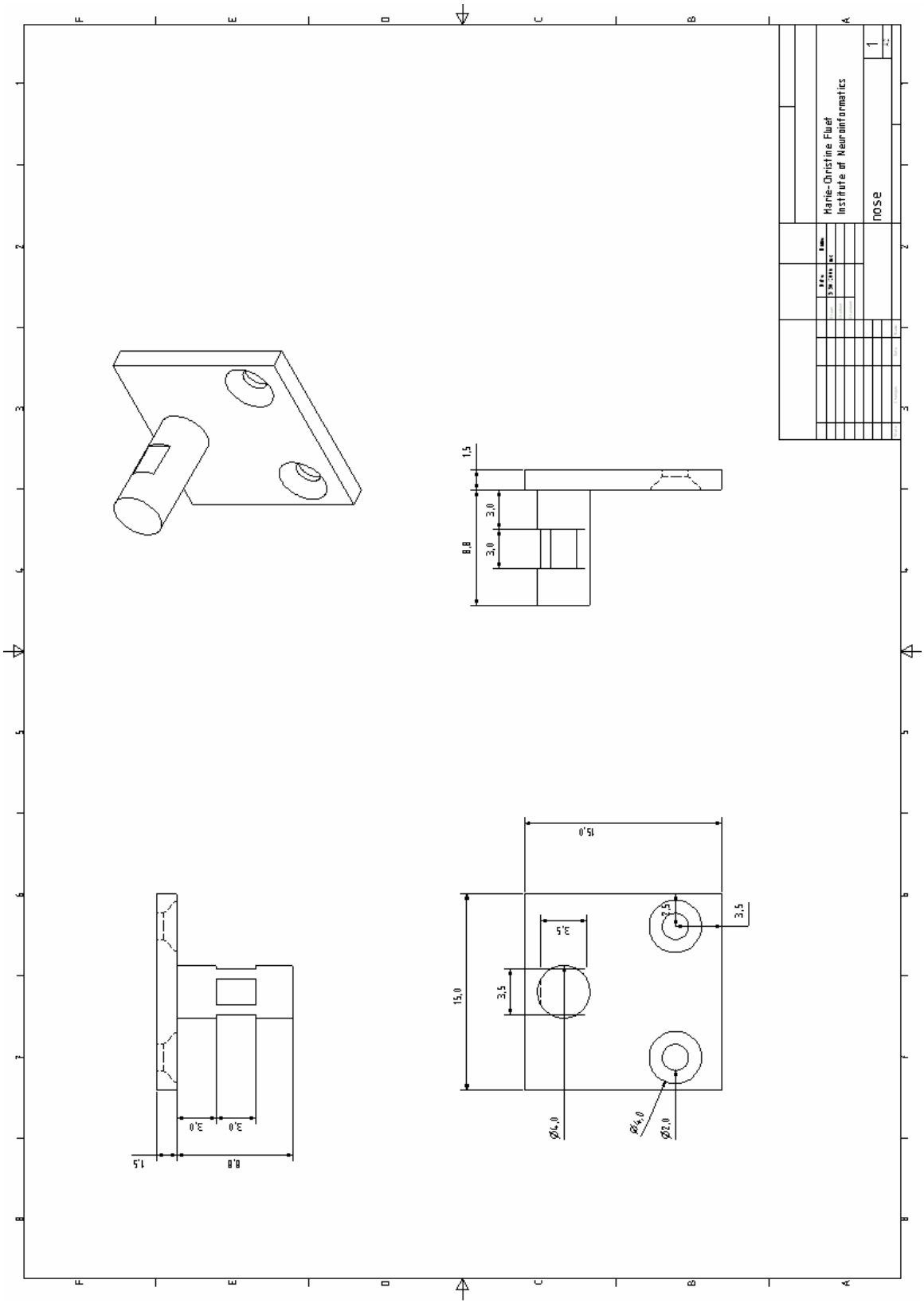

Figure 9.5 Microelectrode drives mounting piece.
This piece was fixed to the xyz-manipulators and served to mount the microelectrode drive.

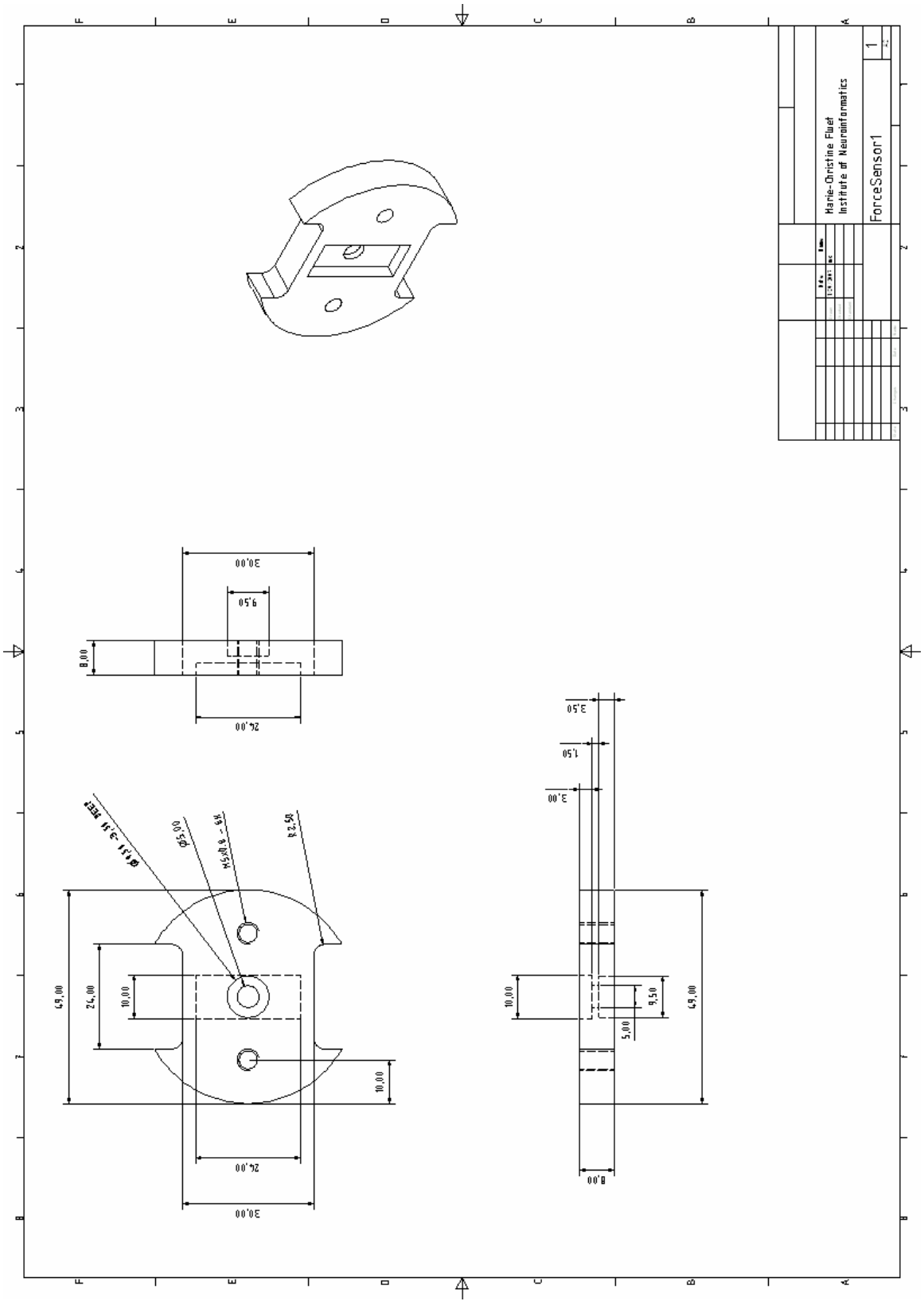

Figure 9.6 First force sensor mounting piece.
This piece was along the axis of the handle and served to link the handle with the pulling force sensor.

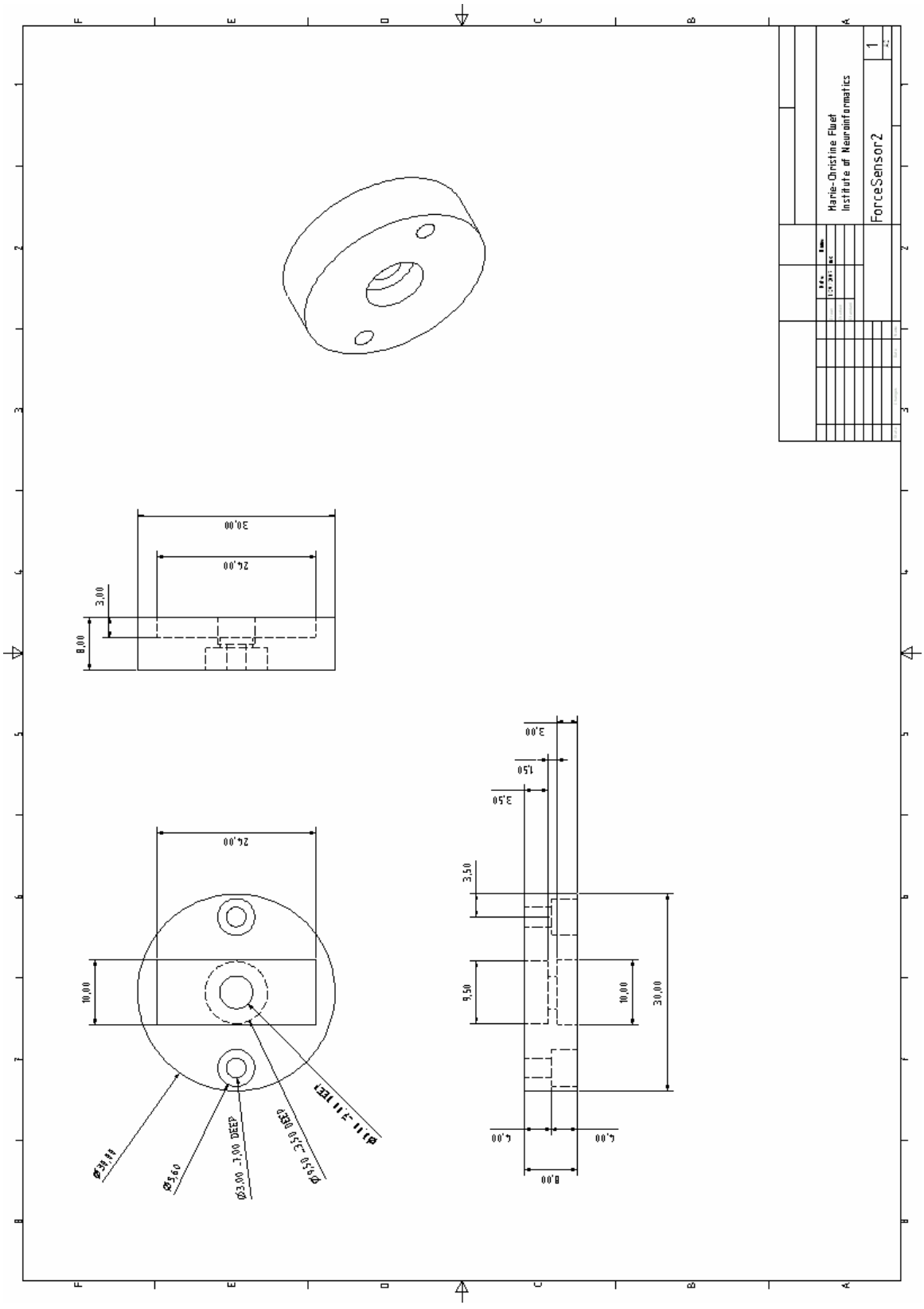

Figure 9.7 Second force sensor mounting piece.
This piece was along the axis of the handle and served to link the pulling force sensor with the motor axis used to turn the handle.

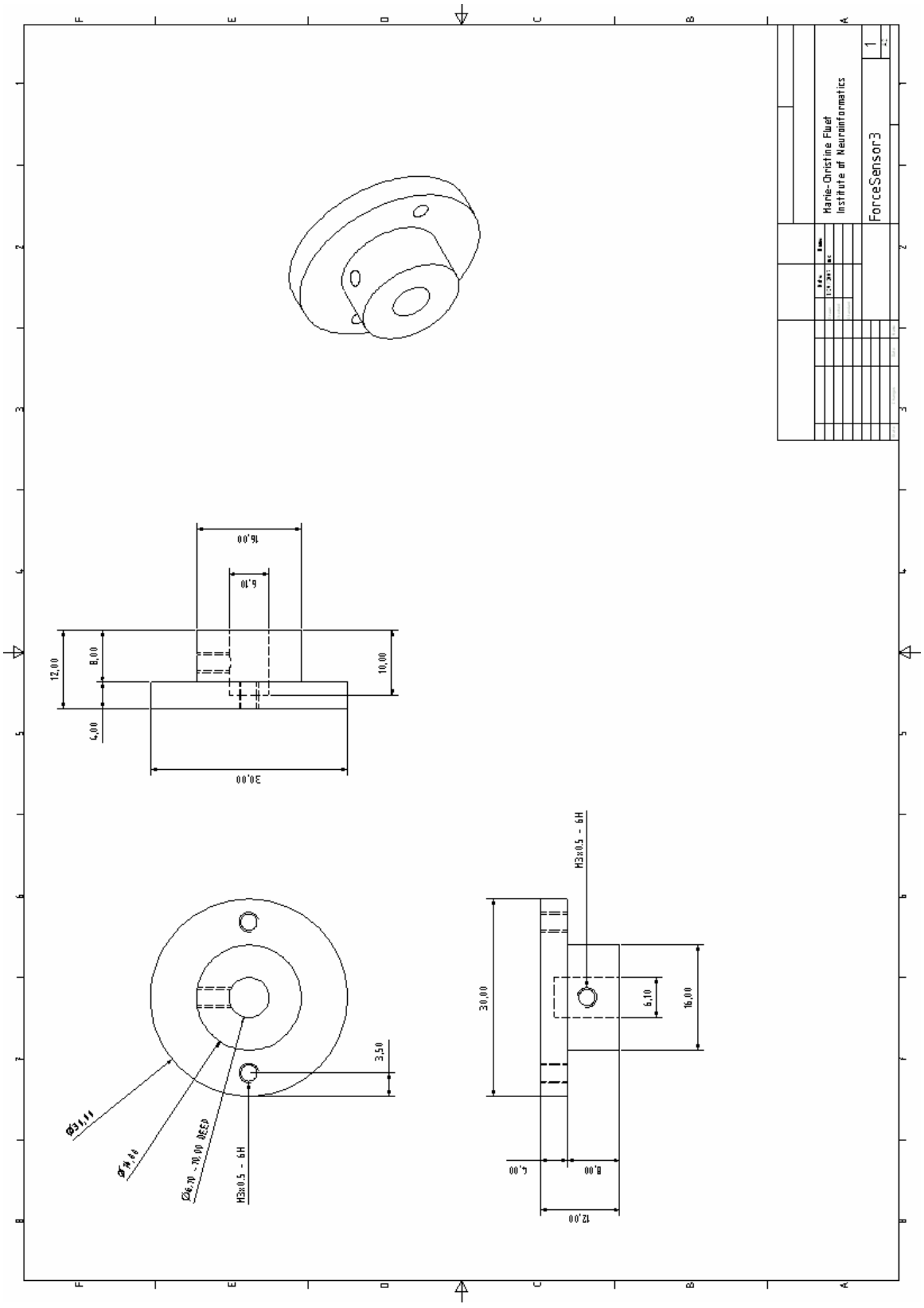

Figure 9.8 Third force sensor mounting piece.
This piece was along the axis of the handle and served to link the pulling force sensor with the motor axis used to turn the handle.

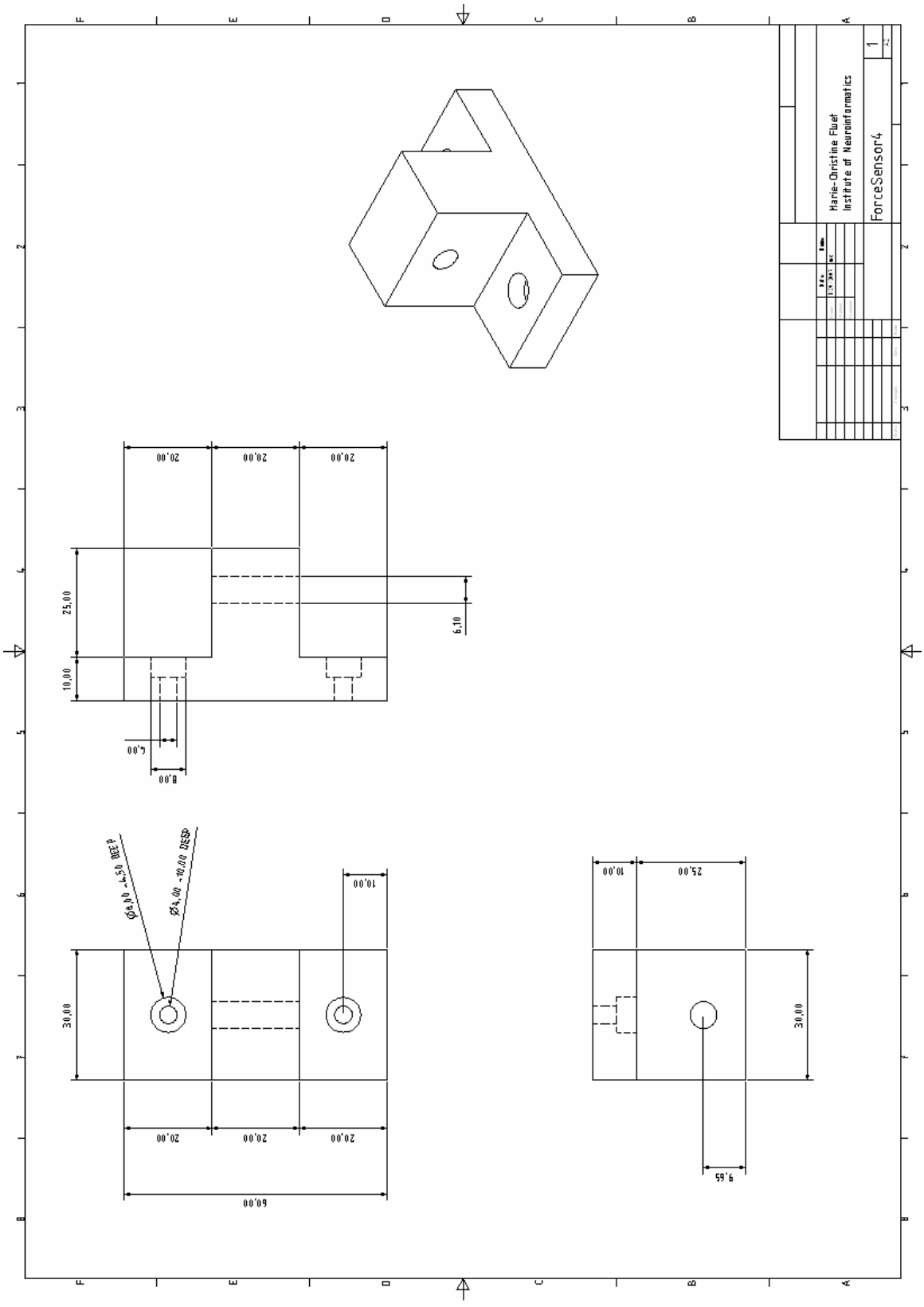

Figure 9.9 Fourth force sensor mounting piece.
This piece was along the axis of the handle and served to link the pulling force sensor with the motor axis used to turn the handle.

REFERENCES

Arbib MA (1985) Schemas for the temporal organization of behaviour. Hum Neurobiol 4:63-72.

Batista AP, Buneo CA, Snyder LH, Andersen RA (1999) Reach plans in eye-centered coordinates. Science 285:257-260.

Baumann MA, Fluet MC, Scherberger H (2009) Context-specific grasp movement representation in the macaque anterior intraparietal area. J Neurosci 29:6436-6448.

Beevor CE, Horsley V (1887) A minute analysis (experimental) of the various movements produced by stimulating in the monkey different regions of the cortical centre for the upper limb, as defined by Professor Ferrier. *Phil Trans R Soc Lond 178*:153-167.

Bernhard CG, Bohm E (1954) Cortical representation and functional significance of the corticomotoneuronal system. AMA Arch Neurol Psychiatry 72:473-502.

Bomze HM, Bulsara KR, Iskandar BJ, Caroni P, Skene JH (2001) Spinal axon regeneration evoked by replacing two growth cone proteins in adult neurons. Nat Neurosci 4:38-43.

Borra E, Belmalih A, Calzavara R, Gerbella M, Murata A, Rozzi S, Luppino G (2008) Cortical connections of the macaque anterior intraparietal (AIP) area. Cereb Cortex 18:1094-1111.

Bunge MB (2001) Bridging areas of injury in the spinal cord. Neuroscientist 7:325-339.

Carmena JM, Lebedev MA, Crist RE, O'Doherty JE, Santucci DM, Dimitrov DF, Patil PG, Henriquez CS, Nicolelis MA (2003) Learning to control a brain-machine interface for reaching and grasping by primates. PLoS Biol 1:E42.

Castiello U (2005) The neuroscience of grasping. Nat Rev Neurosci 6:726-736.

Chapin JK, Moxon KA, Markowitz RS, Nicolelis MA (1999) Real-time control of a robot arm using simultaneously recorded neurons in the motor cortex. Nat Neurosci 2:664-670.

Chavis DA, Pandya DN (1976) Further observations on corticofrontal connections in the rhesus monkey. Brain Res 117:369-386.

Dum RP, Strick PL (1991) The origin of corticospinal projections from the premotor areas in the frontal lobe. J Neurosci 11:667-689.

Dum RP, Strick PL (2005) Frontal lobe inputs to the digit representations of the motor areas on the lateral surface of the hemisphere. J Neurosci 25:1375-1386.

Fattori P, Breveglieri R, Marzocchi N, Filippini D, Bosco A, Galletti C (2009) Hand orientation during reach-to-grasp movements modulates neuronal activity in the medial posterior parietal area V6A. J Neurosci 29:1928-1936.

Ferrari PF, Gallese V, Rizzolatti G, Fogassi L (2003) Mirror neurons responding to the observation of ingestive and communicative mouth actions in the monkey ventral premotor cortex. Eur J Neurosci 17:1703-1714.

Ferrier D (1873) Experimental Researches in Cerebral Physiology and Pathology. J Anat Physiol 8:152-155.

Fogassi L, Gallese V, Buccino G, Craighero L, Fadiga L, Rizzolatti G (2001) Cortical mechanism for the visual guidance of hand grasping movements in the monkey: A reversible inactivation study. Brain 124:571-586.

Fritsch GT, Hitzig E (1870) On the electrical excitability of the cerebrum. In G. von Bonin (1960) transl., *Some papers on the cerebral cortex*. Springfield, Illinois: Thomas.

Fulton JF (1934) Forced grasping in relation to the syndrome of the premotor area. *Arch NeurolPsychiatr* 31:221-235.

Fulton JF (1935) Definition of the motor and premotor areas. *Brain Res* 58:311-316.

Fulton JF, Jacobsen CF, Kennard MA (1932) A note concerning the relation of the frontal lobes to posture and forced grasping in monkeys. *Brain* 55:524-536.

Gallese V, Keysers C, Rizzolatti G (2004) A unifying view of the basis of social cognition. Trends Cogn Sci 8:396-403.

Gallese V, Fadiga L, Fogassi L, Rizzolatti G (1996) Action recognition in the premotor cortex. Brain 119 (Pt 2):593-609.

Gallese V, Murata A, Kaseda M, Niki N, Sakata H (1994) Deficit of hand preshaping after muscimol injection in monkey parietal cortex. Neuroreport 5:1525-1529.

Gamberini M, Passarelli L, Fattori P, Zucchelli M, Bakola S, Luppino G, Galletti C (2009) Cortical connections of the visuomotor parietooccipital area V6Ad of the macaque monkey. J Comp Neurol 513:622-642.

Gentilucci M, Scandolara C, Pigarev IN, Rizzolatti G (1983) Visual responses in the postarcuate cortex (area 6) of the monkey that are independent of eye position. Exp Brain Res 50:464-468.

Godschalk M, Lemon RN, Nijs HG, Kuypers HG (1981) Behaviour of neurons in monkey peri-arcuate and precentral cortex before and during visually guided arm and hand movements. Exp Brain Res 44:113-116.

Godschalk M, Lemon RN, Kuypers HG, Ronday HK (1984) Cortical afferents and efferents of monkey postarcuate area: an anatomical and electrophysiological study. Exp Brain Res 56:410-424.

Goldberg ME, Colby CL, Duhamel JR (1990) Representation of visuomotor space in the parietal lobe of the monkey. Cold Spring Harb Symp Quant Biol 55:729-739.

Goodale MA, Milner AD (1992) Separate visual pathways for perception and action. Trends Neurosci 15:20-25.

Gross CG (2007) The discovery of motor cortex and its background. J Hist Neurosci 16:320-331.

Hitzig E (1870) Ueber die galvanischen Schwindelempfindungen und eine neue Methode galvanischer Reizung der Augenmuskeln. *Berl klin Wschr*:137-138.

Hochberg LR, Serruya MD, Friehs GM, Mukand JA, Saleh M, Caplan AH, Branner A, Chen D, Penn RD, Donoghue JP (2006) Neuronal ensemble control of prosthetic devices by a human with tetraplegia. Nature 442:164-171.

Horsley V, Schafer EA (1888) A record of experiments upon the functions of the cerebral cortex. *Phil Trans R Soc Lond* 179:1-45.

Hoshi E, Tanji J (2006) Differential involvement of neurons in the dorsal and ventral premotor cortex during processing of visual signals for action planning. Journal of neurophysiology 95:3596-3616.

Jeannerod M, Arbib MA, Rizzolatti G, Sakata H (1995) Grasping objects: the cortical mechanisms of visuomotor transformation. Trends Neurosci 18:314-320.

Jones EG, Coulter JD, Hendry SH (1978) Intracortical connectivity of architectonic fields in the somatic sensory, motor and parietal cortex of monkeys. J Comp Neurol 181:291-347.

Kemere C, Santhanam G, Yu BM, Afshar A, Ryu SI, Meng TH, Shenoy KV (2008) Detecting neural-state transitions using hidden Markov models for motor cortical prostheses. Journal of neurophysiology 100:2441-2452.

Kennard MA (1935) Vasomotor disturbances resulting from cortical lesions. *Arch NeurolPsychiatr* 33:537-545.

Kennard MA, Viets HR, Fulton JF (1934) The syndrome of the premotor cortex in man: Impairment in skilled movements, forced grasping, spasticity and vasomotor disturbance. *Brain* 57:69-84.

Kohler E, Keysers C, Umilta MA, Fogassi L, Gallese V, Rizzolatti G (2002) Hearing sounds, understanding actions: action representation in mirror neurons. Science 297:846-848.

Kurata K, Hoffman DS (1994) Differential effects of muscimol microinjection into dorsal and ventral aspects of the premotor cortex of monkeys. Journal of neurophysiology 71:1151-1164.

Kuypers HG, Lawrence DG (1967) Cortical projections to the red nucleus and the brain stem in the Rhesus monkey. Brain Res 4:151-188.

Lemon RN (2008) Descending pathways in motor control. Annu Rev Neurosci 31:195-218.

Luppino G, Rizzolatti G (2000) The Organization of the Frontal Motor Cortex. News Physiol Sci 15:219-224.

Luppino G, Murata A, Govoni P, Matelli M (1999) Largely segregated parietofrontal connections linking rostral intraparietal cortex (areas AIP and VIP) and the ventral premotor cortex (areas F5 and F4). Exp Brain Res 128:181-187.

Martino AM, Strick PL (1987) Corticospinal projections originate from the arcuate premotor area. Brain Res 404:307-312.

Matelli M, Luppino G (2001) Parietofrontal circuits for action and space perception in the macaque monkey. Neuroimage 14:S27-32.

Matelli M, Luppino G, Rizzolatti G (1985) Patterns of cytochrome oxidase activity in the frontal agranular cortex of the macaque monkey. Behav Brain Res 18:125-136.

Matelli M, Luppino G, Rizzolatti G (1991) Architecture of superior and mesial area 6 and the adjacent cingulate cortex in the macaque monkey. J Comp Neurol 311:445-462.

Matelli M, Camarda R, Glickstein M, Rizzolatti G (1986) Afferent and efferent projections of the inferior area 6 in the macaque monkey. J Comp Neurol 251:281-298.

Matsumura M, Kubota K (1979) Cortical projection to hand-arm motor area from post-arcuate area in macaque monkeys: a histological study of retrograde transport of horseradish peroxidase. Neurosci Lett 11:241-246.

Matsumura M, Sawaguchi T, Oishi T, Ueki K, Kubota K (1991) Behavioral deficits induced by local injection of bicuculline and muscimol into the primate motor and premotor cortex. Journal of neurophysiology 65:1542-1553.

Monakow KH, Akert K, Kunzle H (1979) Projections of precentral and premotor cortex to the red nucleus and other midbrain areas in Macaca fascicularis. Exp Brain Res 34:91-105.

Muakkassa KF, Strick PL (1979) Frontal lobe inputs to primate motor cortex: evidence for four somatotopically organized 'premotor' areas. Brain Res 177:176-182.

Murata A, Fadiga L, Fogassi L, Gallese V, Raos V, Rizzolatti G (1997) Object representation in the ventral premotor cortex (area F5) of the monkey. Journal of neurophysiology 78:2226-2230.

Murray EA, Bussey TJ, Wise SP (2000) Role of prefrontal cortex in a network for arbitrary visuomotor mapping. Exp Brain Res 133:114-129.

Musallam S, Corneil BD, Greger B, Scherberger H, Andersen RA (2004) Cognitive control signals for neural prosthetics. Science 305:258-262.

Napier JR (1956) The prehensile movements of the human hand. J Bone Joint Surg Br 38-B:902-913.

Pandya DN, Seltzer B (1982) Intrinsic connections and architectonics of posterior parietal cortex in the rhesus monkey. J Comp Neurol 204:196-210.

Ramon-Cueto A, Plant GW, Avila J, Bunge MB (1998) Long-distance axonal regeneration in the transected adult rat spinal cord is promoted by olfactory ensheathing glia transplants. J Neurosci 18:3803-3815.

Raos V, Umilta MA, Murata A, Fogassi L, Gallese V (2006) Functional properties of grasping-related neurons in the ventral premotor area F5 of the macaque monkey. Journal of neurophysiology 95:709-729.

Rizzolatti G, Luppino G, Matelli M (1998) The organization of the cortical motor system: new concepts. Electroencephalogr Clin Neurophysiol 106:283-296.

Rizzolatti G, Scandolara C, Matelli M, Gentilucci M (1981) Afferent properties of periarcuate neurons in macaque monkeys. I. Somatosensory responses. Behav Brain Res 2:125-146.

Rizzolatti G, Gentilucci M, Fogassi L, Luppino G, Matelli M, Ponzoni-Maggi S (1987) Neurons related to goal-directed motor acts in inferior area 6 of the macaque monkey. Exp Brain Res 67:220-224.

Rizzolatti G, Camarda R, Fogassi L, Gentilucci M, Luppino G, Matelli M (1988) Functional organization of inferior area 6 in the macaque monkey. II. Area F5 and the control of distal movements. Exp Brain Res 71:491-507.

Romo R, Hernandez A, Zainos A (2004) Neuronal correlates of a perceptual decision in ventral premotor cortex. Neuron 41:165-173.

Rozzi S, Ferrari PF, Bonini L, Rizzolatti G, Fogassi L (2008) Functional organization of inferior parietal lobule convexity in the macaque monkey: electrophysiological characterization of motor, sensory and mirror responses and their correlation with cytoarchitectonic areas. Eur J Neurosci 28:1569-1588.

Sakata H, Taira M, Murata A, Mine S (1995) Neural mechanisms of visual guidance of hand action in the parietal cortex of the monkey. Cereb Cortex 5:429-438.

Sanides F (1964) The cyto-myeloarchitecture of the human fronyal labe and its relation to phylogenetic differentiation of the cerebral cortex. J Hirnforsch 47:269-282.

Schall JD (1991) Neuronal activity related to visually guided saccades in the frontal eye fields of rhesus monkeys: comparison with supplementary eye fields. Journal of neurophysiology 66:559-579.

Schell GR, Strick PL (1984) The origin of thalamic inputs to the arcuate premotor and supplementary motor areas. J Neurosci 4:539-560.

Scherberger H, Jarvis MR, Andersen RA (2005) Cortical local field potential encodes movement intentions in the posterior parietal cortex. Neuron 46:347-354.

Schwab ME (2002) Repairing the injured spinal cord. Science 295:1029-1031.

Serruya MD, Hatsopoulos NG, Paninski L, Fellows MR, Donoghue JP (2002) Instant neural control of a movement signal. Nature 416:141-142.

Shain W, Spataro L, Dilgen J, Haverstick K, Retterer S, Isaacson M, Saltzman M, Turner JN (2003) Controlling cellular reactive responses around neural prosthetic devices using peripheral and local intervention strategies. IEEE Trans Neural Syst Rehabil Eng 11:186-188.

Spinks RL, Baker SN, Jackson A, Khaw PT, Lemon RN (2003) Problem of dural scarring in recording from awake, behaving monkeys: a solution using 5-fluorouracil. Journal of neurophysiology 90:1324-1332.

Stark E, Asher I, Abeles M (2007) Encoding of reach and grasp by single neurons in premotor cortex is independent of recording site. Journal of neurophysiology 97:3351-3364.

Swash M (2005) John Hughlings Jackson (1835-1911). J Neurol 252:745-746.

Taira M, Mine S, Georgopoulos AP, Murata A, Sakata H (1990) Parietal cortex neurons of the monkey related to the visual guidance of hand movement. Exp Brain Res 83:29-36.

Taylor DM, Tillery SI, Schwartz AB (2002) Direct cortical control of 3D neuroprosthetic devices. Science 296:1829-1832.

Uchida N, Buck DW, He D, Reitsma MJ, Masek M, Phan TV, Tsukamoto AS, Gage FH, Weissman IL (2000) Direct isolation of human central nervous system stem cells. Proc Natl Acad Sci U S A 97:14720-14725.

Umilta MA, Brochier T, Spinks RL, Lemon RN (2007) Simultaneous recording of macaque premotor and primary motor cortex neuronal populations reveals different functional contributions to visuomotor grasp. Journal of neurophysiology 98:488-501.

Umilta MA, Kohler E, Gallese V, Fogassi L, Fadiga L, Keysers C, Rizzolatti G (2001) I know what you are doing. a neurophysiological study. Neuron 31:155-165.

Wessberg J, Stambaugh CR, Kralik JD, Beck PD, Laubach M, Chapin JK, Kim J, Biggs SJ, Srinivasan MA, Nicolelis MA (2000) Real-time prediction of hand trajectory by ensembles of cortical neurons in primates. Nature 408:361-365.

Wise SP (1985) The primate premotor cortex: past, present, and preparatory. Annu Rev Neurosci 8:1-19.

Wise SP (2006) The evolution of ventral premotor cortex and the primate way of reaching. in *Evolution of Primate Nervous Systems: A Comprehensive Reference* Vol. 4, (ed. Kaas. J.H.) Ch. 11.

Woolsey CN, Settlage PH, Meyer DR, Sencer W, Pinto Hamuy T, Travis AM (1952) Patterns of localization in precentral and "supplementary" motor areas and their relation to the concept of a premotor area. Res Publ Assoc Res Nerv Ment Dis 30:238-264.

CURRICULUM VITAE

Personal Information

Name: Marie-Christine Fluet

Birthday : 1978/03/07

Nationality : Canadian

Languages : French: Native Speaker

English: Fluent

German: Intermediate level

Education

Jan. 2005 – June 2009	PhD Student Institute of Neuroinformatics, University of Zurich, Zurich, Switzerland
Jan. 1998 - Feb. 2002	Bachelor's degree in Electrical Engineering École Polytechnique de Montréal, Montreal, Quebec, Canada Student exchange for one semester at the Ecole Polytechnique Federale de Lausanne, Lausanne, Switzerland
Sep. 1997 - Dec. 1997	Studies in Occupational therapy Mc Gill College, Montreal, Quebec, Canada
Sep. 1995 - May 1997	College degree (Diplôme d'études collégiales) in sciences Collège de Sherbrooke, Sherbrooke, Quebec, Canada

Work experiences

May 2004 - Dec. 2004 — Technician at the Institute of Neuroinformatics, University of Zurich, Zurich, Switzerland

- Development of the set up and experiments for the study of free flying drosophila in a wind tunnel.

Jan. 2003 - Apr. 2004	Research assistant at the Institute of Physiology, University of Zurich, Zurich, Switzerland ❖ Fluorescence microscopy and voltage clamping for the study of sodium ion channels expressed in oocytes.
Apr. 2002 – Dec. 2002	Research assistant in the Ceramic Laboratory, Ecole Polytechnique Federale de Lausanne, Lausanne, Switzerland ❖ Development of the electrical, informatical, mecanical and optical components of an AFM (Atomic Force Microscope).

Publications

Baumann M, Fluet MC, Scherberger H (in press). Context specific grasp movement representation in the macaque anterior intraparietal area. *Journal of Neuroscience*.

Abstracts

2008	Fluet MC, Baumann M, Scherberger H, Hand grasping representation in premotor cortex of macaque monkeys. FENS 2008 Abstracts. Geneva, July 12-16.
2008	Baumann M, Fluet MC, Scherberger H, Hand grasping representation in parietal and premotor cortex of macaque monkeys. Primate neurobiology 2008 Abstracts. Tuebingen, Feb 27-29.
2007	Fluet MC, Baumann M, Scherberger H, Hand grasping representation in ventral premotor cortex of macaque monkeys. Neuroscience 2007 Abstracts. San Diego, Nov 3-7.
2007	Fluet MC, Baumann M, Scherberger H, Hand grasping signals in macaque premotor and parietal cortex. SSN 2007 Abstracts. Bern, Mar 9-10.
2006	Fluet MC, Baumann M, Scherberger H, Hand grasping signals in macaque premotor area F5 during a delayed grasping task.

Neuroscience 2006 Abstracts. Atlanta, Oct 14-18.

2006 Baumann M, Fluet MC, Scherberger H, Coding and decoding of hand grasping signals in the primate parietal and premotor cortex. Areadne 2006 Abstracts. Santorini, June 22-25.

2005 Baumann M, Fluet MC, Scherberger H, A behaviour control system for testing the neural representation of hand grasping signals in the macaque monkey. SSN 2005 Abstracts. Zurich, Feb 17-19.

Awards

2005-2007 Fellowship. University Research Priority Program "Integrative Human Physiology".

2004 Encouragement award for graduation in the field of information technologies and communication. Ministry of education of the government of Quebec.